AD_____

Award Number: DAMD17-98-1-8510

TITLE: Mechanisms of Mechano-Transduction within Osteoblasts

PRINCIPAL INVESTIGATOR: Louis C. Gerstenfeld, Ph.D.

CONTRACTING ORGANIZATION: Boston University Medical Campus
Boston, Massachusetts 02118

REPORT DATE: September 2002

TYPE OF REPORT: Final Addendum

PREPARED FOR: U.S. Army Medical Research and Materiel Command
Fort Detrick, Maryland 21702-5012

REPORT DOCUMENTATION PAGE

Form Approved
OMB No. 074-0188

1. AGENCY USE ONLY (Leave blank)	2. REPORT DATE	3. REPORT TYPE AND DATES COVERED
	September 2002	Final Addendum (1 Sep 01-31 Aug 02)

4. TITLE AND SUBTITLE
Mechanisms of Mechano-Transduction within Osteoblasts

5. FUNDING NUMBERS
DAMD17-98-1-8510

6. AUTHOR(S)
Louis C. Gerstenfeld, Ph.D.

7. PERFORMING ORGANIZATION NAME(S) AND ADDRESS(ES)
Boston University Medical Campus
Boston, Massachusetts 02118

E-Mail: lgersten@bu.edu

8. PERFORMING ORGANIZATION REPORT NUMBER

9. SPONSORING / MONITORING AGENCY NAME(S) AND ADDRESS(ES)
U.S. Army Medical Research and Materiel Command
Fort Detrick, Maryland 21702-5012

10. SPONSORING / MONITORING AGENCY REPORT NUMBER

11. SUPPLEMENTARY NOTES
Original contains color plates. All DTIC reproductions will be in black and white.

12a. DISTRIBUTION / AVAILABILITY STATEMENT
Approved for Public Release; Distribution Unlimited

12b. DISTRIBUTION CODE

13. ABSTRACT ***(Maximum 200 Words)***
Mechanical stimulation is crucial to the homeostasis of adult bone density and mass. The hypothesis of this proposal was that bone cells sense their mechanical environment through specific extracellular matrix (ECM) proteins (integrins) that are the ligands for these receptors. These studies focused on osteoblasts and the activation of specific integrin isotypes in response to adhesion and/or mechanical stimulation. The signal transductions system(s) responsible for mediating osteopontin, bone sialoprotein, and fibronectin gene expression in response to mechanical stimulation were examined as well as cellular response to variants in frequency, intensity, or duration of the mechanical stimuli. Both mechanical stimulation and cell adhesion specifically stimulated the expression of integrin binding proteins, yet while there are common features in the signal transduction processes, each gene was separately induced by unique mechanisms. Our data illustrate that the induction of intracellular kinase activities are related more to the specific nature of the ligand's interactions with its receptor and less with the process of cellular adhesion alone. They further demonstrate that osteoblast adhesion to different integrin ligands selectively mediates osteopontin gene expression. These data were the foundation for two new in vivo models to further define the role of mechanical stimulation on bone growth and healing.

14. SUBJECT TERMS
bone, osteoblasts, mechanical stimulation, signal transduction, genomic regulation

15. NUMBER OF PAGES
106

16. PRICE CODE

17. SECURITY CLASSIFICATION OF REPORT	18. SECURITY CLASSIFICATION OF THIS PAGE	19. SECURITY CLASSIFICATION OF ABSTRACT	20. LIMITATION OF ABSTRACT
Unclassified	Unclassified	Unclassified	Unlimited

Final Addendum Report
Table of Contents

INTRODUCTION

The bone remodeling cycle is known to be intimately involved in the metabolic homeostasis of mineral balance.[1] Bone formation and the remodeling cycle have been shown to be essential in maintaining the structural integrity of skeletal tissue in response to the mechanical loading to which it is subjected.[2,3] Bone remodeling has also been hypothesized to provide the means of repairing bone tissue that has been damaged as a result of mechanical fatigue.[4] Thus, it may be speculated that the skeletal cells (osteoblasts and osteoclasts) which mediate the remodeling process are regulated by their mechanical environment. In order for osteoblasts to respond to their mechanical environment, they must in some way sense it. One mechanism by which cells sense mechanical signals is through the physical deformation of the tissue. The hypothesis of this proposal was that specific cell surface receptors (integrins) that interact with specific extracellular matrix proteins (collagen, osteopontin, bone sialoprotein, and fibronectin) provide the physical link through which mechanical stimuli are transmitted via tissue deformation. As a corollary to this hypothesis, we proposed that the extracellular proteins that are ligands for these receptors are themselves regulated in response to cellular interaction with both the matrix and mechanical stimulation. Thus, these proteins act like autocrine factors that modify cell behavior in response to changes in matrix composition and mechanical deformation, as well as having a structural role in the matrix itself. Maintaining the balance of the extracellular matrix composition within bone then provides a mechanism by which the structural homeostasis of the skeleton may be regulated. This hypothesis and the published data that supports it are found in our review article published in 1999.[5]

The experiments that were carried out with the support of this grant were designed to define how osteoblasts and skeletal cells discriminate mechanical stimuli at a molecular level and how mechanical stimuli and cellular interactions with the extracellular matrix are transduced through integrin receptors and converted to intracellular signals that lead to genomic changes. These experiments defined whether different integrin ligands use common mechanisms in the regulation of their response to these stimuli. A determination of the intracellular second signaling systems (kinases) that are responsible for mediating the altered gene expression of *opn*, *bsp* and *fn* to mechanical stimulation were determined, both by assessing which kinases are activated and through the use of specific inhibitors that block the actions of the different kinase systems. A determination of the specific integrin isotypes that are involved in the different signal transduction processes was made. Other experiments examined if individual gene responses are differentially sensitive to various aspects of the mechanical stimuli (intensity, frequency, duration) or have different thresholds of response to different component parts of the stimuli.

BODY (with Goals as Defined in the Original Proposal)

Goal 1

The first goal of this proposal was directed at defining the molecular mechanisms of signal transduction by which mechanical stimulation regulates the expression of three specific ECM genes (osteopontin, bone sialoprotein and fibronectin) within osteoblasts. These studies tested whether there are common signal transduction pathways that mediate changes in the expression of these genes in response to mechanical stimulation.

a) The involvement of specific integrin isotypes in the mechano-signal transduction process that mediates these gene's genomic responses to mechanical stimulation was assessed in year 1.
b) The mechanistic relationship between the signal transduction pathways that are activated by mechanical stimulation vs. cell adhesion was examined in years 2-3
c) The nature of the second signal transduction pathways that mediate the changes in expression for each of these genes was determined in years 2-3.

Results of Goal 1

The effect of cell adhesion on the expression of these genes was separately examined to determine if these stimuli would mimic the effects of the mechanical stimulation. All three genes showed comparable levels of induction in response to adhesion on the fibronectin coated surfaces in comparison to non-coated surfaces, with maximal levels of induction seen for *bsp* and *opn* at 24 hours after plating while *fn* showed maximal levels of stimulation at 8 hours. Interestingly, while both *opn* and *fn* mRNA expression returned to base line after cell adhesion on fibronectin, *bsp* mRNA levels remained elevated. Examination of the signal transduction pathways that mediated the gene expression in response to attachment on fibronectin coated surfaces showed that both genistein and cycloheximide inhibited the induction of all three genes. This demonstrates that a tyrosine kinase was involved in the cell attachment mediated induction of these genes, and new protein synthesis was a prerequisite to this process. In contrast, the PKA specific inhibitor H-89 only ablated the induction of *fn* expression. Depolymerization of either microtubules or microfilaments with colchicine or cytochalasin D respectively had little effect on the over all expression of these genes in response to cell adhesion, indicating that the adhesion mediated phenomena was not dependent on cytoskeletal integrity. In summary, these results show that both mechanical stimulation and cell adhesion specifically stimulated the expression of integrin binding proteins. These results further demonstrate that while there are common features in the signal transduction processes that mediated the induction of these genes, each gene was separately induced by unique mechanisms. A complete description of these results is in: Carvalho RS, Kostenuik PJ, Salih E, Bumann A, and Gerstenfeld LC *"Selective Adhesion of Osteoblasts to Different Integrin Ligands will Induce Osteopontin Gene Expression."* See appended materials.

In our second study, we examined three interrelated relationships pertaining to osteoblast adhesion and the transduction of molecular signals. The first aspect of this study was to define if osteoblasts have variable adhesion properties to different integrin ligands. The second component of the study was to define the relationship between the selective adhesion of the osteoblasts on the different ligands with the induction of specific second signal kinase activities. The final aspect of this study was to determine if osteoblast adhesion to specific integrin ligands would show specific induction of *opn* mRNA expression. The first series of experiments of this study are depicted in Figure 1, panels A and B. These data show that three different extracellular matrix proteins, fibronectin (FN), fibrillar collagen type I (C), and denatured collagen type I gelatin (G), promote selective adhesion, whereas three other proteins, laminin (LN), osteopontin (OPN), and vitronectin (VN), did not. Bovine serum albumin (Al) was used as a control and is included in Panel B. As can be seen from this study, fibronectin was the most effective protein at promoting selective adhesion. Both native and denatured type I collagen also promoted selective attachment, but unlike fibronectin, both native and denatured collagen showed

saturation at between 1 and 3μg/cm^2 of surface coating. In contrast, fibronectin did not show saturation in promoting cell adhesion until about 30μg/cm^2 (data not shown). These data demonstrate that osteoblast adhesion specifically led to a strong induction of p-tyrosine levels and a generalization of its distribution throughout the cells after adhesion was promoted with a specific integrin binding ligand. These data then reinforce the conclusions reached in the experiments depicted in Figure 2, which suggest that the induction of intracellular kinase activities are related more to the specific nature of the ligand's interactions with its receptor and less with the process of cellular adhesion alone.

The last set of experiments of this study examined the relationship between osteoblast adhesion on specific ligands and the induction of specific genomic changes, using *opn* mRNA levels as a marker of genomic regulation. These studies are depicted in Figure 4. As can be seen in this figure, the induction of increased *opn* mRNA expression was seen as early as four hours after the cells had been allowed to adhere and continued to increase up to 24 hours. It is interesting to note in this study that once again native fibrillar collagen, fibronectin (*fn*), and to a lesser extent laminin, induced osteopontin (*opn*) gene expression to increase. These results suggest that the same integrin receptors that facilitate specific cell attachment also facilitate the induction of osteopontin expression. It is also interesting to note that neither osteopontin nor vitronectin mediated either of these cell responses, suggesting that they are not facilitated through a $\alpha_v\beta_3$ receptor. The one difference that was observed, however, was in the comparison of cell attachment on denatured collagen versus the induction of osteopontin. This result again suggests that signal transduction through the collagen receptor is only mediated when it interacts with native collagen. A complete description of these results is in: *"Osteoblast adhesion to different integrin ligands selectively mediates osteopontin gene expression."* See appended materials.

Goal 2

The second goal of these studies determined the relative importance of each component part of the mechanical stimuli (intensity, frequency and duration) to the mechano-signal transduction process.

a) The components of the mechanical stimuli (intensity, frequency, and duration) that are responsible for producing the signal transduction, which leads to the genomic regulation of specific genes in osteoblasts, were examined in year 3.
b) Short term (<24hr) versus chronic (>72hr) adaptive responses of osteoblasts to variations in duration of mechanical perturbation were defined in year 3.

Results of Goal 2

Towards the completion of goal two, the first series of these experiments was carried out by Emily Samuels, a masters student with the Harvard School of Dental Medicine, and the repeat of these studies was carried out by Annegret Rebehn, a masters student from the Dental School of University of Kiel, Germany (on sabbatical). These experiments were focused to determine the component part of mechanical stimuli that would induce changes in osteopontin gene expression. In both sets of studies we analyzed duration and frequency of the mechanical stimulation and examined the effect of fluid flow-induced shear stress on osteopontin expression. Using our device, which delivers spatially uniform biaxial strain to a membrane surface, osteoblasts were

subjected to 1% strain for 1, 5, 15 and 30 minutes and 1, 2, 4 and 8 hours of strain. Analysis of the induction of osteopontin mRNA expression demonstrated that a maximal 145% induction was observed after 8 hours ($p<0.05$). Osteoblasts were then subjected to varying frequencies of strain (0.1, 0.25, 0.5 and 1 Hz) for 8 hours. There was clearly a 2-3 fold stimulation in response to increasing frequency again with a significant finding ($p<0.05$). The effect of fluid induced shear stress was examined in the third part of this study. This was accomplished in the following manner. The membrane was cut into two equal areas that encompassed the inner and outer circular areas of the membrane. The cells were then subjected to an 8 hour period of mechanical stimulation at the same variations in frequency as used in the first part of these studies. Because of the way the device generates its strains, the inner circular area has several fold lower fluid flow than the outer areas. Similarly, higher frequencies will generate higher fluid flows; thus the combination of inner and outer areas with increasing frequency of strain should produce several orders of magnitude greater fluid movement. Analysis of *opn* mRNA production, however, showed that only the highest frequency (1 Hz) generated altered levels of osteopontin expression when comparing the inner and outer areas of the membrane. These results also showed that it was inversely related to the levels of fluid flow. Thus, the inner areas had the higher levels of osteopontin induction. Because a second student repeated these experiments and obtained the same results, we currently believe that the initial results that we obtained are correct. These results, however, are completely opposite to the hypothesis that fluid shear stress was the major mechanical stimulation that facilitated osteopontin (*opn*) expression. These results also would lead us questions as to whether Ca flux through stress activated channels was a component part of the signal transduction mechanisms that induced osteopontin expression as has been suggested by other research groups. This later suggestion, however, has since been shown to be incorrect.[7] As we moved forward with the third year and finished out these studies, we assessed how to further examine the mechanisms by which strain is effecting osteopontin gene regulation by determining the arrangement of stress fibers and integrin receptor localization within the cells that are found within the various areas of the mechanically stimulated membranes.

Continuation of Ongoing and New Studies

We will continue to pursue the in vitro effects of mechanical stimulation on skeletal stem cell differentiation. New, ongoing studies that were derived from the data generated by funding of this application are a realization of the long-term goals to extrapolate these in vitro model studies into mammalian systems.

Preliminary mechanical stimulation experiments have been undertaken in C3H10T1/2 murine mesenchymal stem cells and mesenchymal stem cells isolated from murine facture calluses at 7 days when the tissue is predominantly cartilage. These new experiments have the goal of determining how these cells respond to mechanical stimulation and if mechanical stimulation will change the time course of differentiation that is induced by BMP-7 treatment. Initial experiments will focus on examining osteopontin. Further experiments will assess the markers of both osteogenic and chondrogenic differentiation to determine if mechanical stimulation promotes chondrogenic or osteogenic differentiation selectively.

In conjunction with these in vitro studies, we have established two in vivo models to complement the in vitro studies as well as further define the role of mechanical stimulation on bone growth and healing. The first in vivo model involves introducing precisely defined motion into an osteotomy gap. These experiments are thoroughly described in: *"Induction of a neoarthrosis by precisely controlled motion in an experimental mid-femoral defect,"* and *"The role of the local mechanical environment on tissue differentiation during skeletal defect repair."* See appended materials.

The second in vivo model we developed is a murine tibial distraction osteogenesis model. Distraction osteogenesis is known to primarily induce intramembranous bone formation, and the motion is in a relatively stable environment with the mechanical stimulation in only one direction. This model will allow us to define the molecular and structural processes that occur during intramembranous bone formation and through this type of mechanical stimulation. These experiments are described in detail in: *"The role of Angiogenesis in a murine tibial model of distraction osteogenesis."* See appended materials.

KEY RESEARCH ACCOMPLISHMENTS

1. We have completed all of the experiments outlined in goal one.

2. We have completed all of the experiments outlined in goal two, as well as any repeated experiments from the first year.

3. Using data generated from this application, we have published (or are in the process of publishing) five full-length manuscripts, one masters thesis, and six abstracts, as well as given four presentations.

4. We established a new model of in vivo mechanical stimulation to study the role of mechanical forces in promoting chondrogenic differentiation in an osteotomy gap in a rat model.

5. We established a new model of in vivo mechanical stimulation to study murine tibial (long bone) distraction osteogenesis.

REPORTABLE OUTCOMES, 2001/2002

Manuscripts, Abstracts, and Presentations

Manuscripts:

1. Carvalho RS, Schaffer JL, Bumann A, and Gerstenfeld LC (2002) The predominant integrin ligands expressed by osteoblasts show preferential regulation in response to both cell adhesion and mechanical stimulation. J. Cellular Biochem. 84:497-508.

2. Cullinane DM, Frederick A, Eisenberg SR, Paccica D, Elaman MV, Lee C, Salisbury K, Gerstenfeld LC and Einhorn T. (2001) Induction of neoarthrosis by precisely controlled motion in an experimental mid-femoral defect. J. Orthopaedic Res. 20: 579-586.

3. Carvalho RS. Kostenuick P, Bumann A, Salih E and Gerstenfeld LC (2002) Selective Adhesion of Osteoblasts to Different Integrin Ligands will Induce Osteopontin Gene Expression. (Submitted, Matrix Biology)

4. Cullinane DM, Salisbury KT, Alkhiary Y, Gerstenfeld LC, and Einhorn TA (2002) The Role of the Local Mechanical Environment on Tissue Differentiation During Skeletal Defect Repair, (Manuscript).

Abstracts:
1. Carvalho RS, Kostenuick P, Bumann A, and Gerstenfeld LC. (2002) Differential Mechanisms of Signal Transduction that Mediate the Induction of Gene Expression by Cell Adhesion or Mechanical Stimulation within Osteoblasts. Orthopaedic Research Society.

2. Cullinane DM, Salisbury KT, Alkhiary Y, Sanabria G, Cottetta N, Gerstenfeld LC, and Einhorn TA. (2003) Mechanobiologically directed skeletal regeneration: Induced differentiation of cartilage, collagen type II and GDF-5 expression, and modified matrix architecture. Submitted for the 48th Annual Meeting of the Orthopaedic Research Society.

3. Carvalho RS, Einhorn TA, Lehmann W, Edgar C, Alyamani A, Apazidis A, Pacicca D, and Gerstenfeld LC. (2003) The role of Angiogenesis in a murine tibial model of distraction osteogenesis. Submitted for the 48th Annual Meeting of the Orthopaedic Research Society.

Presentations:
Cullinane M. Mechanobiology of bone and cartilage differentiation. SICB, Harvard University, March 2002.

Cullinane M. Biomechanics & Mechanobiology. Cambridge University, Dept. of Anatomy, UK, Sept. 2002

Patents and Licenses applied for or issued: None

Degrees obtained supported by this award: None

Development of cell lines, tissue or serum repositories: None

Informatics such as databases and animal models, etc:
New Animal Model: Dr. Dennis Cullinane, a classically trained anatomist who received partial support from this application, developed a new research area related to mechanical stimulation in bone repair. This new research project is focused on a new model of bone repair in which an external fixator is used to apply precisely controlled motion to an osteotomy. Using this surgical approach, new joint-like structures are able to be formed in a rat model. This approach may have clinical applications for use in the reconstruction of finger joints. This new animal model is now being applied to study cartilage formation. **These experiments are thoroughly described in:** *"Induction of a neoarthrosis by precisely controlled motion in an*

experimental mid-femoral defect," and *"The role of the local mechanical environment on tissue differentiation during skeletal defect repair."* See appended materials.

New Animal Model: Dr. Roberto Carvalho, who joined our laboratory to continue his research and was supported by data and materials provided by this grant's funding, has developed a murine tibial distraction osteogenesis model. Distraction osteogenesis is known to primarily induce intramembranous bone formation, and the motion is in a relatively stable environment with the mechanical stimulation in only one direction. The true innovation is in making the device tiny enough to work in the mouse, which is a widely used and characterized model with many transgenic variations available. This model will allow us to define the molecular and structural processes that occur during intramembranous bone formation and through this type of mechanical stimulation. **The specifics of this technique are described in:** *"The role of Angiogenesis in a murine tibial model of distraction osteogenesis."* See appended materials.

Funding applied for based on work supported by this award:
Whittaker Foundation; Dennis M. Cullinane, Ph.D., applied for additional funding for the joint-like structure/precisely controlled motion to an osteotomy project.

NIH R03; Roberto S. Carvalho, D.M.D., Ph.D., applied for funding in order to continue study of the role of osteopontin and in-vivo mechanical signaling in a mouse tibial distraction osteogenesis model.

NIH PO1; Louis Gerstenfeld, Ph.D., Dennis M. Cullinane, Ph.D., and Roberto S. Carvalho, D.M.D., Ph.D., are all part of a pending program grant that the Boston University School of Medicine, Department of Orthopaedic Surgery, which includes elements of the rat joint induction project and the murine distraction osteogenesis experiments.

Employment or research opportunities applied for and/or received on experiences/training supported by this award:
In the last year, two M.D./Ph.D. candidates have been working in the laboratory on areas of biomechanical stimulation of bone healing and bone cell response. Ms. Kristy Salisbury, a bioengineering student, is doing her thesis work on the new project area of joint regeneration by biomechanical stimulation. Mr. Alexios Apazidis, a biochemistry student, is currently obtaining experience using cultured cells and mechanical stimulation. Dr. Roberto Carvalho, D.D.S., MSc., D.M.D., Ph.D., has continued his affiliation with our laboratory to further his research in the area of osteopontin and mechanical stimulation. Dr. Carvalho has recently been appointed an Assistant Professor of Orthodontics at Boston University School of Dental Medicine, and a joint appointment as an Assistant Professor of Orthopaedic Surgery at Boston University School of Medicine is currently pending.

In the past year, the funding applied for or received based on the research performed with this application's funding is as follows: Dr. Cullinane has received funding from the Arthritis Foundation for the joint induction project, and he has applied for additional funding from the Whittaker Foundation. Dr. Carvalho is applying to the NIH for RO3 funding to continue the

distraction osteogenesis experiments. Drs. Gerstenfeld, Cullinane, and Carvalho are also collaborators on a pending program grant that incorporates aspects of both mammalian models described above.

CONCLUSIONS

The major conclusions from this proposal are as follows:

1. Integrin ligands as a class are induced in osteoblasts in response to mechanical stimulation and adhesion. Such findings provide strong evidence to support the hypothesis that these molecules act like autocrine or paracrine factors.

2. Cell adhesion of osteoblasts is specifically mediated by β1 class of integrins. This same class of integrins appears to be responsible for the signal transduction process that stimulates osteopontin induction. The β3 integrin ligands vitronectin and osteopontin neither mediate specific adhesion nor induce osteopontin gene expression, but they do selectively induce specific kinase activities.

3. Component aspects of the mechanical stimulation do affect the induction of the gene. Both greater duration and increasing frequency clearly appear to enhance response to the mechanical signal. Shear stress induced by fluid flow does not appear to be a mediating factor in osteopontin induction in response to mechanical stimulation.

FINAL REPORT BIBLIOGRAPHY

1. Gerstenfeld, LC. (1999) Osteopontin in skeletal tissue homeostasis: an emerging picture of the autocrine/paracrine functions of the extracellular matrix. Research Prospective, J. Bone and Mineral Research, 14:850-855

2. Carvalho RS, Schaffer JL, Bumann A and Gerstenfeld LC. (2002) Predominant Integrin Ligands Expressed by Osteoblasts Show Preferential Regulation in Response to both Cell Adhesion and Mechanical Perturbation. J. Cellular Biochem. 84:497-508.

3. Cullinane DM, Frederick A, Eisenberg SR, Paccica D, Elaman MV, Lee C, Salisbury K, Gerstenfeld LC and Einhorn T. (2002) Induction of neoarthrosis by precisely controlled motion in an experimental mid-femoral defect. J. Orthopaedic. Res. 20: 579-586.

4. Carvalho RS, Kostenuick P, Bumann A, Salih E and Gerstenfeld LC (2002) Selective Adhesion of Osteoblasts to Different Integrin Ligands will Induce Osteopontin Gene Expression. (Submitted, Matrix Biology)

5. Cullinane DM, Salisbury KT, Alkhiary Y, Gerstenfeld LC, and Einhorn TA (2002) The Role of the Local Mechanical Environment on Tissue Differentiation During Skeletal Defect Repair. (Manuscript).

6. Samuel, E J. Osteoblast induction of osteopontin expression: response to changes in duration and frequency of mechanical strain, and to variation in flow induced shear stress. Masters thesis, Harvard School of Dental Medicine; Copyright, Harvard School of Dental Medicine.

Abstracts:

1. Carvalho RS, Schaffer JL, Bumann A, and Gerstenfeld LC (2000) RGD containing proteins of osteoblasts are responsive to mechanical stimulation and matrix attachment. *Trans. 46th Ann. Meeting, Orthop. Res. Soc.*

2. Cullinane, D.M., Frederick, A., Gerstenfeld, L., Eisenberg, Pacicca, D., Altuwairgi, O., Lee, C., Salisbury, K., Hellenbrand, L., Einhorn, T.A. (2000) Induction of joint morphology and articular-like cartilage in a bone gap using controlled micromotion. *Trans. 47th Ann. Meeting Orthop. Res. Soc., San Francisco.*

3. Carvalho RS. Kostenuick P, Bumann A, Salih E and Gerstenfeld LC. (2001) Selective induction of osteopontin expression in osteoblasts is mediated by different integrin ligands. J. Bone Mineral Res. 16:S1:S:240

4. Carvalho RS, Kostenuick P, Bumann A and Gerstenfeld LC. (2002) Differential Mechanisms of Signal Transduction that Mediate the Induction of Gene Expression by Cell Adhesion or Mechanical Stimulation within Osteoblasts. *Trans. 47th Ann. Meeting Orthop. Res. Soc., San Francisco.*

5. Cullinane DM, Salisbury KT, Alkhiary Y, Sanabria G, Cottetta N, Gerstenfeld LC, and Einhorn TA. (2003) Mechanobiologically directed skeletal regeneration: Induced differentiation of cartilage, collagen type II and GDF-5 expression, and modified matrix architecture. Submitted for the 48th Annual Meeting of the Orthopaedic Research Society.

6. Carvalho RS, Einhorn TA, Lehmann W, Edgar C, Alyamani A, Apazidis A, Pacicca D, and Gerstenfeld LC. (2003) The role of Angiogenesis in a murine tibial model of distraction osteogenesis. Submitted for the 48th Annual Meeting of the Orthopaedic Research Society.

Presentations:

Differential Mechanisms of Signal Transduction that Mediate the Induction of Gene Expression by Cell Adhesion or Mechanical Stimulation within Osteoblasts. Presented at "Osteoporosis as a failure of bone's adaptation to functional load bearing." The Wellecome Trust Foundation, Highgate, England, 1999.

Cullinane D, Frederick A, Gerstenfeld L, Eisenberg S, Pacicca D, Altuwairgi O, Lee C, Salisbury K, Hellenbrand L and Einhorn T (2001) Induction of joint morphology and articualar-like cartilage in a bone gap using controlled micromotion. Transactions of Ortho Res. Soc, 26:364

Cullinane D (2002) Mechanobiology of bone and cartilage differentiation. SICB, Harvard University.

Presentations (continued):
Cullinane D (2002) Biomechanics & Mechanobiology. Cambridge University, Dept. of Anatomy, UK, Sept. 2002

Final List of Personnel:

Louis C. Gerstenfeld, Ph.D.
Paul Kostenuick, Ph.D.
George L. Barnes, Ph.D.
Dennis Cullinane, Ph.D.
Irene Simkina, M.S.
Bohus Svagar, M.D.
Colleen Keyes, B.S., M.Sc.
Johanna Cruceta, B.S.
Thomas Dellatorre, B.S.
Michael Elman, B.S.
Erjan Salih, Ph.D. (Subcontract)

REFERENCES:

1. Jilka RL, Manologas SC 1994 In *Osteoporosis* Chapter 2 The cellular and biochemical basis of bone remodeling. Pg 17-47 ed. R. Marcus, Blackwell Scientific Publications, Cambridge MA

2. Lanyon LE, Goodship AE, Pye C, McFie H 1982 Mechanically adaptive bone remodeling. Biomechanics **17**: 897-906.

3. Lanyon LE, Rubin CT 1987 Functional strain on bone tissue as an objective and controlling stimulus for adaptive bone remodeling. J Biomech **15**:141-154.

4. Mori S, Burr DB 1993 Increased intracortical remodeling following fatigue damage. Bone **14**:103-109.

5. Gerstenfeld LC 1999 Editorial\Perspective Osteopontin in skeletal tissue homeostasis: an emerging picture of the autocrine\paracrine functions of the extracellular matrix. J Bone Miner Res **14**:850-855.

6 Owan I, Burr DB, Turner CH, Qiu J, Tu Y, Onyia JE, Duncan RL 1997 Mechanotransduction in bone: osteoblasts are more responsive to fluid forces than mechanical strain . Am J Physiol **273**:C810

7. Chen NX, Ryder KD, Pavalko FM, Turner CH, Burr DB, Qiu J, Duncan RL. 2000 Ca(2+) regulates fluid shear-induced cytoskeletal reorganization and gene expression in osteoblasts.Am J Physiol Cell Physiol **278**:C989-97

BOSTON UNIVERSITY MEDICAL CENTER

Radiation Protection
Office

88 East Newton Street, D-604
Boston, Massachusetts
02118-2394
617 638-7052

To: Dr. Gerstenfeld Date: June 24, 1998

From: Victor Evdokimoff, Secretary Radioisotope Committee VNE/CM

Subject: Authorization to use radioisotopes at BUMC

On June 24, 1998 your application _X_, renewal ___, amendment____ to use radioisotopes at BUMC was approved. You are only authorized for the following isotope(s), quantities, etc.

Isotope(s)	Form	Max./order	Max./year	Possession limit
H-3	Amino acid, Nucleotide	5 mCi	N/A	N/A
P-32	Phosphorous, Nucleotide	5 mCi	N/A	N/A
C-14	Chloramphenicol, Amino acids	1 mCi	N/A	N/A
S-35	Na Sulfate, Nucleotide, Amino acids	1 mCi	N/A	N/A
P-33	Phosphorous, Nucleotides	1 mCi	N/A	N/A

Your authorization code number is G-16 . This number must appear on all requisitions for isotopes. In addition, the following **conditions** apply to your authorization:

1) The Radioisotope Committee is recommending you consider alternatives to using 3H/14C such as non-radioactive tracers.

2) All personnel under your permit planning on using P-32 must complete the individual training requirements. In addition, any user of 1 mCi or more of P-32 at one time is required to be monitored by TLD. Please contact the RPO for assistance.

Boston University
Medical Campus

Office of Research
Administration
715 Albany Street, 560
Boston, Massachusetts
02118-2394
617 638-4600

BOSTON UNIVERSITY MEDICAL CENTER

Institutional Biosafety Committee

Renewal Letter: Biohazard Project

IBC Coordinator: Mary Gistis

Principal Investigator:	Dr. Louis Gerstenfeld
Project Title:	Musculoskeletal Research
Approval Number:	# A-168
Renewal Date:	November 4, 1998
Containment Level:	BL-2/Universal Precautions
Comments:	related to rDNA projects 497, 500, 501

For your records, make several copies of this document to avoid delays when filing your grant applications with federal agencies.

IBC APPROVAL LETTER

Boston University
School of Medicine

Institutional Animal
Care and Use
Committee

700 Albany Street, W707
Boston, Massachusetts
02118
TEL: 617 638-4263
FAX: 617 638-4055

Louis C. Gerstenfeld PhD
Associate Professor
Orthopedic Surgery
Boston University Medical Center
715 Albany Street, Housman 2
Boston . MA 02118

7/11/2000

RE: Application No. 98-096 Agency: Department of the Army

Title: Mechanisms of Mechano-Transduction Within Osteoblasts

Protocol Status: APPROVED, 7/22/1998
ANIMAL NUMBERS/YR. 1248 chicken embryos/year x 4 yrs

BIOHAZAPDS:

Dear Dr. Gerstenfeld

Your application for use of animals in research or education has been reviewed by the Institutional Animal Care a Use Committee at Boston University Medical Center. The protocol is APPROVED as being consistent with humane treatme of laboratory animals and with standards set forth in the Guide for the Care and Use of Laboratory Animals and the Animal Welfare Act.

The Laboratory Animal Science Center at Boston University Medical Center has been accredited by the Americar Association for Accreditation of Laboratory Animal Care since 1971. Boston University Medical Center has had an Animal Welfare Assurance on file with the Office for Protection from Research Risks (OPRR) since January 1, 1986. Boston University's Animal Welfare Assurance number is A-3316-01.

Animal protocols may be approved for up to three years. However, if the study extends beyond one year from the approval date, an annual continuation form (1 page) must be submitted. If a project is to extend beyond three years, a full application must be resubmitted and reviewed at the end of the initial three year period.

Sincerely,

Colleen A. Cody, Coordinator
Institutional Animal Care and Use Committee

c: Wayne W. LaMorte, M.D., Ph.D., M.P.H. Chairman, IACUC
Veterinary Staff, LASC

APPENDICES:

A. Predominant Integrin Ligands Expressed by Osteoblasts Show Preferential Regulation in Response to both Cell Adhesion and Mechanical Perturbation. J. Cellular Biochem. 84:497-508 (2002)

B. Induction of a Neoarthrosis by Precisely Controlled Motion in an Experimental Mid-Femoral Defect. J. Orthopaedic Res. 20: 579-586 (2002)

C. Mechanobiologically directed skeletal regeneration: Induced differentiation of cartilage, collagen type II and GDF-5 expression, and modified matrix architecture. Submitted for the 48th Annual Meeting of the Orthopaedic Research Society.

D. The role of Angiogenesis in a murine tibial model of distraction osteogenesis. Submitted for the 48th Annual Meeting of the Orthopaedic Research Society.

E. Selective Adhesion of Osteoblasts to Different Integrin Ligands will Induce Osteopontin Gene Expression. (Submitted, Matrix Biology)

F. The Role of the Local Mechanical Environment on Tissue Differentiation During Skeletal Defect Repair (Manuscript)

Journal of Cellular Biochemistry 84:497–508 (2002)

Predominant Integrin Ligands Expressed by Osteoblasts Show Preferential Regulation in Response to Both Cell Adhesion and Mechanical Perturbation

R.S. Carvalho,[1,2] A. Bumann,[3] J.L. Schaffer,[4] and L.C. Gerstenfeld[1]*

[1]Orthopaedic Research Laboratory, Department of Orthopaedic Surgery, Boston University Medical Center, 715 Albany Street, R-205, Boston, Massachusetts 02118-2526
[2]Department of Orthodontics, School of Dental Medicine, Boston University, 100 East Newton St., Boston, Massachusetts 02118
[3]Department of Experimental Dentistry, Free University, D-14197, Berlin, Germany
[4]Department of Orthopaedic Surgery, The Cleveland Clinic, 9500 Euclid Avenue, Desk A-41, Cleveland, Ohio 44195

Abstract Previous studies have demonstrated that both mechanical perturbation and cell adhesion induced the expression of osteopontin (*opn*) by osteoblasts (Carvalho et al. [1998] J. Cell. Biochem. 70:376–390). The present study examined if these same stimuli on osteoblasts would induce the expression of other integrin binding proteins, specifically fibronectin (*fn*) and bone sialoprotein (*bsp*). All three genes showed three- to four-fold maximal induction in response to both cell adhesion and a single 2-h period of an applied spatially uniform, dynamic biaxial strain of 1.3% at 0.25 Hz. Each gene, however, responded with a different time course of induction to mechanical strain, with *bsp*, *fn*, and *opn* showing their maximal response at 1, 3, and 9 h, respectively, after the perturbation period. In contrast, peak induction to cell adhesion was observed at 24 h for *bsp* and *opn*, while *fn* levels peaked at 8 h. Interestingly, while both *opn* and *fn* mRNA expression returned to base line after cell adhesion, *bsp* mRNA levels remained elevated. Examination of collagen type I and osteocalcin mRNAs showed unaltered levels of expression in response to either type of perturbation. A common feature of the signal transduction pathways, which mediate the gene expression in response to both cell adhesion and mechanical perturbation, was the activation of specific tyrosine kinases based on the ablation of the induction of these genes by the tyrosine kinase inhibitor genistein. While cycloheximide blocked the induction of all three mRNAs in response cell adhesion, it failed to block the induction of any of these genes in response to mechanical perturbation. Such results suggest that the induction of these genes after mechanical perturbation was mediated by an immediate response to signal transduction, while cell adhesion mediated effects secondary to signal transduction. Depolymerization of microfilaments with cytochalasin D had no effect on the overall expression of any of these genes in response to cell adhesion and only blocked the induction of *opn* expression in response to mechanical perturbation. These results suggest that cytoskeletal integrity is only selectively important in the signal transduction of certain types of stimuli and for the regulation of certain genes. In summary, both mechanical perturbation and cell adhesion stimulated the expression of integrin binding proteins. Furthermore, while there are common features in the signal transduction processes that mediate the induction of these genes in response to both stimuli, specific genes are separately regulated by precise mechanisms that are unique to both forms of stimuli. J. Cell. Biochem. 84: 497–508, 2002.

Key words: integrin; osteopontin; osteoblasts; mechanical stimulation

The mediation of cellular responses to mechanical stimuli depends in part on the recognition and interaction of selected cell-surface receptors with the extracellular matrix (ECM). Integrins are one class of cell surface receptors that mediate cell adhesion to the ECM. The integrins are a family of heterodimeric membrane receptors composed of multiple α and β isotypes. Variations in the extracellular

Grant sponsor: The Department of Defense, Bone Health and Military Readiness Program; Grant number: DAMD17-98-1-8510.

*Correspondence to: L.C. Gerstenfeld, Ph.D., Department of Orthopaedic Surgery, Orthopaedic Research Laboratory, Boston University Medical Center, 715 Albany Street, R-205, Boston, MA 02118. E-mail: lgersten@bu.edu

Received 21 March 2001; Accepted 4 September 2001

Published online December 4, 2001.
DOI 10.1002/jcb.10021

domains of the individual isotypes of integrin receptors impart their specificity for unique ECM proteins [Hynes, 1992; Miyauchi et al., 1995]. The interaction of many integrin isotypes with their specific ligands is mediated by their recognition of the amino acid sequence, arginine–glycine–aspartic acid–serine (RGDS) [Hynes, 1992]. It has been demonstrated that the binding of specific adhesion proteins to their integrin receptors generates a cascade of intracellular signals that are responsible for the regulation of a wide variety of cellular responses [Damsky and Werb, 1992; Juliano and Haskill, 1993]. Such interactions facilitate the appropriate functioning of essential cell functions such as cell adhesion, cell migration, and survival of many cell types. These many functions are in turn mediated through integrin receptor activation of specific signal transduction mechanisms or by their mediation of structural alterations in the cytoskeletal architecture of cells [Juliano and Haskill, 1993].

In bone tissue, osteoblasts express high levels of several different RGD-containing proteins, the most predominant being osteopontin (*opn*), bone sialoprotein (*bsp*), and fibronectin (*fn*) [Puleo and Bizios, 1992; Gotoh et al., 1995; Winnard et al., 1995]. Osteopontin has been shown to interact with both osteoblasts and osteoclasts [Oldberg et al., 1988; Gotoh et al., 1990; Ross et al., 1993], and it is thought to play a role in mediating osteoclast resorption of bone tissue [Reinholt et al., 1990; Denhart and Guo, 1993]. The expression of *opn* is seen concurrently with alkaline phosphatase, and it has been identified as an early marker of osteoblast differentiation [Gerstenfeld et al., 1990]. Bone sialoprotein is another specific integrin ligand that is expressed by osteoblasts. It has a very restricted expression to only cells within the skeletal lineage and is seen predominantly in areas of mineralized growth cartilage and osteoid [Chen et al., 1994; Yang and Gerstenfeld, 1996, 1997]. Bone sialoprotein has been shown to initiate calcification through its binding properties to collagen, calcium, and hydroxyapatite [Hunter and Goldberg, 1994]. Unlike the former two proteins, fibronectin is expressed ubiquitously in most connective tissues. However, this protein appears to play an important role in the mechanisms of cell attachment, spreading, and migration during early osteoblast differentiation [Curtis, 1987; Winnard et al., 1995]. In addition to the RGDS peptide, fibronectin contains a synergistic adhesion site to the RGD sequence. It also contains two adhesion sites in the type III connecting segment of the whole molecule, the CS1 portion and the arginine–glutamic acid–aspartic acid–valine (REDV) sequence within the CS5 portion of fibronectin [Puleo and Bizios, 1992]. Some studies suggest that fibronectin also acts as an activator of cell adhesion rather than as a direct adhesion molecule [Curtis et al., 1992]. Thus fibronectin may mediate multiple interactions and responses by cells. Currently, there is a large body of data to suggest that the RGD-containing proteins *opn*, *bsp*, and *fn* play essential roles in the cellular differentiation and migration of osteoblasts during skeletal growth and/or in the initiation of spatial deposition of mineral in the ECM [Curtis et al., 1992; Hunter and Goldberg, 1993; Gerstenfeld et al., 1995; Schaffer et al., 1996].

Previous studies have shown that both the mechanical environment of osteoblasts and cell adhesion induce *opn* gene expression [Toma et al., 1997; Carvalho et al., 1998]. These studies suggest that the interactions of cells with the ECM are integral components to the mediation of these stimuli. However, cellular perturbation through receptors may occur both through the occupancy of the receptor as well as the deformation through the engagement of the receptors with matrix attachment [Miyauchi et al., 1995]. Furthermore, it has been shown that precise reverse phosphorylation of specific proteins appears to regulate various intracellular pathways exclusively upon cellular attachment [Guan et al., 1991]. These results raise the possibility that signal transduction may be dependent on the matrix composition and that the cellular matrix components themselves may function as autocrine factors that regulate their own expression [Gerstenfeld, 1999]. Mechanical perturbation through receptor deformation and stimuli through receptor-ligation then may share overlapping molecular elements that mediate intracellular signal transduction and lead to common genomic responses. Such modulations may also involve cytoskeletal integrity and its relation with the integrin receptors. It has been hypothesized that cellular shape changes determine signal transduction pathways through the direct deformation of cellular membranes and reorientation of the microfilament network, thereby affecting integrin behavior [Ingber, 1991].

In previous studies from our laboratory, we have shown that the continuous application of a dynamic, spatially uniform biaxial mechanical perturbation to osteoblasts leads to cytoskeletal rearrangement as well as changes in the ECM composition cellular response [Meazzini et al., 1998]. Other studies have shown that mechanical strain in cells of osteoblastic lineage only showed increased DNA synthesis when the cells were attached to specific ligands such as fibronectin [Wilson et al., 1995]. Thus, it seems that mechanical perturbation leads to both physical alteration of ECM proteins and alterations in cellular architecture, which suggests that cells reach a homeostatic balance that is regulated through a complex set of receptor-mediated interactions between the cells and the ECM proteins. In this study we examined if genes such as *opn*, *bsp*, and *fn*, which specifically interact with integrins, would be commonly induced following either mechanical perturbation and/or cell-ligand binding. It was further examined if there are common signal transduction pathways by which the expression of these proteins were modified following cellular attachment or mechanical perturbation, and if these pathways are unique or have overlapping mechanisms.

MATERIALS AND METHODS

Materials

All tissue culture supplies, cytochalasin D, colchicine, and cycloheximide were from Sigma Chemical Company (St. Louis, MO). H89 genistein was from LC Laboratories (Woburn, MA). Nylon membranes for Northern blots were from Biotrans, ICN Corp. (Aurora, OH).

Cell Culture

Seventeen-day embryonic chicken calvaria osteoblasts were isolated and grown in culture as previously described [Gerstenfeld et al., 1988]. These cells were plated at a density of 2×10^6 cells in 100-mm tissue culture dishes either left uncoated or coated with purified fibronectin (1 mg/ml) as previously described [Schaffer et al., 1994]. Cultures were grown for 2 weeks until they reached confluence in minimum essential media supplemented with 10% fetal bovine serum (FBS). The medium was changed to BGJ_b supplemented with 10% FBS with the addition of 10 mM β-glycerophosphate and 12.5 μg/ml ascorbic acid. All analyses were performed on at least three separate preparations of cells, and all data are presented as a percent increase in expression over that of the controls which were determined from parallel cultures grown under identical conditions. All error bars represent the standard deviation (SD) of the determinations from separate experiments and the number of replicates that were used for each measurement is denoted in each figure.

Mechanical Perturbation/Attachment Assays

The mechanical stretch apparatus used for these experiments was as previously described [Schaffer et al., 1994]. The design of the device imposes a verified temporal and spatial displacement profile to an optically transparent elastomeric membrane in which the strain magnitude was experimentally demonstrated to be homogeneous and isotropic (i.e., radial strain = circumferential strain = constant over the culture surface) [Schaffer et al., 1994]. A polyurethane membrane (a generous gift from Dow Chemical Corporation, Midland, MI) was used in the culture dishes allowing for a constant 1.3% uniform biaxial strain at 0.25 Hz to be applied for a single 2 h period. For each experiment, non-stimulated controls were performed on identical culture surfaces at the same time and from the same preparation of cells grown at identical conditions as the mechanically stimulated cultures. In all experiments for mechanical stretch (perturbation), determinations were carried out 6 h after the end of the 2 h period of active cellular perturbation. For the attachment/integrin ligation assays, the cells were allowed to attach to fibronectin coated (1 mg/ml) dishes at the same concentration as those of mechanical stimulated cultures for 24 h. Fibronectin served as the basic ligand and uncoated plastic plates as controls.

Signal Transduction Studies

Signal transduction pathways that mediate the cell responses of the mechanical perturbation and/or attachment/ligation were investigated by the use of specific chemical inhibitors. The final concentration for each of these compounds was: 50 mM cycloheximide, 20 mg/ml genistein, 1 μM H89 (Sigma), 50 μM cytochalasin D (Sigma), and 1 μM colchicine (Sigma). Cycloheximide and genistein were incubated for 30 min, while cytochalasin D was incubated for

1 h and colchicine for 6 h. Controls were separately determined for each compound in cultures treated identically with the various compounds but in which the cells were either not mechanically stimulated or were attached to uncoated dishes.

Isolation and Analysis of RNA

Total RNA was isolated using tri-Reagent™ (Molecular Center, Cincinati, OH) according to the manufacturer's instructions. RNA was resolved on 1% agarose gels containing 2.2 M formaldehyde [Toma et al., 1997] and 5 mg of total RNA was loaded per gel per lane. Chicken cDNAs used for these studies were pro α1[I] collagen [Lehrach et al., 1979], osteocalcin [Neugebauer et al., 1995], *opn* [Moore et al., 1991], and *bsp* [Yang et al., 1995]. Northern blots with ^{32}P cDNA-labeled probes were carried out at 65°C in 2.5 × SSC, 50 mM Na-phosphate buffer, 100 μg/ml single stranded salmon sperm DNA, and for 18–24 h in a rotating hybridization oven (Robins Scientific, Sunnyvale, CA). Autoradiograms were quantified using an LKB Ultra II scanning densitometer (LKB, Broma, Sweden), and values were normalized against 18S ribosomal RNA obtained by hybridization of each blot to a conserved nucleotide sequence probe of 18S ribosomal subunit (Ambion Corp., Austin, TX). All analyses were performed at least three times, and all data are presented as a percentage in expression over that of the control, which were determined from parallel cultures. All data were evaluated as a mean ± 2 standard deviations with a minimum of three experiments from different populations of primary cells, and appropriate statistical analysis were performed.

RESULTS

Osteoblast-Adhesion and Mechanical Perturbation Increase Levels of RGD-Containing Proteins

Initial studies were carried out to assess the expression of mRNA levels for *opn*, *bsp*, and *fn* osteoblasts following either cell adhesion or mechanical perturbation. Fibronectin was used as the adhesion substrate in these experiments. The temporal profiles of *opn* expression were shown to peak at 24 h. This induction was three- to four-fold above that of control samples. At time periods beyond 24 h, there was a sharp reduction in *opn* expression, which returned to its baseline levels of expression (Fig. 1). Bone sialoprotein expression followed a similar profile to that seen for *opn* also peaking at 24 h (three-fold). However, there was no marked decrease in the expression of *bsp*, which remained elevated (two-fold) at 48 h and even 72 h (Fig. 2). In contrast, the expression of *fn* mRNA started at significantly higher levels when compared to the other two mRNAs (Fig. 3). Expression of *fn* peaked at 8 h from the onset of the perturbation (two-fold) and showed a sharp reduction to its baseline levels soon thereafter.

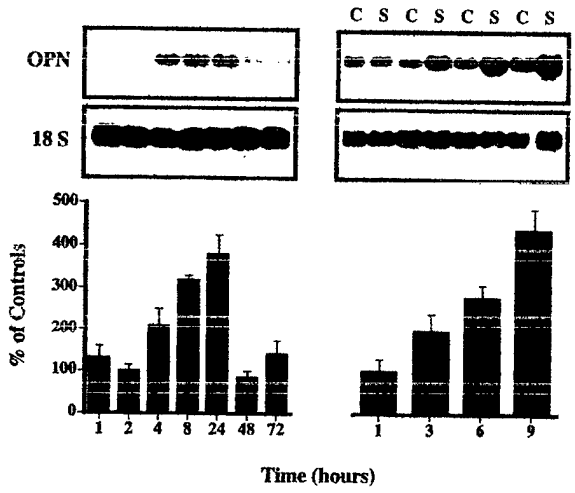

Fig. 1. Effect of cell adhesion and mechanical perturbation on the temporal expression of osteopontin (*opn*) mRNA expression by osteoblasts. Northern blot analysis of *opn* mRNA expression following cell adhesion of osteoblasts to fibronectin is seen on the left and that of induction in response to mechanical perturbation is seen on the right. The expression of the 18S rRNA is seen in the lower panel of each figure. The graphic representation of the temporal expression for the mRNA levels is shown for 1, 2, 4, 8, 24, 48, and 72 h after an initial 24-h period of attachment relative to the control samples at identical times. The graphic representation of the temporal expression for the mRNA levels is shown for 1, 3, 6, and 9 h post-mechanical perturbation. Controls = C and strained samples = S. All data are presented as percent induction of expression of the mRNAs relative to their control samples. Error bars are the SD determined from at least three experiments.

The expression of these mRNAs was then examined after the application of mechanical perturbation. As expected, mechanical perturbation of osteoblasts increased *opn* expression by two to threefold, peaking at 9 h post-stretch (Fig. 1). This clearly contrasted with adhesion, which showed a peak induction in *opn* expression at 24 h. In the case of *fn*, mechanical perturbation also showed an increase in expression peaking at 3 and 6 h from the onset of the perturbation (Fig. 3). It is interesting to note, however, that mechanical perturbation was

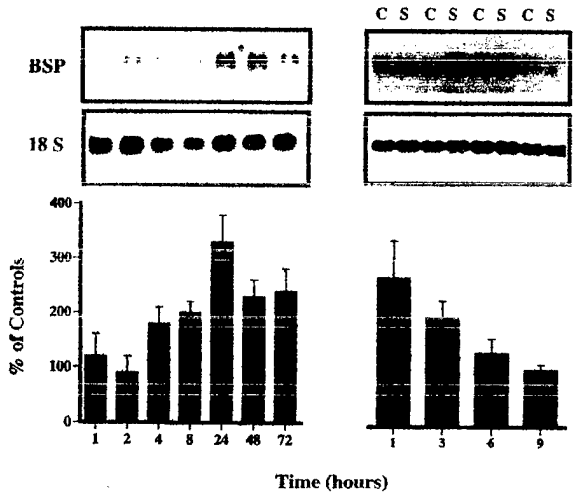

Fig. 2. Effect of cell adhesion and mechanical perturbation on the temporal expression of *bsp* mRNA expression by osteoblasts. Northern blot analysis of bone sialoprotein mRNA expression following cell adhesion of osteoblasts to fibronectin is seen on the left and that of induction in response to mechanical perturbation is seen on the right. The expression of the 18S rRNA is seen in the lower panel of each figure. The graphic representation of the temporal expression for the mRNA levels is shown for 1, 2, 4, 8, 24, 48, and 72 h after an initial 24-h period of attachment relative to the control samples at identical times. The graphic representation of the temporal expression for the mRNA levels is shown for 1, 3, 6, and 9 h post-mechanical perturbation. Controls = C and strained samples = S. All data are presented as percent induction of expression of the mRNAs relative to their control samples. Error bars are the SD determined from at least three experiments.

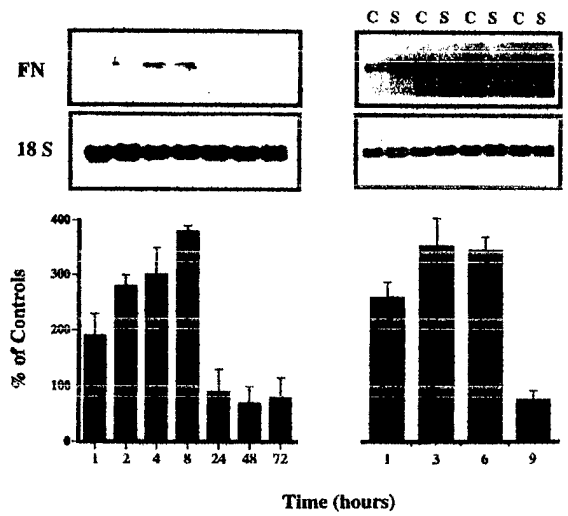

Fig. 3. Effect of cell adhesion and mechanical perturbation on the temporal expression of *fn* mRNA expression by osteoblasts. Northern blot analysis of fibronectin mRNA expression following cell adhesion of osteoblasts to fibronectin is seen in the left and that of induction in response to mechanical perturbation is seen on the right. The expression of the 18S rRNA is seen in the lower panel of each figure. The graphic representation of the temporal expression for the mRNA levels is shown for 1, 2, 4, 8, 24, 48, and 72 h after an initial 24-h period of attachment relative to the control samples at identical times. The graphic representation of the temporal expression for the mRNA levels is shown for 1, 3, 6, and 9 h post-mechanical perturbation. Controls = C and strained samples = S. All data are presented as percent induction of expression of the mRNAs relative to their control samples. Error bars are the SD determined from at least three experiments.

inhibitory for *bsp* expression. In Figure 2, *bsp* levels started at twofold of control samples at 1 h post-stretch and quickly decreased to baseline levels at 9 h post-stretch.

These results would suggest that integrin binding-ECM molecules are selectively responsive to perturbation via either mechanical perturbation or cell adhesion-mediated signal transduction. Two other prevalent ECM genes, collagen type I and osteocalcin, were then examined as a comparison to these RGD containing integrin ligands. Both collagen type I (*col1*) and osteocalcin (*oc*) mRNAs were examined after mechanical perturbation. Interestingly, neither of these genes showed alterations in their expression when the cells were subjected to mechanical perturbation (Fig. 4).

Different Matrix Proteins Require Different Signal Transduction Pathways Following Cell Adhesion

In order to further understand if common signal transduction processes mediated the

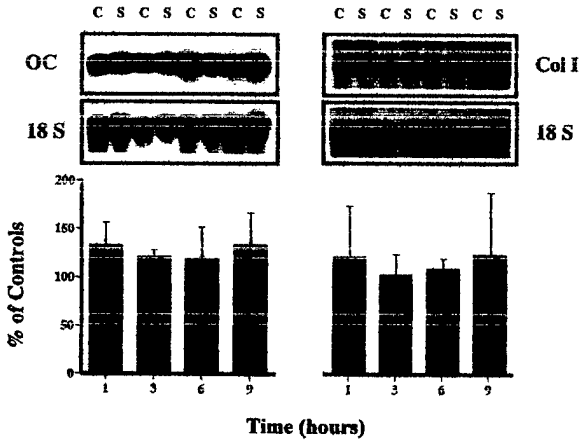

Fig. 4. Effect of mechanical perturbation on the temporal expression of *col1* and *oc* mRNA expression by osteoblasts. Northern blot analysis of osteocalcin and collagen type I mRNA expression following mechanical perturbation of osteoblasts are denoted in the figure. The graphic representation of the temporal expression for these mRNAs is shown by the times of 1, 3, 6, and 9 h post-perturbation. All the panels show the percent induction of expression of the steady mRNA levels relative to their control samples. Controls = C and strained samples = S. Error bars are the SD determined from at least three experiments.

induction of the three RGD integrin ligand genes, pharmacological inhibitors of specific signal transduction pathways were used. From the slow increase in *opn* levels following cell adhesion, it appears that this protein is involved in a secondary, down-stream event to other genomic changes. Indeed, the compound cycloheximide, a known inhibitor of de novo protein synthesis, blocked the induction of *opn* mRNA expression following adhesion to fibronectin (Fig. 5). Cycloheximide also inhibited the expression levels of *fn* and *bsp* genes (Figs. 6 and 7), showing that these genes were also dependent on new protein synthesis following cellular adhesion. Even though the maximum levels of *fn* occurred at 9 h post cellular adhesion, this finding was consistent with the relative long period for maximum induction of *opn* and *bsp* (Figs. 1–3).

Previous observations had shown that changes in *opn* mRNA expression in response to mechanical perturbation were dependent on the integrity of the microfilament structure of the cell [Toma et al., 1997]. This finding is consistent to the results seen in this study (Fig. 5). The role of the cytoskeleton in the signal transduction pathways for each of these mRNAs was examined in these studies. Incubation of the osteoblast cultures with the microtubule depolymerizing agent colchicine did not affect the expression of any of the mRNAs (Figs. 5–7). However, cultures treated with cytochalsin-D, a microfilament disruption agent, inhibited the levels of *opn* mRNA below those of control levels (Fig. 5), following mechanical perturbation. This change was not seen for either *bsp* or *fn* mRNAs (Figs. 6 and 7).

Finally, specific inhibitors for second messenger systems were used. The use of genistein, a potent inhibitor of tyrosine kinase phosphorylation, was shown to significantly inhibit the expression of *opn*, *bsp*, and *fn* mRNAs. As shown in Figure 5, this finding has also been observed previously for *opn* expression in mechanically stimulated cells [Toma et al., 1997; Carvalho et al., 1998]. Genistein treatment in cells subjected to mechanical perturbation also inhibited the levels of *fn* and *bsp* mRNAs (Figs. 6 and 7). The pharmacological inhibitor of PKA-like kinases, H-89, also caused an

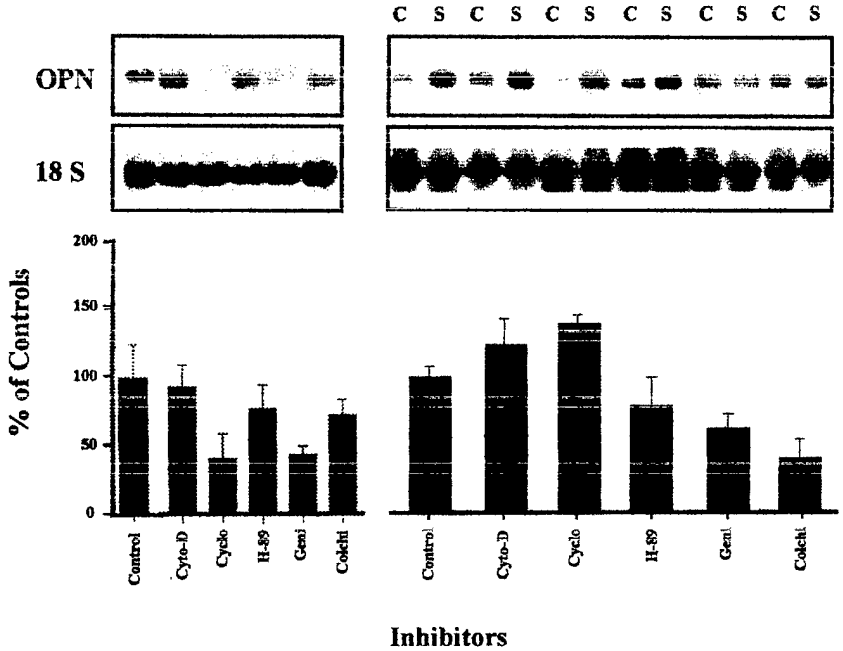

Fig. 5. Effect of pharmacological inhibitors on the mRNA expression of *opn* by osteoblasts in response to cell adhesion and mechanical perturbation. Effects of various second messenger inhibitors and cytoskeletal disrupters on the expression of *opn* mRNA in response to cell adhesion and mechanical perturbation were examined. Cells were treated with the microfilament depolymerizing agent cytochalasin-D (Cyto-D), the microtubule disrupting agent colchicine (Colchi), the protein synthesis inhibitor cycloheximide (Cyclo), the PKA inhibitor H-89 (H-89), and the tyrosine kinase inhibitor genistein (Geni). Autoradiographs for the Northern blot analysis of the steady state levels of each mRNA and of the 18S RNA are presented separately. Graphic analysis shows the percent induction or inhibition of the various mRNAs compared to that of controls. Error bars are the SD of three experiments.

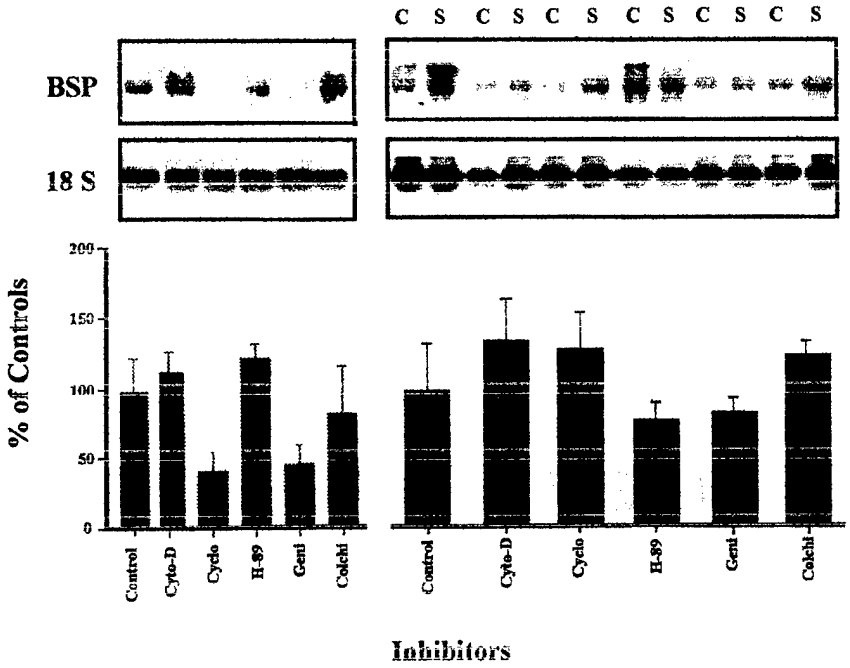

Fig. 6. Effect of pharmacological inhibitors on the mRNA expression of *bsp* by osteoblasts in response to cell adhesion and mechanical perturbation. Effects of various second messenger inhibitors and cytoskeletal disrupters on the expression of *bsp* mRNA in response to cell adhesion and mechanical perturbation were examined. Cells were treated with the microfilament depolymerizing agent cytochalasin-D (Cyto-D), the microtubule disrupting agent colchicine (Colchi), the protein synthesis inhibitor cycloheximide (Cyclo), the PKA inhibitor H-89 (H-89), and the tyrosine kinase inhibitor genistein (Geni). Autoradiographs for the Northern blot analysis of the steady state levels of each mRNA and of the 18 S RNA are presented separately. Graphic analysis shows the percent induction or inhibition of the various mRNAs compared to that of controls. Error bars are the SD of three experiments.

inhibition of *fn* levels, but it did not effect the expression of *opn* or *bsp* following cell adhesion. However, when H-89 was given to cells that had undergone mechanical perturbation, the expression of both *bsp* and *opn* mRNAs were inhibited, but not that of *fn* mRNA (Figs. 5–7). These findings suggest that the perturbation in expression of the RGD-containing extracellular proteins, which are studied here in response to cell adhesion, is distinct from that of mechanical perturbation, yet both responses appear to be uniquely dependent on the activation of specific subsets of kinases.

DISCUSSION

In previous studies, we have shown that both mechanical perturbation and cell adhesion led to the induction of increased *opn* expression. While both types of stimuli were dependent on integrin receptors, each of them was mediated by a specific set of intracellular signals that were distinct for each type of perturbation [Carvalho et al., 1998]. The present study provides further evidence that both cellular adhesion and mechanical perturbation lead to the selective induction of multiple integrin binding proteins within osteoblasts. Furthermore, while these data suggest that there may be some common mechanisms of signal transduction that stimulate the increased expression of these genes, each of the genes was uniquely and separately regulated by both stimuli (Table I).

In the bone extracellular matrix, RGD-containing glycoproteins including *opn*, *bsp*, and *fn* are presumed to interact with cell adhesion receptors (integrins) on the surface of the bone cells [Grzesik and Robey, 1994]. Studies suggest that that these extracellular components directly affect gene expression [Pienta et al., 1991], which takes place following mechanical perturbation [Resnick et al., 1993; Toma et al., 1997; Carvalho et al., 1998]. When considering adhesion separately from mechanical perturbation, one needs to take into account the effects of the former over the latter, as it may be speculated then that adhesion or integrin-ligation acts as a "primer" prior to any response due to the mechanical perturbation. In particular, it is interesting to note that the effects of the dynamic,

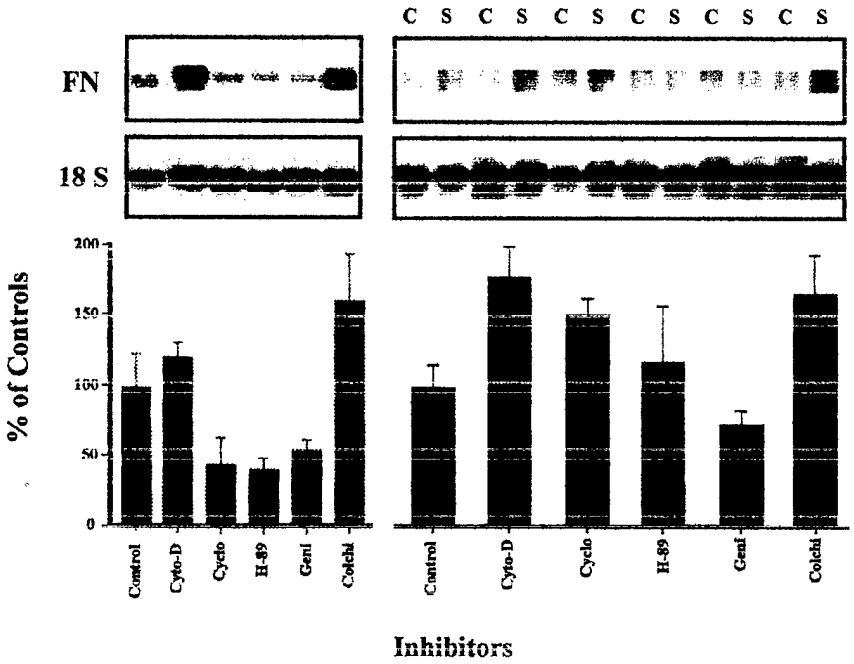

Fig. 7. Effect of pharmacological inhibitors on the mRNA expression of *fn* by osteoblasts in response to cell adhesion and mechanical perturbation. Effects of various second messenger inhibitors and cytoskeletal disrupters on the expression of *fn* mRNA in response to cell adhesion and mechanical perturbation were examined. Cells were treated with the microfilament depolymerizing agent cytochalasin-D (Cyto D), the microtubule disrupting agent colchicine (Colchi), the protein synthesis inhibitor cycloheximide (Cyclo), the PKA inhibitor H-89 (H-89), and the tyrosine kinase inhibitor genistein (Geni). Autoradiographs for the Northern blot analysis of the steady state levels of each mRNA and of the 18S RNA are presented separately. Graphic analysis shows the percent induction or inhibition of the various mRNAs compared to that of controls. Error bars are the SD of three experiments.

spatially uniform mechanical perturbation on cells that are in the process of adhesion enhances the formation of new receptor-ligand bonds. In studies by Kuo et al. [1977], mechanical perturbation was shown to alter the kinetic regulation of cell adhesion, thus interfering with binding rate. However, once the cells are adherent, specific RGD tri-peptides inhibited both adhesion and mechanical perturbation responses [Carvalho et al., 1998]. Wilson et al. [1995] also presented evidence that RGD peptides, fibronectin, and certain integrin antibodies disrupted integrin-ligand interaction, which in turn ablated strain induced mechanotransduction responses, without disrupting adhesion of the same cells.

It has been proposed that receptors such as integrins can behave as a homeostatic system for modulating the ECM structure and organization in response to the structural needs of the

TABLE I. Comparison of Signal Transduction Pathways for the mRNA Expression of Osteopontin (*opn*), Bone Sialoprotein (*bsp*), and Fibronectin (*fn*) Between Cell Adhesion and Mechanical Stretching

	Genes					
	opn		*bsp*		*fn*	
Perturbation	Adhesion	Stretch	Adhesion	Stretch	Adhesion	Stretch
Time after peak expression (h)	24	9	24	1	8	3
De novo protein synthesis	Yes	No	Yes	No	Yes	No
Tyrosine kinase-mediated	Yes	Yes	Yes	Yes	Yes	Yes
PKA-mediated	No	Yes	No	Yes	Yes	No
Requires microfilaments	No	Yes	No	No	No	No
Requires microtubules	Yes	No	No	No	No	No

cell [Werb et al., 1989; Gerstenfeld, 1999]. In this context, it is interesting to note that the mechanical forces that are applied to tissues should be structurally deformed at their anchorage points to the extracellular matrix. These sites should be the focal points at which mechanical strains are specifically transmitted to the cells. The strains to which a cell is subjected, therefore, will be effected by both the compositional properties of the matrix and the receptors on the surfaces of the cells, which can interact with these ECM proteins. The importance of extracellular interactions for the process of mechanosensation has been shown by Du et al. [1996]. They demonstrated in their experiments that isolated genes of the touch receptor neurons in *C. elegans* encoded for extracellular proteins. These authors [Du et al., 1996] further hypothesized that the ECM mediates the anchoring properties of specialized cells, enabling their mechanosensory response.

Concerning the intercellular components of mechanosignal transduction, both Davies and Tripathi [1993] and Ingber [1997] have suggested that the transduction of mechanical stimuli in anchorage-dependent cells is due to a combination of signal transduction processes via the cytoskeleton through integrin receptors that interact with the cytoskeleton, as well as through biochemical signals. In order for mechanosignal transduction to occur through the cytoskeleton, it is necessary that cooperative interactions occur between the three component parts of cytoskeleton: the micofilaments, intermediate filaments, and microtubles. Studies of osteoblasts have also shown that the cytoskeleton changes both its structural architecture and its composition in response to mechanical perturbation [Meazzini et al., 1998]. However, signal transduction of different types of signals may not depend on the integrity of all of these structural elements. In this study, this is shown by following the selective inhibition of microtubules and microfilaments. The results presented in Figure 5 and Table I demonstrate that *opn*–cell adhesion dependent mRNA expression was inhibited following colchicine treatment, yet adhesion was not affected after the addition of cytochalasin-D. The inverse effect was seen when the cells were mechanically stimulated [Toma et al., 1997]. In contrast, alterations in cytoskeletal architecture via pharmacological manipulation did not change the expression of *bsp* or *fn* mRNAs in response to either mechanical perturbation or cell adhesion. These latter results suggest the involvement of microfilaments in the selective regulation of some genes but not others. Indeed, recent studies have shown that the induction of COX 2 enzyme expression within osteoblasts in response to fluid flow mediated shear stress was also regulated via alteration in the cells cytoskeletal architecture [Pavalko et al., 1998]. Such results suggest that there may be specific subsets of genes that are commonly regulated and are dependent on the cytoarchitecture of the cell, yet others may not be dependant on the cytoarchitecture, even though they are regulated by cell adhesion or mechanical perturbation.

This differentiation between mechanical perturbation and adhesion appears to follow unique mechanisms. Since each ECM ligand interacts with different integrins, it may be speculated that selective interactions or mediation of the various signals occur through specific integrin receptors. For instance, while $\alpha v\beta 3$ deficient cell populations were not capable of migrating in response to *opn*, these same cells did migrate significantly in response to fibronectin and vitronectin [Liaw et al., 1995]. Furthermore, specific ligand interactions may mediate a variety of intracellular signals ranging from ion flux to selective G-protein kinase and/or phosphatase activation. The transduction of the mechanosignal at the cellular membrane leads to a cascade of downstream signaling events, many of which are mediated by tyrosine kinases, which in turn phosphorylate other kinases [Berk et al., 1995]. Kinases that have been associated with mechanotransduction include mitogen-activated protein kinase (MAPK). MAPK activation has been shown to follow mechanical perturbation in cardiac cells [Yamazaki et al., 1993] and fluid flow in endothelial cells [Tseng and Berk, 1993]. It has been suggested that such responses are part of a multiplicity of pathways and might be grouped functionally into those that are either calcium-dependent or -independent [Berk et al., 1995; Ishida et al., 1997]. The presence of calcium is important for the activation of a putative shear stress receptor (membrane level), which regulates a pertussis toxin-sensitive G protein-coupled K + channel (SSR) [Ohno et al., 1993] and the enzyme phospholipase C [Nollert et al., 1990]. The levels of PIP2, in turn will be regulated by rho, a small GTP-binding protein [Chong et al., 1994]. The calcium-independent

pathway involves the activation of MAPK [Berk et al., 1995]; however, other calcium-independent tyrosine kinases such as src and FAK may also be involved in the shear stress transduction.

A common feature in the signal transduction processes that regulate the expression of all the integrin binding genes in response to either adhesion or mechanical perturbation was the inhibition of the induction of their expression by genistein. This suggests that a tyrosine kinase(s) is involved in the signal transduction, which stimulates the expression of all of these proteins. In contrast, PKA inhibition through H-89 treatment demonstrated a selective effect for *opn* and *bsp* in response to mechanical perturbation but not with cell adhesion (Figs. 5 and 6). As for *fn*, H-89 inhibited the effects of adhesion but not those of mechanical perturbation (Table I; Fig. 7). In the experiments reported herein, there were no changes in the non-RGD containing proteins collagen type I and osteocalcin (Fig. 4). Integrin receptors have been described as potential mediators of mechanical perturbation [Ingber et al., 1994; Ishida et al., 1997]. Activation of integrins has been shown to induce the tyrosine phosphorylation of FAK at focal adhesion complexes [Schaller et al., 1994]. In addition, other proteins within these focal adhesion contacts, such as paxillin and src, will also be phosphorylated when exposed to flow [Girard and Nehem, 1993; Bull et al., 1994]. Our laboratory has shown that FAK phosphorylation was regulated by mechanical perturbation [Toma et al., 1997], also suggesting that the disruption of microtubules does not affect the expression of any gene studied following mechanical perturbation. This is an interesting finding as it relates to MAPK, as this kinase has been shown as the earliest signal activated by flow at physiological stress [Tseng and Berk, 1993]. MAPK is also known as a microtubule-associated kinase [Sabe et al., 1994], suggesting a role in the cytoskeleton. However, as disruption of microtubules did not affect gene expression following perturbation, one may only speculate on the role of MAPK as a mechanical perturbation-dependent kinase. On the other hand, we have observed that adhesion alone in the presence of the microtubule-disrupting drug colchicine, blocked the induction of *opn* expression in particular. Thus, it is conceivable that MAPK plays a role in this mechanism, since this kinase has been shown to be activated by cell binding to fibronectin [Morino et al., 1995]. It has been suggested that activation of integrins is associated with the same signal events that occur when cells are exposed to flow [Vuori and Ruoslahti, 1993; Schwartz and Deninghoff, 1994; Berk et al., 1995]. However, further study is needed, as the complexity of such a response can not be understood if the responses of mechanical perturbation and adhesion are not taken into account individually.

Integrin-ligation is thought to stimulate the same signal events as mechanical perturbation [Berk et al., 1995]. Indeed, we have shown here that this is the case, even though the mechanisms that mediate both responses are uniquely different. If integrins are the mediators for mechanotransduction in both forms of activation, then there maybe several different integrin receptors acting in concert with other sensors that are specific to the mechanical activation. The dependency of mechanical perturbation effects on RGD-containing proteins in this study and the lack of response in either collagen type I or osteocalcin further demonstrate an active role of integrins in adhesion and perturbation. It is clear that integrins and focal contacts play important roles in mechanotransduction. It remains to be determined, however, how the mechanisms of adhesion cross talk with those of mechanical perturbation and which kinases and second signals are common in regulating downstream events prior to any activation in gene expression.

ACKNOWLEDGMENTS

The authors acknowledge the expert technical assistance of Irina Simkina in preparation and maintenance of the osteoblast cell cultures. We thank Becton Dickinson Labware and Dow Chemical Company for their generous support of this project. R.S.C. acknowledges the support of the American Association of Orthodontists Foundation.

REFERENCES

Berk BC, Corson MA, Peterson TE, Tseng H. 1995. Protein kinases as mediators of fluid shear stress stimulated signal transduction in endothelial cells: a hypothesis for calcium-dependent and calcium-independent events activated by flow. J Biomech 28:1439–1450.

Bull HA, Brickell PM, Dowd PM. 1994. Src-related protein tyrosine kinases are physically associated with the surface antigen CD36 in human dermal microvascular endothelial cells. FEBS Let 351:41–44.

Carvalho RS, Schaffer JL, Gerstenfeld LC. 1998. Osteoblast induction of osteopontin expression in response to cell attachment or mechanical perturbation shows common mediation through integrin receptors. J Cell Biochem 70:376–390.

Chen J, McKee MD, Nanci A, Sodek J. 1994. Bone sialoprotein mRNA expression and ultrastructural localization in fetal procine calvarial bone: comparisons with osteopontin. Histochem J 26:67–78.

Chong LD, Traynor-Kaplan A, Bokoch GM, Schwartz MA. 1994. The small GTP-binding protein Rho regulates a phosphatidylinositol 4-phosphate 5-kinase in mammalian cells. Cell 79:507–513.

Curtis ASG. 1987. Cell activation and adhesion. J Cell Sci 87:609–611.

Curtis ASG, McGrath M, Gasmi L. 1992. Localised application of an activating signal to a cell: experimental use of fibronectin bound to beads and the implications for mechanisms of adhesion. J Cell Sci 101:427–436.

Damsky CH, Werb Z. 1992. Signal transduction by integrin receptors for extracellular matrix: cooperative processing of extracellular information. Curr Opin Cell Biol 4:772–781.

Davies PF, Tripathi SC. 1993. Mechanical stress mechanisms and the cell: an endothelial paradigm. Circ Res 72:239–245.

Denhart DT, Guo X. 1993. Osteopontin: a protein with diverse functions. FASEB J 17:1476–1481.

Du H, Gu G, William CM, Chalfie M. 1996. Extracellular proteins needed for *C. elegans* mechanosensation. Neuron 16:183–194.

Gerstenfeld LC. 1999. Osteopontin in skeletal tissue homeostasis: an emerging picture of autocrine/paracrine functions of the extracellular matrix. J Bone Min Res 14:850–855.

Gerstenfeld LC, Chipman S, Kelly C, Lee DD, Landis WJ. 1988. Collagen expression, ultrastructural assembly, and mineralization in cultures of chicken embryo osteoblasts. J Cell Biol 106:979–989.

Gerstenfeld LC, Gotoh Y, Mckee MD, Nanci A, Landis WJ, Glimcher MJ. 1990. Expression and ultrastructural localization of the major phosphoprotein synthesized by chicken osteoblasts during in vitro mineralization. Anat Rec 228:93–103.

Gerstenfeld LC, Uporova T, Ashkar S, Salih E, Glimcher MJ. 1995. Regulation of avian osteopontin pre- and post-translational expression in skeletal tissues. Annals NY Acad Sci 270:67–82.

Girard PR, Nehem RM. 1993. Endothelial cell signalling and cytoskeletal changes in response to shear stress. Front Med Biol Eng 5:121–125.

Gotoh Y, Gerstenfeld LC, Glimcher MJ. 1990. Identification and characterization of the major chicken bone phosphoprotein. Analysis of its synthesis by cultured embryonic chick osteoblasts. Eur J Biochem 187:49–58.

Gotoh Y, Salih E, Glimcher MJ, Gerstenfeld LC. 1995. Characterization of the major non-collagenous proteins of chicken bone: identification of a novel 60 kDa non-collagenous phosphoprotein. Biochem Biophys Res Commun 208:863–870.

Grzesik W, Robey PG. 1994. Bone matrix RGD glycoproteins: immunolocalization and interaction with primary osteoblastic bone cells in vitro. J Bone Min Res 9:487–496.

Guan J-L, Trevithick JE, Hynes RO. 1991. Fibronectin/integrin interaction induces tyrosine phosphorylation of a 120-kDa protein. Cell Regul 2:951–964.

Hunter GK, Goldberg HA. 1993. Nucleation of hydroxyapatite by bone sialoprotein. Proc Natl Acad Sci USA 90:8562–8565.

Hunter GK, Goldberg HA. 1994. Modulation of crystal formation by bone phosphoproteins: role of glutamic acid-rich sequences in the nucleation of hydroxyapatite by bone sialoprotein. Biochem J 302:175–179.

Hynes RO. 1992. Integrins: versatility, modulation, and signaling in cell adhesion. Cell 69:11–25.

Ingber DE. 1991. Integrins as mechanochemical transducers. Curr Opin Cell Biol 3:841–848.

Ingber DE. 1997. Tensegrity: the architectural basis of cellular mechanotransduction. Ann Rev Physiol 59:575–599.

Ingber DE, Dike L, Hansen L, Karp S, Liley H. 1994. Cellular tensegrity: exploring how mechanical changes in the cytoskeleton regulated cell growth, migration, and tissue pattern during morphogenesis. Int Rev Cytol 150:173–224.

Ishida T, Takahashi M, Corson MA, Berk BC. 1997. Fluid shear stress-mediated signal transduction: how do endothelial cells transduce mechanical force into a biological response? Ann NY Acad Sci USA 811:12–23.

Juliano RL, Haskill S. 1993. Signal transduction from the extracellular matrix. J Cell Biol 120:577–585.

Kuo SC, Hammer DA, Lauffenburger DA. 1977. Simulation of detachment of specifically bound particles from surfaces by shear flow. Biophys J 73(1):517–531.

Lehrach H, Frischauf AM, Hanahan D, Wozney J, Fuller F, Boedtker H. 1979. Construction and characterization of pro alpha 1 collagen complementary deoxyribonucleic acid clones. Biophys J 73(1):517–531.

Liaw L, Skinner MP, Raines EW, Ross R, Cheresh DA, Schwartz SM, Giachelli CM. 1995. The adhesive and migratory effects of osteopontin are mediated via distinct cell surface integrins. J Clin Invest 95:713–724.

Meazzini MC, Schaffer JL, Toma CD, Gray ML, Gerstenfeld LC. 1998. Osteoblast cytoskeletal modulation in response to mechanical strain in vitro. J Orthop Res 16:170–180.

Miyauchi AJ, Alvarez JI, Greenfield EM, Teti A, Grano M, Colucci S, Zambonin-Zallone A, Ross FP, Teitelbaum SM, Cheresh D, Hruska KA. 1995. Recognition of osteopontin and related peptides by an avb3 integrin stimulates immediate cell signals in osteoclasts. J Biol Chem 266: 20369–20374.

Moore MA, Gotoh Y, Rafidi K, Gerstenfeld LC. 1991. Characterization of a cDNA for chicken osteopontin: expression during bone development, osteoblast differentiation, and tissue distribution. Biochemistry 30: 2501–2508.

Morino N, Mimura T, Hamasaki K, Tobe K, Ueki K, Kikuchi K, Takehara K, Kadowaki T, Yazaki Y, Nojima Y. 1995. Matrix/integrin interaction activates the mitogen activated protein kinase pp44*erk-1* and p42*erk-2*. J Biol Chem 270:269–273.

Neugebauer BM, Moore MA, Broess M, Gerstenfeld LC, Hauschka PV. 1995. Characterization of structural sequences in the chicken osteocalcin gene: expression of osteocalcin by maturing osteoblasts and by hypertrophic chondrocytes in vitro. J Bone Miner Res 10:157–163.

Nollert MU, Eskin SG, McIntire LV. 1990. Shear stress increases inositol trisphosphate levels in human endothelial cells. Biochem Biophys Res Commun 170: 281–287.

Ohno M, Cooke JP, Gibbons GH. 1993. Shear stress induced TCF-beta-1 gene transcription via a flow activated potassium channel. Circulation 88:103i.

Oldberg A, Franzen A, Heinegard D, Pierschbacher M, Ruoslahti E. 1988. Identification of a one sialoprotein receptor in osteosarcoma cells. J Biol Chem 263:19433–19436.

Pavalko FM, Chen NX, Turner CH, Burr DB, Atkinson S, Hsieh YF, Qiu J, Duncan RL. 1998. Fluid shear-induced mechanical signaling in MC3T3-E1 osteoblasts requires cytoskeleton-integrin interactions. Am J Physiol 275: C1591–C1601.

Pienta KJ, Murphy BC, getzenmber RH, Coffey DS. 1991. The effect of extracellular matrix interaction on morphologic transformation in vitro. Biochem Biophys Res Comm 179:333–339.

Puleo DA, Bizios R. 1992. Mechanisms of fibronectin-mediated attachment of osteoblasts to substrates in vitro. Bone Min 18:215–226.

Reinholt FP, Hultenby K, Oldberg A, Heinegard D. 1990. Osteopontin: possible anchor of osteoblasts to bone. Proc Natl Acad Sci USA 87:4473–4475.

Resnick NT, Collins W, Atkinson DT, Bonthron CF, Dewey CF, Gimbrone MA. 1993. Platelet-derived growth factor B chain promoter contains a cis-acting fluid shear stress-responsive element. Proc Natl Acad Sci USA 90:4591–4595.

Ross FP, Chappel J, Alvarez JI, Sander D, Butler WT, Farach-Carson MC, Mintz KA, Robey PG, Teitelbaum SL, Cheresh DA. 1993. Interaction between the bone matrix proteins osteopontin and bone sialoprotein and the osteoclast integrin alpha v beta 3 potentiate bone resorption. J Biol Chem 5:9901–9907.

Sabe H, Hata A, Okada M, Nakagawa H, Hanafusa H. 1994. Analysis of the binding of the src homology 2 domain of Csk to tyrosine-phosphorylated protein in the suppression and mitotic activation of c-Src. Proc Natl Acad Sci USA 91:3984–3988.

Schaffer JL, Rizen M, L'Italien GJ, Megerman J, Gerstenfeld LC, Gray ML. 1994. A Device for the application of a dynamic biaxially uniform and isotropic strain to a flexible cell culture membrane. J Orthop Res 12:709–719.

Schaffer JL, Toma CD, Meazzini MC, Gray ML, Gerstenfeld LC. 1996. Mechanical perturbation of osteopontin gene expression and its relationship to microfilament structure. In: Davidovitch Z, Norton L, editors. The biological mechanisms of tooth movement and cranial facial adaptation, Boston, MA: Harvard society for the advancement of orthodontics. p 113–121.

Schaller MD, Hildebrand JD, Dhannon JD, Fox JW, Vines RR, Parsons JT. 1994. Autophosphorylation of the focal adhesion kinase, pp125FAK, directs SH 2-dependent binding of pp60src. Mol Cell Biol 14:1680–1688.

Schwartz MA, Deninghoff K. 1994. αv Integrins mediate the rise in intracellular calcium in endothelial cells on fibronectin even though they may play a minor role in adhesion. J Biol Chem 269(11):133–137.

Toma CD, Ashkar S, Gray ML, Schaffer JL, Gerstenfeld LC. 1997. Mechano-induction of osteopontin expression in osteoblasts: dependency of signal transduction on microfilanment integrity. J Bone Min Res 12:1626–1636.

Tseng H, Berk BC. 1993. Fluid shear stress stimulates mitogen-activated protein kinase in bovine aortic endothelial cells. Circulation 88:1–184.

Vuori K, Ruoslahti E. 1993. Activation of protein kinase C precedes alpha 5 beta 1 integrin-mediated cell spreading to fibronectin. J Biol Chem 268:459–462.

Werb Z, Tremble PM, Behrendtsen O, Crowley E, Damsky CH. 1989. Signal transduction through the fibronectin receptor induces collagenase and stromelysin gene expression. J Cell Biol 109:877–889.

Wilson E, Sudhir K, Ives H. 1995. Mechanical strain of rat vascular smooth muscle cells is sensed by specific extracellular matrix/integrins interactions. J Clin Invest 96:2364–2372.

Winnard RG, Gerstenfeld LC, Toma C, Franceschi RT. 1995. Fibronectin gene expression synthesis and accumulation during in vitro differentiation of chicken osteoblasts. J Bone Min Res 12:1969–1977.

Yamazaki TK, Tobe E, Maemura K, Kaida T, Komuro I, Tamemoto H, Kadowaki T, Nagai R, Yazaki Y. 1993. Mechanical loading activates mitogen-activated protein kinase and S-6 peptide kinase in cultured rat cariac myocites. J Biol Chem 268:12069–12076.

Yang R, Gerstenfeld LC. 1996. Signal transduction pathways mediating parathyroid hormone perturbation of bone sialoprotein gene expression in osteoblasts. J Biol Chem 271:29839–29846.

Yang R, Gerstenfeld LC. 1997. Structural analysis and characterization of tissue and hormonal responsive expression of the avian bone sialoprotein (*BSP*) gene. J Cellular Biochem 64:77–93.

Yang R, Gotoh Y, Moore MA, Rafidi K, Gerstenfeld LC. 1995. Characterization of an avian bone sialoprotein (*bsp*) cDNA. Comparisons to mammalian *BSP* and identification of conserved structural domains. J Bone Miner Res 10:632–640.

ELSEVIER

Journal of Orthopaedic Research 20 (2002) 579–586

Journal of Orthopaedic Research

www.elsevier.com/locate/orthres

Induction of a neoarthrosis by precisely controlled motion in an experimental mid-femoral defect

Dennis M. Cullinane [a,b], Amy Fredrick [a,b], Solomon R. Eisenberg [b], Donna Pacicca [a], Michael V. Elman [a], Cassandra Lee [a], Kristy Salisbury [a], Louis C. Gerstenfeld [a], Thomas A. Einhorn [a,*]

[a] *Musculoskeletal Research Laboratory, Department of Orthopaedic Surgery, Boston University Medical Center, Boston, MA, USA*
[b] *Department of Biomedical Engineering, Boston University School of Engineering, Boston, MA, USA*

Received 14 February 2001; accepted 8 August 2001

Abstract

Bone regeneration during fracture healing has been demonstrated repeatedly, yet the regeneration of articular cartilage and joints has not yet been achieved. It has been recognized however that the mechanical environment during fracture healing can be correlated to the contributions of either the endochondral or intramembranous processes of bone formation, and to resultant tissue architecture. Using this information, the goal of this study was to test the hypothesis that induced motion can directly regulate osteogenic and chondrogenic tissue formation in a rat mid-femoral bone defect and thereby influence the anatomical result. Sixteen male Sprague Dawley rats (400 ± 20 g) underwent production of a mid-diaphyseal, non-critical sized 3.0 mm segmental femoral defect with rigid external fixation using a custom designed four pin fixator. One group of eight animals represented the controls and underwent surgery and constant rigid fixation. In the treatment group the custom external fixator was used to introduce daily interfragmentary bending strain in the eight treatment animals (12° angular excursion), with a hypothetical symmetrical bending load centered within the gap. The eight animals in the treatment group received motion at 1.0 Hz, for 10 min a day, with a 3 days on, one day off loading protocol for the first two weeks, and 2 days on, one day off for the remaining three weeks. Data collection included histological and immunohistological identification of tissue types, and mean collagen fiber angles and angular conformity between individual fibers in superficial, intermediate, and deep zones within the cartilage. These parameters were compared between the treatment group, rat knee articular cartilage, and the control group as a structural outcome assessment. After 35 days the control animals demonstrated varying degrees of osseous union of the defect with some animals showing partial union. In every individual within the mechanical treatment group the defect completely failed to unite. Bony arcades developed in the experimental group, capping the termini of the bone segments on both sides of the defect in four out of six animals completing the study. These new structures were typically covered with cartilage, as identified by specific histological staining for Type II collagen and proteoglycans. The distribution of collagen within analogous superficial, intermediate, and deep zones of the newly formed cartilage tissue demonstrated preferred fiber angles consistent with those seen in articular cartilage. Although not resulting in complete joint development, these *neoarthroses* show that the induced motion selectively controlled the formation of cartilage and bone during fracture repair, and that it can be specifically directed. They further demonstrate that the spatial organization of molecular components within the newly formed tissue, at both microanatomical and gross levels, are influenced by their local mechanical environment, confirming previous theoretical models. © 2002 Orthopaedic Research Society. Published by Elsevier Science Ltd. All rights reserved.

Introduction

Joint diseases such as osteoarthritis or traumatic arthritis are characterized by the loss of articular cartilage and altered joint anatomy with resulting pain, incapacitation, and substantially lowered quality of life. While total joint arthroplasty is a successful treatment for these conditions, it is not a lasting solution for the young active person. Indeed, the repair of articular cartilage would be a major advance in the treatment of arthritic diseases. However, although bone regeneration during fracture healing has been demonstrated repeatedly, the regeneration of a joint structure and its articular cartilage remain elusive goals [7,8,12,24].

* Corresponding author. Tel.: +1-617-638-8435; fax: +1-617-638-8493.
E-mail address: thomas.einhorn@bmc.org (T.A. Einhorn).

PII: S0736-0266(01)00131-0

It has long been recognized though that the mechanical environment influences the formation of cartilage, bone, and resultant tissue architecture during skeletal healing and in response to normal activity. The mechanical environment has been implicated in the upregulation of cartilage matrix synthesis both experimentally [16,30] and as a result of exercise [28]. Moreover, the specific development of cartilage versus bone in healing fractures is related to the mechanical environment, a concept supported by theoretical models [2,4,6, 9,11,18,27].

Fracture repair involves the interaction of cells with their local mechanical environment in a cascade of molecular events, resulting in a repaired and remodeled fracture site [6,14,29]. A comparable series of interactive events also occurs in limb joint ontogeny [3,5,21,22]. Indeed, it has been demonstrated that the normal in vivo development of a joint depends on a relatively consistent mechanical load being applied [3,13,18–22]. Models of non-union have even been developed using manually applied mechanical stimulation [1]. Yet, despite the general understanding that the mechanical environment plays an important role in tissue development and repair, incorporation of mechanical stimulation into studies of cartilage and bone repair have been limited.

This study was undertaken as an empirical test of the hypothesis that precise mechanical stimulation, induced on a daily basis, can regulate osteogenic and chondrogenic tissue formation in a rat femoral defect model. Our study was designed as a confirmation of theoretical models of mechanobiological influences during skeletal healing. We demonstrate that the differentiation processes of cartilage and bone during fracture healing can be experimentally manipulated into desired tissue and structural level outcomes. This study may provide the basis for future research approaches to examine the molecular regulatory processes by which the mechanical environment regulates cartilage and bone formation, and potentially joint formation.

Materials and methods

Operative procedure

Animal care and experimental protocols were followed in accordance with NIH guidelines and approved by our institution's Laboratory Animal Science Center IACUC. Following a minimum 48 h acclimation period, sixteen skeletally mature male Sprague Dawley rats (400 ± 20 g) were transported to a dedicated surgical procedure room. Each animal was anesthetized with an isofluorene inhalation system (4.0% induction, 2.0% maintenance). The right thigh was shaved, prepped with betadine, and given an intramuscular (all injections were given via this route) injection of Cefazolin antibiotic (200 mg/kg).

A 2 cm incision was made on the lateral aspect of the thigh, creating a plane through the lateral intermuscular septum to expose the femur. The periosteum was elevated on the anterolateral aspect of the femur and a drill guide template was positioned on the femur using two cable ties. Special care was taken in placing the template to allow the pins to be inserted centrally on the diaphysis of the femur, reducing the chances of fracture due to inappropriate pin insertion. Once the template was securely placed, the proximal-most pinhole was drilled using a drill guide and a 0.7 mm drill bit. The hole was tapped with a 0.9 mm tap and the pin was secured into the femur. The other pins were placed using the same technique in order from the distal-most pin to the inner proximal and inner distal pins. The template was removed and the skin pulled over the pins by placing fourteen gauge needle heads over the pin locations. The fixator was secured to the pins as close to the skin as possible without potentially causing skin ulcerations.

Following the application of the fixator, a defect was made using a rotating saw blade attached to a Dremmel Tool (Dremmel, Racine, WI). A 3 mm gap size was chosen so that it would function as a non-critical sized defect allowing healing with delayed union to occur [15]. After completion of the defect, the site was irrigated with sterile saline and the fascia and skin closed. The incision was cleansed with betadine and the animal given an injection of Buprenex analgesic (0.2 mg/kg). During the 2 days following surgery each animal received an injection of Cefazolin (200 mg/kg) once per day, and an injection of Buprenex (0.2 mg/kg) twice per day. Each animal was housed in its own individual cage, and for the duration of the experiment all animals were monitored daily for pain and infection.

Fixator design and application

A custom designed external fixator was used to introduce 40% (vertical displacement as a function of the cortex diameter) interfragmentary bending strain (12° angular excursion) with a hypothetical symmetrical bending load distribution centered within the gap (Fig. 1). It was felt that 12° was well within the physiological range of angular excursion of normal developing joints such as the knee or elbow. To perform this motion an oscillating linkage was built such that the amount of interfragmentary displacement could be set between 1.0 and 1.5 mm relative to the locked position, providing for the 12° of total angular excursion. The motion was applied using a stepper motor (model #2602-010, Hurst Motors, Detroit, MI). The speed of the motor was controlled using an EPC-013 stepper motor control (Hurst Motors, Detroit, MI). The shaft of the stepper motor was coupled to one of two eccentric shafts of a torque transducer (model #1102-50, Lebow Products, Troy, MI). The other eccentric shaft of the transducer was connected to the linkage. A torque sensor connected to an external data acquisition board (model #100, Instrunet, Cambridge, MA) acted as a bridge voltage sensor and controlled the torque transduced to the fixator. Based on manufacturer's specifications the torque sensor was mapped to 1.967 mV/oz in., with the input torque sampled at 60 Hz for the duration of each experimental session. The peak torque required to induce motion was recorded as the baseline value. The loading apparatus was then calibrated prior to every application using Fourier transforms of the stepper motor moment application.

Each of the sixteen animals had an external fixator applied to its right femur and a 3 mm defect created at the mid-diaphysis. One group ($n = 8$ animals) represented the controls and remained rigidly fixed for the entire experimental period, receiving no motion treatment. The treatment group ($n = 8$ animals) received mechanical stimulation at 1.0 Hz for 10 min a day, with a 3 days on, one day off loading protocol for the first two weeks. The loading protocol for the final three weeks was 2 days on and 2 days off. The loading protocol was designed to give the animals weekly rest time from the anesthesia. The treatment frequency of 1.0 Hz was chosen because it falls well within the physiological range of normal joint function. A total of 600 symmetrical bending cycles per day were induced on the defect of the treatment animals for a total of 35 days (24 days of actual stimulation). The experimental time period of five weeks was determined to be the point of bony bridging under rigid fixation based upon the results of the control specimens.

Radiological assessment

High resolution radiographs (Ultraspeed DF-50, Kodak, Rochester, NY) of the harvested specimens were performed weekly until the termination of the experiment. Radiographs were taken in order to monitor fixator stability and placement, and to follow callus mineralization and bony healing.

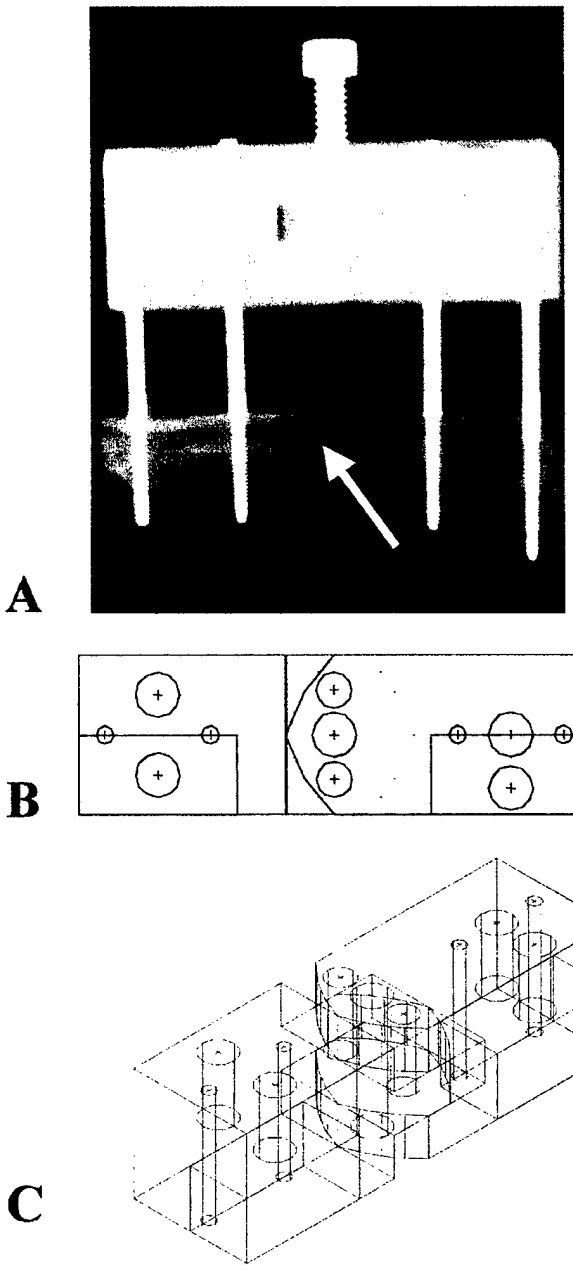

Fig. 1. Radiograph of the fixator and 3.0 mm defect on a rat femur (A) with an Autocad drawing of the fixator in lateral view (B) and obliquely in 3D (C). An arcade can be seen developing within the defect as a result of the micromotion bending treatment (arrow). The action of the fixator in (A) is in and out of the paper. In (B) the pins would be positioned in the small holes along the length of the small rectangles. Note the axis of the fixator is aligned with the theoretical center of the defect.

Histological assessment

Animals were euthanized at day 35, the femora were excised and specimens placed in 4.0% paraformaldehyde for 12 h. They were then decalcified for two weeks in TBD-2 decalcifying solution (Shannon, Baltimore, MD). The bones were then dehydrated via a series of increasing alcohol solutions and cleared in xylene for 1 h. They were infiltrated with paraffin, with the solution changed at 1 and 2 h, and maintained at 60 °C under a 25 mm Hg vacuum. The bones were embedded so as to expose the sagittal plane for sectioning. Specimens were sectioned at 5–7 μm thickness and stained with hematoxylin and eosin, or alcian blue. Immunohistochemical staining for Type II collagen was performed using a primary antibody of Collagen II (Neomarkers, Fremont, CA) and a Vector Stain Kit (Vector Laboratories, Burlingame, CA). Articular cartilage specimens were obtained from the knees of cohort rats.

Fourier transform analysis

Histological slides were utilized to quantify preferred fiber angle and fiber angle conformity in the collagen fibers of the newly formed cartilage tissues (Fig. 2). These values were determined for deep, intermediate, and superficial layers and were compared between the treatment group, the controls, and normal rat knee articular cartilage. First, standard H & E histologic sections of demineralized treatment, control, and normal rat knee cartilage specimens were prepared and collagen fiber orientation within the tissues was graphically visualized under polarized light with an Olympus OMT2 microscope at 200× magnification. Two deep, two intermediate, and two superficial fields were generated and mapped for each of the 16 cartilage surfaces (8 distal and 8 proximal). The superficial zone was determined as the area immediately under the cartilage surface, the deep zone was the area immediately adjacent to the underlying subchondral bone, and the

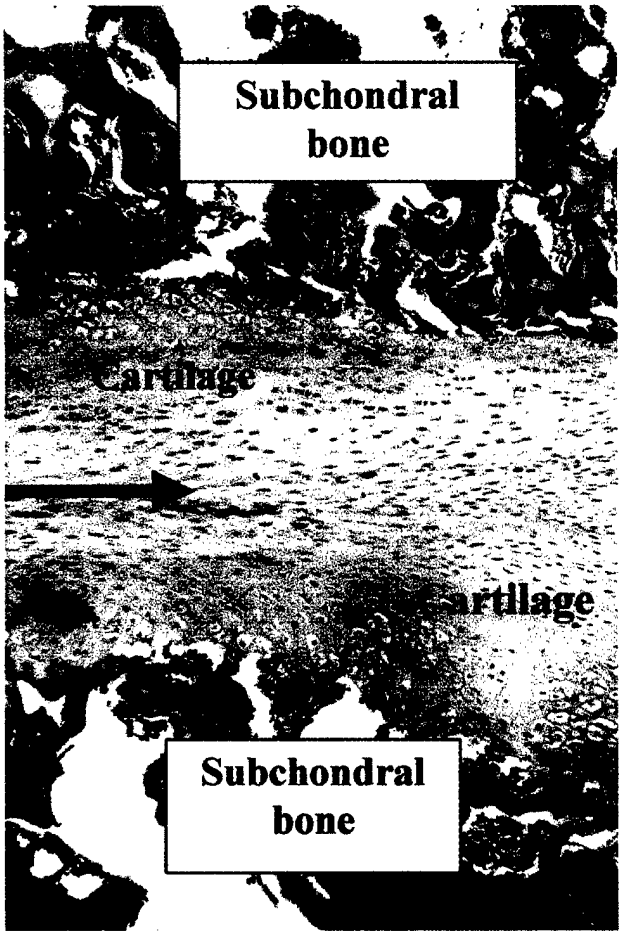

Fig. 2. Cartilage tissue formed in a *neoarthrosis* via controlled motion (from Fig. 4(D)). Red tissue at top and bottom are distal and proximal subchondral bone arcades. The morphology of the cartilage cells changes from the arcades to the midline, becoming more flattened. A distinctive cleavage can be seen beginning between the distal and proximal cartilage bands (arrow). It is believed that the introduction of shear motion would further enhance the cleavage of this cartilage zone into two discontiguous cartilage surfaces.

intermediate zone was exactly half way between the deep and superficial zones. The polarized microscopic images were captured using a digital camera (Kodak DCS-420, Kodak, Rochester, NY) affixed to the microscope. The digital images were imported into Matlab and thresholds were set to obtain high contrast images (Fig. 3(A)). Preferred fiber orientation within each field was determined by creating Fourier transforms of the digitized images (Matlab, Mathworks, Natick, MA), which generate an elliptical signal (Fig. 3(B)). The gray level of each pixel was processed using a 2D fast Fourier transform $F(m,n)$, where m and n are spatial frequencies corresponding to the x and y axes of the original image. The gray level of each pixel, represented by a function, $f(m,n)$, was then transformed using a 2D discrete Fourier transform.

$$\mathrm{F}(\mathrm{p},\mathrm{q}) \quad \sum_{m=0}^{M-1}\sum_{n=0}^{N-1} f(m,n)\mathrm{e}^{-j(2\pi/M)mn}\mathrm{e}^{-j(2\pi/N)qn},$$

$$p = 0,1,\ldots,M-1, \quad q = 0,1,\ldots,N-1.$$

The preferred orientation in the original image was represented by a peak in the power spectrum ($|F(m,n)|^2$, a 2D array, (Fig. 3(C))). To quantify the orientation its intensity was determined as the angular distribution of the power spectrum. The angular distribution was computed as the average of the power spectrum within a narrow fan-shaped region. The largest peak of the intensity of orientation was perpendicular to the preferred orientation of the fibers. Collagen fiber conformity was determined by the ratio of the major and minor axes of the power spectrum peak, with larger values corresponding to greater angle conformity.

Statistical analyses

Data are presented as mean ± S.D. All histomorphometric results including collagen preferred fiber angle and fiber angle conformity were compared between the control and treatment groups using an ANOVA and Tukey's post hoc test at an level of 0.05, and with p values less than 0.05 interpreted as significant. All sample sizes for the specific groups were determined by power statistics calculations: based on a coefficient of variation of 25% in the data, and accepting α and β errors of 5.0%.

Results

All six specimens of the control group demonstrated at least partial bony union, with two showing complete union (Fig. 4). Radiological and histological analyses of the treatment group showed the creation of an organized pseudoarthrosis with opposing bone arcade structures capping the defect termini contrasting with the healed controls (Figs. 4 and 5). Additionally, a cartilage tissue with articular cartilage-like organization developed on the defect side of the bone arcades (Fig. 2). This complex structure was maintained in the mechanical stimulation group past the time of healing in the controls, with the shape of the arcades corresponding to the pivoting action of the fixator. No control animals demonstrated development of a bony arcade or cartilaginous band across the medullary canal. These arcades, especially when present on both sides (Fig. 4(B) (D)), had the effect of segmenting the femur into two bones via a joint-like structure. This *neoarthrosis* was maintained in the treatment group past the time of healing in the controls. The tissue arising from the arcades stained positively for sulfated proteoglycan specific alcian blue staining, an indication of the presence of cartilage. Likewise, type II collagen was prevalent throughout the tissue, confirming it to be cartilage. However, the cartilage band was not thick enough to quantitatively determine a trend in staining intensity, as is normally found in articular cartilage. The presence of other specific cartilage types (i.e., Type IX, Type X, Type XI, etc.) was not determined in this study.

The distribution and orientation of collagen fibers within the experimental cartilage closely resembled that of collagen in articular cartilage from rat knee joints, with an alignment parallel to the articulating surface in the superficial zone and an increasingly perpendicular alignment, relative to the articulating surface, in the intermediate and deeper zones (Table 1). The control cartilage (residual from the endochondral osteogenesis process of healing), was fragmented in its distribution within the defect and demonstrated no superficial-to-deep polarity in the level of organization. The greatest similarity in collagen fiber angle was found between the treatment ($4.47° \pm 2.65$) and knee articular cartilage ($4.5° \pm 4.69$) in the superficial zone ($p = 0.89$). The

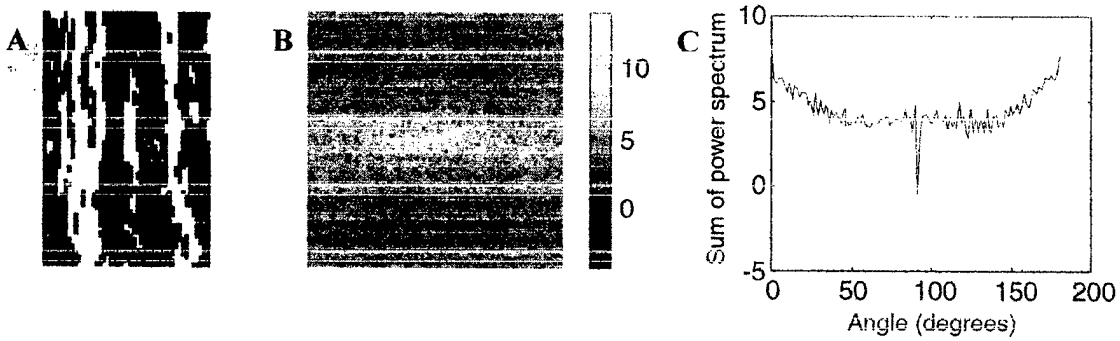

Fig. 3. Stages and results of Fourier transform of polarized neoarthrotic collagen fiber images. (A) Thresholded polarized image of collagen fibers in the superficial zone of the cartilage. (B) Elliptical transform of image in 3A with horizontal major axis and (C) power spectrum analysis of fiber angle preference (90°). The ratio of the major axis to the minor axis in the ellipse in (B) determines fiber angle conformity. Higher ratios denote higher fiber conformity to preferred angle.

Fig. 4. Bony arcades (arrows) clearly formed in four out of six treatment animals as a result of the controlled micromotion. The bony arcade develops as an extension of the cortices and the convex formation is sometimes matched by a corresponding concave formation on the other side of the defect (B, C, D). The arcades support an articular-like cartilage tissue on the defect side (asterisk). The boxed in area (D) shows the articular-like cartilage forming on the subchondral bone, and at higher magnifications a cleavage line can be seen between distinct cartilage bands (Fig. 2).

values from the control superficial zone (101.67° ± 105.7) were significantly different from the articular cartilage ($p < 0.01$) and treatment groups ($p = 0.04$). In the intermediate zone the knee articular cartilage and treatment groups were not significantly different (7.1° ± 4.62 and 6.55° ± 4.9, respectively, $p = 0.83$). The collagen in the intermediate zone of the control group (35.89° ± 12.72) demonstrated a somewhat perpendicular fiber angle relative to a hypothetical articular surface at the midpoint of the defect. There was a significant difference between the articular cartilage and the controls ($p < 0.01$), and between the neoarthrotic cartilage and the controls ($p < 0.01$). The deep layer in all three groups demonstrated perpendicular preferred collagen fiber angles (relative to the articular surface), with no significant differences between the three groups.

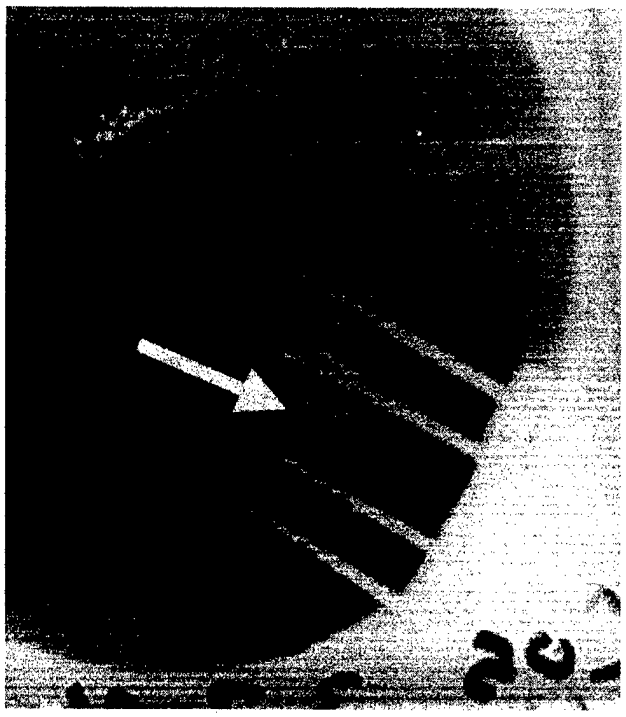

Fig. 5. A high resolution radiograph of a control specimen demonstrating bony bridging of the defect via direct periosteal bone formation (arrow). Note the lack of endochondral bone formation within the defect space which is the result of ideally rigid fixation (asterisks). Two control specimens demonstrated bony healing while four showed delayed union. No control specimen developed a bony arcade or articular-like cartilage as seen in the treatment group (Fig. 4).

The conformity ratios (angular agreement of the individual collagen fibers) were highest in the superficial zones of both the knee articular cartilage and the treatment cartilage (6.88 ± 3.83 and 4.04 ± 0.45, respectively, $p = 0.16$) while the control group demonstrated relatively low fiber organization (1.49 ± 0.11). However, a significant difference was found between both the articular and neoarthrotic fiber angle conformities versus the control conformity ($p = 0.02$ and $p < 0.01$, respectively). The only significant difference in fiber conformity in the intermediate zone was found between the articular cartilage and the control groups ($p < 0.01$). There were no significant differences in fiber conformity between the groups in the deep zone. In summary, the collagen within the neoarthrotic cartilage appeared to not be statistically different from that seen in rat knee articular cartilage, while the control cartilage was statistically different.

Discussion

It is well known that humans are capable of forming a cartilaginous joint-like structure in a long bone, as is observed in the pathological condition pseudoarthrosis [12,25]. Although the precise mechanical and biological events which lead to this condition are not known, theoretical modeling of tissue development within a fracture site predict that such an outcome is possible [2,4,6,9,18,27]. Experimental models of pseudoarthroses have even been established using manually applied mechanical stimulation [1], but precisely controlled mechanical treatments and their effects on tissue differentiation have not been established.

Our results suggest that the application of precisely controlled bending motion in a non-critical sized defect leads to the directed formation of specific tissues such as cartilage (as specified by theoretical models), and that the architectural organization of the resulting anatomical structures relate directly to the action and magnitude of the induced motion. Thus, the resulting pseudoarthrotic structures were likely a response to the symmetri-

Table 1
Results of the collagen fiber preferred orientation and conformity analyses using Fourier transforms of polarized histological specimens

		Superficial layer		Intermediate layer		Deep layer	
		Angle (°)	Ratio	Angle (°)	Ratio	Angle (°)	Ratio
Articular cartilage	Mean	4.5α	6.88α	7.1α	4.87α	64.1	2.97
	S.D.	4.69	3.83	4.62	1.34	31.71	1.39
Neo arthrosis	Mean	4.47β	4.04β	6.55β	3.33	53.2	1.83
	S.D.	2.65	0.45	4.9	1.16	70.09	0.56
Healing controls	Mean	101.67$\alpha\beta$	1.49$\alpha\beta$	35.89$\alpha\beta$	2.16α	76.65	2.32
	S.D.	105.76	0.11	12.72	0.35	82.24	1.29

Preferred fiber angle is relative to the articulating surface except in the healing controls which were referrenced to a homologous line perpendicular to the long axis of the bone and through the center of the osteotomy. The fiber angle conformity ratio is the similarity of each individual fiber angle to the average angle, with higher values indicating greater conformity. A striking similarity existed between the neoarthrotic cartilage (Neo Arthrosis) and rat knee articular cartilage (Articular Cartilage) in the intermediate and superficial layers. These were in contrast to the endochondral cartilage found in typical healing fractures such as that represented by the controls. Fiber angle conformity was relatively low in the controls and the standard deviation of the mean preferred fiber angle was very high. Significant differences are denoted as (α) for articular cartilage and (β) for neoarthrotic cartilage.

cal bending motion, as are the analogous structures in in utero joint development largely a product of their mechanical environment [3,5,13,22,23]. This cyclical and symmetrical bending motion created a mechanical environment of alternating hydrostatic compression and tension in one axis, symmetrically increasing in magnitude with increased distance from the center of the defect to the outer cortex. A neutral axis with respect to tension and compression was created along the theoretical bending axis of the defect. Additionally, the initiation of a line of cavitation between the newly developing surfaces resulted from the shear component of the bending action (Fig. 2, see arrow).

The bone arcades that formed across the termini of the defect effectively capped the segments and created what could be considered two bones out of the single femur. This segmenting of a single skeletal element is a crucial event in joint formation. The bone caps were likely the result of the forces induced by the alternating compressive loads caused by the fixator, compressing the material and cells recruited to repair the defect. In some instances clearly reciprocal convex and concave shaped arcades formed from this bone; likely a result of the pivoting action of the fixator. The arcades that developed were aligned with the fixator bending axis and as the fixator pivoted on its axis so did the healing defect.

The cartilage tissue that developed on these bony caps demonstrated an organized collagen fiber architecture (with respect to the perpendicular of the long axis of the bone segments). Likewise, collagen fiber architecture in articular cartilage is well organized showing superficial to deep polarity [10,26]. In contrast, collagen fiber architecture in cartilage of the endochondral ossification pathway is typically much less organized, having little to no deep-to-superficial polarity in its structure. Although not identical to articular cartilage, the ultrastructure of the cartilage that developed on the bony termini of the experimental group demonstrated a degree of organization which was strikingly similar.

A shear component was also induced on the surface of the defect tissues as they developed, another result of the pivoting action imposed by the fixator. As the tissue initially began to differentiate, the plane of shearing action defined the dividing point between the segments. As the tissues further differentiated into bone and cartilage, the shear component was likely responsible for the specialized orientation of the collagen fibers within the superficial layer of cartilage. Shear forces would be greatest superficially at the opposing surfaces (the location of greatest shear displacement during bending), and be reduced in magnitude proximally and distally from the defect center. Thus, shear would be lower in magnitude in the deeper cartilage tissues where the collagen fiber orientation was increasingly less tangential to the presumptive surface, and deeper still where subchondral bone formed. This is analogous to the mechanical environment responsible for articular cartilage formation in utero.

Studies of the influence of the mechanical environment on fracture healing suggest that less rigid fixation leads to preferred endochondral osteogenesis while more rigid fixation leads to preferred intramembranous ossification [2–4,9,11,18,27]. Our stimulation protocol provided motion, but in precisely controlled directions, followed by 23 h of rigid fixation. We believe the defect segmentation, bone and cartilage differentiation and cartilage architecture are all the result of the controlled mechanical stimulation imposed by the fixator. This is analogous to the case for articular cartilage developing in utero, whose structure results largely from its loading history during development [3,5,13,22,23]. The results of this study indicate that precise control of the mechanical environment during bone defect healing can influence differentiation at both the tissue (cartilage versus bone) and molecular (organized versus disorganized collagen fiber architecture) levels. The significance of this study lies in the parallels of defect healing and in utero joint development [17], and in its potential use in directed tissue differentiation for joint repair.

Acknowledgements

The authors would like to recognize Robert Sjostrum for machining the fixators and linkage system. Amy Frederick's salary was partially funded by the NIH, HD22400, and Dr. Cullinane's salary was partially funded by the Department of Defence, DAMD 17981. The authors received no commercial funds for this experiment.

References

[1] Brighton CT, Krebs AG. Oxygen tension of nonunion of fractured femurs in the rabbit. Surg Gynecol Obstet 1972;135:379–85.
[2] Carter DR. Mechanobiology of skeletal tissue growth and adaptation. In: Proceedings of the 12th Conference on Europ Soc Biomech, 2000. p. 7.
[3] Carter DR, van der Meulen MCH, Beaupre GS. Mechanobiologic regulation of osteogenesis and athrogenesis. In: Buckwalter JA, Ehrlich MG, Sandell LJ, Trippel SB, editors. Skeletal growth and development: clinical issues and basic science advances. Rosemont, IL: Am Acad Orthop Surg; 1998a. p. 99–130.
[4] Carter DR, Beaupre GS, Giori NJ, Helms JA. Mechanobiology of skeletal regeneration. Clin Orthop Suppl 1998b;355:S41–55.
[5] Carter DR, Wong M. Mechanical stresses in joint morphogenesis and maintenance. In: Mow VC, Woo SLY, Ratcliffe A, editors. Biomechanics of diarthrodial joints, vol. 2. New York: Springer; 1990. p. 155–74.
[6] Carter DR, Blenman PR, Beaupre GS. Correlations between mechanical stress history and tissue differentiation in initial fracture healing. J Orthop Res 1988;6:736–48.

[7] Chen FS, Chao Y, Shang Q. Advances in the research on repairing cartilagenous defects of synovial joint. Chung Kuo Hsiu Fu Chung Chien Wai Ko Tsa Chih 1998;12(5):297–300.
[8] Chen FS, Frenkel SR, Di Cesare PE. Repair of articular cartilage defects: part II. Treatment options. Am J Orthop 1999;28(2): 88–96.
[9] Claes LE, Heigele CA. Magnitudes of local stress and strain along bony surfaces predict the course and type of fracture healing. J Biomech 1999;32:255–66.
[10] Cova M, Toffanin R, Frezza F, Pozzi-Mucelli M, Mlynarik V, Pozzi-Mucelli RS, Vittur F, Dalla-Palma L. Magnetic resonance imaging of articular cartilage: ex vivo study on normal cartilage correlated with magnetic microscopy. Eur Radiol 1998;8(7): 1130–6.
[11] Cullinane DM, Inoue N, Meffert R, Tis J, Rafiee B, Chao EYS. Regulating bone at the cellular level: A little evidence for Wolff's Law. Am Zool 1999;39(5):96.
[12] Dorr LD. Continuous passive motion offers no benefit to the patient. Orthopaedics 1999;22(4):393.
[13] Drachman DB, Sokoloff L. The role of movement in embryonic joint development. Dev Biol 1966;14:401–20.
[14] Einhorn TA. The cell and molecular biology of fracture healing. Clin Orthop 1998;355(Suppl.):S7–21.
[15] Einhorn TA. Clinically applied models of bone regeneration in tissue engineering research. Clin Orthop 1999;367(Suppl.): S59–67.
[16] Elder SH, Kimura JH, Soslowsky LJ, Lavagnino M, Goldstein SA. Effect of compressive loading on chondrocyte differentiation in agrose cultures of chick lim-bud cells. J Orthop Res 2000;18(1):78–86.
[17] Ferguson C, Alpern E, Miclau T, Helms JA. Does adult fracture repair recapitulate embryonic skeletal formation. Mech Dev 1999;87(1–2):57–66.
[18] Gardner TN, Stoll T, Marks L, Mishra S, Tate MK. The influence of mechanical stimulus on the pattern of tissue differentiation in a long bone fracture-an FEM study. J Biomech 2000; 33:415–25.
[19] Hall BK. In vitro studies on the mechanical evocation of adventitious cartilage into bone. J Exp Zool 1968;168:283–305.
[20] Hall BK. Immobilization and cartilage transformation into bone in the embryonic chick. Anat Rev 1972;173:391–403.
[21] Hamrick MW. A chondral modeling theory revisited. J Theor Biol 1999;201(3):201–8.
[22] Heegaard JH, Beaupre GS, Carter DR. Mechanically modulated cartilage growth may regulate joint surface morphogenesis. J Orthop Res 1999;17(4):509–17.
[23] Heegaard JH, Carter DR, Beaupre GS. A mathematical model for simulating mechanically modulated growth in developing diarthrodial joints. Trans Orthop Res Soc 1995;20:73.
[24] Hunziker EB. Articular cartilage repair: are the intrinsic biological constraints undermining this process insuperable. Osteoarthritis Cartilage 1999;7(1):15–28.
[25] Lehman WB, Atar D, Feldman DS, Gordon JC, Grant AD. Congenital pseudoarthrosis of the tibia. J Ped Orthop 2000;9: 103–7.
[26] Luder HU. Frequency and distribution of articular tissue features in adult human mandibular condyles: a semiquanititative light microscopic study. Anat Rec 1997;248(1):18–28.
[27] Martin RB. Toward a unifying theory of bone remodeling. Bone 2000;26(1):1–6.
[28] Murray RC, Zhu CF, Goodship AE, Lakhani KH, Agrawal CM, Athanasiou KA. Exercise affects the mechanical properties and histological appearance of equine articular cartilage. J Orthop Res 1999;17(5):725–31.
[29] Probst A, Spiegel HU. Cellular mechanisms of bone repair. J Invest Surg 1997;10(3):77–86.
[30] Wu QQ, Chen Q. Mechanoregulation of chondrocyte proliferation, maturation, and hypertrophy: ion-channel dependent transduction of matrix deformation signals. Exp Cell Res 2000;256(2): 383–91.

MECHANOBIOLOGICALLY DIRECTED SKELETAL REGENERATION: INDUCED DIFFERENTIATION OF CARTILAGE, COLLAGEN TYPE II AND GDF-5 EXPRESSION, AND MODIFIED MATRIX ARCHITECTURE

+*Cullinane, DM; *Salisbury, KT; *Alkhiary, Y; **Sanabria, G; **Cottetta, N;*Gerstenfeld, LC;* Einhorn, TA
+*Boston University Medical Center, Boston, MA
**Boston University College of Engineering, Boston, MA

INTRODUCTION

The local mechanical environment is a crucial factor in determining the type of tissues that will form during bone defect healing[1]. This is true at the tissue level as well as for genetic expression, specific tissue molecular structure, and tissue mechanical properties[3]. Theoretical[2], *in vitro*[5], and *in vivo*[3,4] models have demonstrated that the regulation of gene expression and/or the directed development of specific tissue types can be achieved by manipulation of the local mechanical environment. This study tests the hypothesis that precisely controlled mechanical stimulation can induce specific skeletal tissue formation in a healing bone defect, regulating gene expression, cell differentiation, and tissue molecular structure. We mechanically stimulated in bending and shear, healing bone defects in an adult rat model, investigating resulting molecular expression, tissue type, and collagen architecture quantitative characterization.

METHODS

Custom-designed external fixators introduced daily bending (12°), shear (10%), or a combination of bending and shear load regimens at 1 Hz to healing 2mm femoral defects in 12 (4 ea) Sprague Dawley rats (Figure 1). These devices precisely controlled the mechanical environment within the healing defects, allowing the correlation of specific mechanical loads to resulting tissue types, tissue histomorphometrics, and molecular analyses. We anticipated tissue outcomes typically and spatially based on finite element model-derived local stress and strain magnitudes, and mechanobiological principles. Tissue type composition and collagen fibril architecture were quantified using ImagePro and MatLab Fourier transforms, respectively. We also conducted *in situ* hybridization for the expression of Type II collagen and immunohistologically stained for the expression of the joint development-related gene Growth and Differentiation Factor-5 (GDF-5).

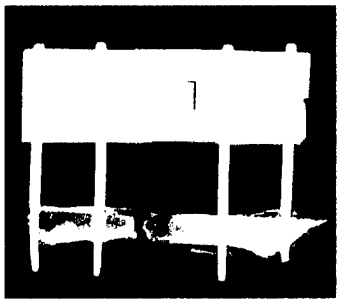

Figure 1. Radiograph of external fixator on femur. Bending treatment specimen following 35 days of stimulation. The bending action is in an out of the page. Note translucency in the area of the defect consistent with the presence of cartilage.

RESULTS

After 35 days all treatment specimens failed to unite, demonstrating cartilage across the defect (Figure 2). The FEM outlined stress and strain distributions within the defects which accurately predict the presence and maintenance of cartilage. Collagen fibril architecture differences occurred between superficial, intermediate, and deep layers in all treatment groups ($p<0.0001$). Ratios of cartilage:bone in all treatment groups were not significantly different from the knee (Table 1). Further, the experimental tissues demonstrated the expression of collagen Type II (confirming cartilage) and GDF-5 (Figure 3).

Category	% Bone (S.D.)	% Cartilage (S.D.)
Control	94.27 ± 4.11	5.73 ± 4.80
Bending	78.40 ± 2.63	21.57 ± 2.60
Shear	80.18 ± 5.78	19.82 ± 3.03
Combination	81.89 ± 13.17	18.11 ± 13.15
Native knee	83.57 ± 1.88	16.43 ± 2.64
Native intervertebral	53.87 ± 13.02	46.13 ±

Table 1. Histomorphometrics of cartilage:bone in the defect. In all treatment groups, the cartilage:bone ratio is not significantly different from the native knee ratio but all are different from native spine joints.

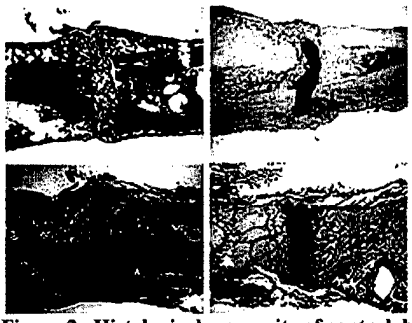

Figure 2. Histological composite of control, bending, shear, and combination specimens (clockwise from top left). Safranin-O and Fast Green stained histological sections. The control (top left) demonstrates complete bony bridging, whereas all three treatment groups maintain cartilage in the defect. Cartilage (red) is reduced in the controls due to constant rigid fixation which minimizes compressive stress. The identification of cartilage was confirmed molecularly with *in situ* hybridization of Type II collagen. Note the bending specimen (top right) has an arched configuration which mirrors the bending action of the fixator. This arch-shaped structure is likely a result of stress distribution from the neutral axis of bending (centerline of defect).

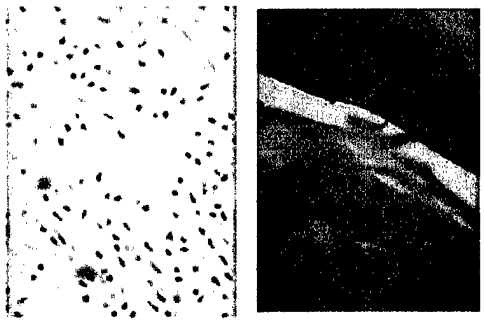

Figure 3. Immunohistological assay for GDF-5. The control (left) shows no reaction, whereas the bending specimen (right) demonstrates a positive reaction (brown stain). GDF-5 is an early joint development-related gene.

DISCUSSION

We demonstrate that cartilage differentiation can be specified within a mechanically controlled, healing, adult bone defect, and that the tissue is maintained past the time of control healing. Beyond a simple pseudoarthrosis, our results show, on multiple levels, that the mechanical interventions are precisely directing specific developmental processes; to some degree mirroring joint development (GDF-5 expression). We have determined that specific molecular expression, tissue type, and tissue architecture are all influenced by the local mechanical environment. These findings support the importance of mechanical intervention in tissue development, repair, and maintenance.

REFERENCES

1. Carter DR, Blenman PR, Beaupre GS (1988) J Orthop Res 6:736-748. 2. Carter DR, Beaupre GS, Giori NJ, Helms JA (1998) Clin Orthop 355S:S41-S55. 3. Cullinane DM, Fredrick A, Eisenberg SR, Pacicca D, Elman MV, Lee C, Salisbury K, Gerstenfeld LC, Einhorn TA (2002) J Orthop Res 20(3):579-586. 4. Eckstein F, Faber S, Muhlbauer R, Hohe J, Englmeier KH, Reiser M, Putz R. (2002) Osteoarthritis Cartilage 10(1):44-50. 5. Elder SH, Goldstein SA, Kimura JH, Soslowsky LJ, Spengler DM (2001) Ann Biomed Eng 29(6):476-82.

THE ROLE OF ANGIOGENESIS IN A MURINE TIBIAL MODEL OF DISTRACTION OSTEOGENESIS

*Carvalho, RS; *Einhorn,TA; **Lehmann,W; *Edgar, C; *Alyamani, A; *Apazidis, A; *Pacicca, D; +*Gerstenfeld, LC
+# Boston University Medical Center, Boston, MA, 02118

INTRODUCTION

Distraction osteogenesis (DO) is a widely used orthopaedic treatment for the correction of limb length discrepancies, congenital deformities, non-unions, and the regeneration of large amounts of bone that have been lost due to trauma. It is one of the most dramatic applications of mechanical stimulation as a means of inducing the regeneration of up to 20% the length of a long bone[1]. While DO procedures are used clinically and the surgical techniques have been refined, the basic mechanisms by which this procedure promotes new bone formation is not well understood. One of the primary descriptive features of DO is that it induces new bone formation through an intramembranous process devoid of extensive amounts of cartilage. However, the most intriguing observation is that the regeneration of abundant amounts of bone is accompanied by robust vascularity of the repair tissue throughout the regenerative process[2]. In order to assess the relationship of bone regeneration during DO to the process of angiogenesis, we have developed a murine model of DO. Using this model, we defined the temporal and spatial expression of the angiogenic and bone morphogenetic signals that drive new bone formation during this process.

METHODS

Surgical Procedure: All procedures were performed under an approved IACUC protocol. BALBc mice (Charles River Labs, Cambridge, MA) weighing 25 to 35 g were used for these studies. All surgeries were performed under general anesthesia by inhalation of isofluorane and O_2. The left leg of the animal was shaved and disinfected with an iodine solution. An anterior longitudinal incision was made over the tibia, and the underlying muscles were retracted with care being taken to minimize damage to the periosteum. A 6 mm distraction device (KLS Martin, Jacksonville, FL), which is used for oral surgical augmentation of alveolar bone, was adapted for use in this procedure. It was attached to the upper part of the tibia by means of a 0.01 inch ligature wire (3M Unitek, Monrovia, CA) that was wrapped around the tibia and secured with bone cement. The distance between the arms of the device attached to the tibia was usually 3-4 mm. Because the fibula and tibia are fused in mice both were bisected with a transverse osteotomy. The osteotomy was created with the use of a serrated scalpel blade under constant cold saline irrigation and placed symmetrically between the arms of the distractor. Immediately after the osteotomy, both proximal and distal segments were approximated (if needed), and alignment of the device with the tibia was confirmed by x-ray (Gendex Oralix AC, Milan, Italy). The soft tissue was closed with a no.5-0 gut absorbable suture. After surgery, the animals were individually caged and started to bear weight on the operated leg minutes after recovery. The distraction protocol consisted of three phases: 1) latency phase of 7 days duration, 2) active distraction of 10 days duration, and 3) consolidation phase of at least 14 days duration. The rate of distraction was 0.15 mm twice a day (0.3 mm/day). X-rays were taken on the day of the surgery, at the end of the latency period (7 days post-surgery), at the middle of the distraction period (11 or 12 days post-surgery), at the end of the active distraction (17 days post-surgery), at the middle of the consolidation period (23 or 24 days post-surgery), and at the end of the consolidation period (31 days post-surgery).

Tissue and Gene Analysis: Histological assessment was made using standard light microscopy. Gene expression levels for end point marker genes defining skeletal tissue differentiation and BMP expression were analyzed by RNase Protection analysis (RPA) using commercially available template sets per the manufacturer's recommended protocol (Pharmingen, Inc., San Jose, CA)[3]. For the analysis of the differential expression of the multiple metalloproteinase and angiogenesis associated genes, we used a number of specific micro-arrays purchased from SuperArray, Inc. (Bethesda, MD). Arrays were carried out and scanned, and gene expression was normalized to housekeeping genes and controls as per the manufacturer's instructions[4].

RESULTS

Whole Tissue Analysis: Characterization of both the x-ray assessment and the histological progression of bone repair in this model of distraction osteogenesis demonstrated that the tibia remained aligned throughout the procedure, and expansion of the device over a ten day period was able to produce robust new bone formation during the period of distraction. After the two weeks of consolidation after distraction was completed histological inspection showed a mixture of both lamellar and primary woven bone in the distraction gap.

BMP and ECM Gene Expression: Analysis of extracellular matrix gene expression at the end of the latency period, at two times during the ten day distraction period, and at the end of the consolidation period, showed that new bone formation was induced throughout the period of bone distraction. Interestingly, the expression of SPARC, osteopontin, bone sialoprotein and fibronectin were maximally expressed during the active distraction period. In contrast, osteocalcin and type I collagen, while elevated during the distraction period, showed persistent high levels of expression throughout the consolidation phase. During the period of active distraction both types II and X collagen were expressed at low levels, yet the expression of these genes disappeared completely during the consolidation phase. Examination of the profiles of BMP expression showed similar results with very high levels of expression of BMPs 2, 3, 3b, 4, 5, 6, 7 and 8. These genes were all seen maximally during the period of active distraction and persisted into the consolidation period. It is interesting to note that BMPs 8A, 3 and 2 showed maximal induction during the distraction period.

Angiogenesis and MMP Gene Expression: Of the 96 angiogenesis associated genes that were analyzed with the microarray used for this study, a number of genes were shown to be selectively induced during the distraction period. These included Hif1A (hypoxia induced factor 1A), gelatinase A and B, PEDF, VEGFA, TGFβ–1, endostatin, FGF receptor 3 (FGFR3), angiopoietin 2 and pleiotrophin. We also examined a selected microarray series that is specific for the metalloproteinase (MMP) genes and their inhibitors, as previous studies have shown that the expression of specific metalloproteinases (MMPs) is elevated during periods of active angiogenesis. This particular array contained 20 cDNA fragments from genes encoding the sequences of MMPs and the four specific inhibitors (TIMPs) of the MMPs. These results showed that MMP2, MMP8, MMP9, MMP13, and MMP14 were induced as a consequence of the surgical treatment and remained elevated above base line levels during the tissue repair process. Interestingly, MMP14 appeared to be further elevated during the distraction phase while MMP8 showed a very strong induction during the consolidation phase.

DISCUSSION

We report here the development of a usable and easily adaptable procedure to carry out distraction osteogenesis in mice. We specifically examined the molecular processes related to bone formation during distraction osteogenesis, focusing on both the induction of morphogenetic proteins that promote new bone formation and the expression of angiogenic factors that promote the formation of new blood supply to injured and growing tissues. Our results suggest that the mechanical signals generated during the distraction process induce the expression of select BMPs and angiogenic factors. Multiple BMPs are expressed during DO, and the pattern of their expression is most like late fracture repair[3]. It is of particular interest to note that Hif1a, one of the key transcription factors that is most proximal in the angiogenic regulatory cascade, was induced during the distraction period. These data show the concurrent expression of both angiogenic and bone morphogenetic factors during distraction and suggest complementary and synergistic roles in bone repair and regeneration.

1. Ilizarov GA Clin Orthop: 250:34-42, 1990
2. Aronson et al. J Orthop Res: 241:106-116, 1997
3. Cho et al. J Bone and Mineral Res: 17:513-20, 2002
4. Gerstenfeld et al. Conn Tiss Res: (in press)
5. Schipani et al. Genes Dev: 15(21):2865-76, 2001

**Department of Trauma and Reconstructive Surgery, University Clinic Hamburg-Eppendorf, Hamburg, Germany

Selective Adhesion of Osteoblasts to Different Integrin Ligands Induces Osteopontin Gene Expression

R.S. Carvalho[1,2], P.J. Kostenuik[3], E. Salih[4], A. Bumann[5], and L.C. Gerstenfeld[1*]

1) Orthopaedic Research Laboratory, Department of Orthopaedic Surgery,
Boston University School of Medicine, 715 Albany Street, R-205,
Boston, MA 02118-2526, U.S.A.
2) Department of Orthodontics, School of Dental Medicine, Boston University,
100 East Newton St., Boston, MA 02118.
3) Current Address: Amgen Corp., Thousand Oaks, CA
4) Department of Orthopaedics, Children's Hospital,
320 Longwood Ave, Boston, MA 02115
5) Department of Orthodontics, Faculty of Dentistry, University of Southern California, Los Angeles, CA and Private Practice of Orthodontics, Berlin, Germany

Running title: Osteoblast Adhesion Mediates OPN Expression

Key Words: Osteoblasts, Adhesion, Integrins, Osteopontin

This work was supported by Supported by a grant from the Department of Defense Bone Health and Military Readiness Program DAMD17-98-1-8510

*Correspondence:
Louis C. Gerstenfeld Ph.D.
Orthopaedic Research Laboratory
Department of Orthopaedic Surgery
Boston University School of Medicine
715 Albany Street, R-205
Boston, MA 02118
Phone: 617-414-1660,
Fax: 617-414-1661
E-mail: lgersten@bu.edu

Abstract

Skeletal homeostasis is partly regulated by the mechanical environment and specific signals derived from cellular adhesion with their matrix. Previous studies demonstrated that osteopontin expression is stimulated in response to both cellular adhesion and mechanical stimulation. The present studies examine if specific integrin ligands mediate osteoblast selective adhesion and whether *opn* mRNA expression is induced in response to these same ligands. Embryonic chicken calvaria osteoblasts were plated on tissue culture surfaces coated with fibronectin (FN), collagen type I (ColI), denatured collagen/gelatin (G), osteopontin (OPN), vitronectin (VN), laminin (LN) or albumin (BSA). Osteoblasts were shown to selectively adhere to FN, Col1, G, and LN, yet not to VN, OPN, or BSA. *Opn* mRNA expression was induced by adhesion to Col1, FN, LN, and G, but neither OPN nor VN induced this expression. Examination of the activation of the protein kinases A and C second signaling systems showed that only adhesion to FN induced PKA and PKC activity while adherence to Col1 induced PKC. Evaluation of the intracellular distribution of focal adhesion kinase (FAK) and p-tyrosine within cells after adherence to FN, VN or BSA demonstrated that adherence to FN stimulated FAK translocation from the nucleus to the cytoplasm and high levels of p-tyrosine localization at the cell surface. However, cell adherence to VN or BSA did not show these morphological changes. These data illustrate that osteoblast selective adhesion is mediated by specific integrin ligands, and induction of intracellular second signal kinase activity is related to the nature of the ligand.

1. Introduction

The bone remodeling cycle is known to be intimately involved in the metabolic homeostasis of mineral balance (Jilka and Manologas, 1994). Bone formation and the remodeling cycle are essential in maintaining the structural integrity of skeletal tissue in response to the mechanical loading to which it is subjected (Lanyon et al., 1982; Lanyon, 1987). It has also been suggested that bone remodeling provides the means of repairing bone tissue damaged as a result of mechanical fatigue (Mori and Burr, 1993). Thus, it may be speculated that skeletal cells that mediate the remodeling process are regulated by their mechanical environment. It has been shown that most cell types are subjected to various forms of loading, including shear stresses due to fluid flow and pressure, tensile stresses exerted by neighboring cells and the extracellular matrix (ECM), and the internal tension of the cytoskeleton (Shyy and Chien, 1997). In order for osteoblasts to respond to their mechanical environment, they must somehow interpret the signal generated by the stimuli. One mechanism by which cells sense these signals is through the physical deformation of the tissue (Carvalho et al., 1998). Many current reports show that signal transduction of biochemical signals following mechanical stimualtion or adhesion involves cell surface ligands, such as integrins (Ingber, 1991; Wang et al., 1993; Carvalho et al., 1998; Urbich et al., 2000). This observation is supported by the fact that mechanical stimulation-derived signals can only be perceived by osteoblasts and other responsive cells after cell adhesion (i.e. integrin-mediated) has taken place. Moreover, some of the signal transduction and gene expression events activated by mechanical stresses are similar, if not identical, to those induced by integrin-mediated cell adhesion (Shyy and Chien, 1997). This may be explained by changes in cell shape caused by either form of stimulation resulting in

the reorientation of the microfilament network, which then affects integrin behavior (Ingber, 1991). Receptor-ligation stimulations also appear to be dependent on the positional parameters provided by the matrix. Physical alteration of ECM proteins may also change integrin conformation, facilitating the activation of specific signal transduction molecules, which in turn regulate cytoskeletal arrangement and cellular response (Meazzini et al., 1998). Integrin ligands may, in fact, have an autocrine and/or paracrine function in regulating cellular function in the ECM (Gerstenfeld, 1999). ECM proteins may also function as initiators of specific cellular functions through their interactions with cell surface receptors.

In bone tissue, osteopontin (OPN) is one of the predominant RGD-containing ECM proteins (Gotoh et al., 1995) and is ubiquitously expressed in all skeletal tissues during embryogenesis (Gerstenfeld, 1999). Ultrastructural localization of OPN in areas adjacent to resorptive osteoclasts (Reinholt et al., 1990) suggests that this protein has an important role in anchoring osteoclasts to bone, which then allows for the resorption process. In addition, osteoclasts have been shown to synthesize OPN during active bone remodeling (Dodds et al., 1995) which further demonstrates that OPN has a major role in the maintenance of bone homeostasis (Gerstenfeld, 1999). It was also demonstrated that osteopontin is induced and then involved in the facilitation of bone remodeling stimulated by mechanical stresses during tooth movement (Terai et al., 1999). We have previously shown that both mechanical stimulation (Toma et al., 1997; Carvalho et al., 1998) and cellular adhesion (Carvalho et al., 1998) result in *opn* induction, and that integrin receptors may have a common role in the signal transduction processes of both forms of stimulation. Thus, our current experiments are designed to ascertain if osteoblasts discriminate at a molecular level different ECM ligands to mediate adhesion, and, if so, would these same ligands be responsible for the induction of osteopontin expression.

2. Experimental Procedures

2.1 Materials

All tissue culture supplies were from Sigma Chemical Company (St. Louis, MO). Antibodies mouse anti-chicken Vinculin, rabbit anti-human focal adhesion kinase, $p125^{FAK}$, mouse pTyr, goat anti-mouse FITC conjugated, and sheep anti-rabbit Cy3 conjugated were also from Sigma Chemical Company (St. Louis, MO). Nylon membranes for Northern blots were from Biotrans, ICN Corp. (Aurora, OH).

2.2 Cell Culture

Seventeen-day embryonic chicken calvaria osteoblasts were grown in culture as previously described (Gerstenfeld et al., 1988). These cells were plated at a density of 2×10^6 cells in 100 mm tissue culture dishes as described in Schaffer et al. (1994). Cultures were grown for two weeks until they reached confluence in minimum essential media supplemented with 10% fetal bovine serum (FBS). All analyses were performed on second passage cells using at least three separate preparations of cells, and all data is presented as a percent increase in expression over that of the controls, which were determined from parallel cultures grown under identical conditions. All error bars represent the standard deviation (SD) of the determinations from separate experiments and the number of replicates that were used for each measurement is denoted in each figure.

2.3 Attachment Assays

For the attachment (integrin ligation) assays, the cells were allowed to attach to selective protein coatings. Petri dishes were coated with 2 $\mu g/cm^2$ to 10 $\mu g/cm^2$ of each of the proteins

studied here. Fibronectin (FN), vitronectin (VN), laminin (LN), denatured collagen/gelatin (G), and collagen type I (Col1) were obtained from Sigma Chemical Company (St Louis, MO). Osteopontin (OPN) was purified as described by Gotoh et al. (1995). FN served as the basic ligand. Dishes coated with polyL-lysine (PL) or bovine serum albumin (BSA), also from Sigma Chemical Company (St. Louis, MO) served as controls. Petri plates were coated with the different proteins under sterile conditions and incubated for 24 hours at 37°C. For all attachment assays, 100,000 cells per 33 mm tissue culture well were used. Cells were allowed to attach for one, four, or twenty-four hours, and assays were performed at least three times for each protein. Values were calculated as the percentage of the cells on the experimental surfaces relative to the cell numbers observed on the plates coated with PL.

2.4 Signal Transduction Studies

Signal transduction pathways that mediate cell responses as a result of attachment/ligation were investigated by measuring the specific kinase activity of the cells plated into each separate protein coating. General protein kinase C (PKC) and protein kinase A (PKA) activities were measured using specific fluorescent substrates. Enzyme activities were first normalized per total protein content used in each assay. All measurements were based on the average of determinations from triplicate culture experiments. Values were then calculated as the percentage of activities seen in cells plated on polyL-lysine coated dishes. Controls were separately determined for each compound in cultures treated identically with the various compounds but in which the cells were attached to uncoated dishes.

2.5 Immunohistochemical studies

The intracellular distribution of focal adhesion kinase (FAK), phosphotyrosine (PT), and vinculin (VN) were examined after adhesion on surfaces coated with either PL or FN. Cell layers were washed with phosphate buffer saline (PBS) and fixed in 3.7% paraformaldehyde for 5 minutes at 4°C. Cells were then permeabilized with 0.02% triton X-100 in PBS for 10 minutes and the background was blocked with blocking solution (Pierce). Cells were washed in washing buffer (0.05% casein acid hydrolysate, 0.015% Tween 20) for 10 minutes and incubated with primary antibodies (mouse anti-chicken Vinculin, rabbit anti-human FAK, or mouse PT antibody) for 45 minutes at 37°C. Once again cells were washed with washing buffer, then incubated with secondary goat anti-mouse FITC conjugated antibodies or sheep anti-rabbit Cy3 conjugated antibodies for 30 minutes at room temperature, and finally washed and visualized/photographed under the light microscope.

2.6 Isolation and Analysis of RNA

Total RNA was isolated using Tri-Reagent™ (Molecular Center, Cincinnati, OH) according to the manufactures instructions. RNA was resolved on 1% agarose gels containing 2.2 M formaldehyde (Toma et al., 1997) and 5 mg of total RNA was loaded per gel lane. Chicken cDNA used for these studies was that of osteopontin (Moore et al., 1991). Northern blots with P^{32} cDNA-labeled+ probes were carried out at 65°C in 2.5 X SSC, 50 mM Na phosphate buffer, made 100 μg/ml single stranded salmon sperm DNA, and for 18 to 24 hours in a rotating hybridization oven (Robins Scientific, Sunnyvalle, CA). Autoradiograms were quantified using an LKB Ultra II scanning densitometer (LKB, Broma, Sweden) and values were normalized to the 18 S ribosomal RNA obtained by hybridization of each blot to a conserved nucleotide

sequence probe of 18 S ribosomal subunit (Ambion Corp., Austin, TX). All analyses were performed at least three times,and all data is presented as a percentage in expression over that of the controls determined from parallel cultures. All data were evaluated as the mean ±2 standard deviation, with a minimum of three experiments from different populations of primary cells and performance of appropriate statistical analysis.

3. Results

3.1 Osteoblasts have variable adhesion properties to different ligands

Initial studies were carried out to determine if chicken calvaria-osteoblasts demonstrate selective adhesion properties to different extracellular matrix proteins that serve as cell ligands. Osteoblasts were allowed to attach for four hours to FN, Col1, G, LN, OPN, VN, or BSA. These results are seen in Figure 1, panels A and B. These data show that FN, Col1, and G promoted selective adhesion. Dishes coated with VN, OPN, and BSA did not. While low concentrations of LN showed a small and selective effect, higher concentrations did not. As can be seen from these data, FN was the most effective protein in promoting selective adhesion. In addition, both native and denatured collagen (Col1 and G) also promoted adhesion, however, these showed saturation at between 1 and 3 $\mu g/cm^2$ of surface coating. In contrast, FN did not show saturation in promoting cell adhesion until about 30 $\mu g/cm^2$ (data not shown). These results demonstrate that adhesion of osteoblasts is specifically promoted by different types of integrin ligands.

3.2 Attachment of osteoblasts to different ECM proteins selectively increases the expression of opn mRNA

In previous studies, we demonstrated that cellular adhesion to fibronectin-coated surfaces would induce the expression of osteopontin. The current study examined if the induction of osteopontin expression was dependent on the adhesion of the osteoblasts to specific integrin ligands. These results are depicted in Figure 2. As can be seen in this figure, induction of *opn* mRNA was seen in cells that had been adhered to surfaces coated with specific extracellular matrix proteins. Induction of new mRNA expression was observed as early as 4 hours after the cells had been allowed to adhere and continued to increase up to 24 hours. At 4 hours of cell attachment, only coatings of FN and Coll resulted in an increase in *opn* mRNA expression. At the second time point of 24 hours, surfaces coated with Coll, FN, and to a lesser extent, LN, once again generated an increase in *opn* mRNA expression. The induction of osteopontin mRNA expression was significant with a 4 fold increase following osteoblast attachment to FN and almost 3 fold increase following osteoblast attachment to Coll. By contrast, results showed that G, OPN and VN did not increase *opn* mRNA. Taken together, these results suggest that a subset of ECM proteins both promoted specific cell adhesion and also mediated intracellular signal events that selectively induced the expression of *opn*. It is interesting to note, however, that none of the proteins that failed to promote specific cell attachment were able to independently promote induction of osteopontin expression.

3.3 Selective induction of kinase activity is related to specific protein ligands

The relationship of cell adhesion to the selective induction of specific intracellular kinase activities was next examined. In this study, cell adhesion was carried out at a fixed concentration of coating (10 $\mu g/cm^2$), considered the best concentration in preliminary observations. Figure 3, panels A and B, demonstrates that the profiles of selectively mediated attachment of embryonic osteoblasts was seen after only 60 minutes, compared to the profiles in Figure 1 in which attachment had been assessed for 4 hours. The induction of two classes of kinases, protein kinase A (PKA) and protein kinase C (PKC), that are involved in second signaling were then determined in cultures that were identically prepared in parallel. It is interesting to note that attachment to FN showed induction of both PKA and PKC activities, while Col1 showed the strongest induction of PKA activity with no induction of the activity of PKC. In addition, OPN also stimulated PKA activity, contrasting to G and LN, which strongly inhibited PKA activity. These data show that specific effects on broad classes of second signaling kinase activities are dependent on the specific ligand interactions and not solely on the processes of cell adhesion (Figures 1 and 2). Indeed, the strongest inhibitory effect on both PKA and PKC activities was seen when the cells were plated on gelatin (G), which at the same time strongly promoted cell adhesion.

3.4 Fibronectin stimulates the distribution of phosphotyrosine following osteoblast adhesion

Our previous studies of the signal transduction mechanisms associated with the mechanical stimulation of osteopontin expression demonstrated the involvement of both p-tyrosine kinase(s) in general and FAK in particular (Toma et al. 1997). The studies presented here examined if the intracellular distribution of focal adhesion kinase (FAK) and p-tyrosine would be altered as a consequence of the selective adhesion to different integrin binding ligands.

Since FN was shown to be the most effective attachment ligand, this protein was compared to either vitronectin or BSA, which do not promote selective adhesion (Figure 4). These experiments showed that adhesion to surfaces coated FN altered the general intracellular localization of FAK from the nucleus to the cytoplasm. In contrast, neither BSA nor VN had an effect on these morphological parameters within an one-hour period. There was also a strong induction of PT levels and a specific distribution of p-tyrosine associated proteins along the cell surface after adhesion was promoted with a FN. These data further reinforce the conclusion illustrated by Figure 3, which suggests that the induction of intracellular kinase activities are related to the specific nature of the ligand's interactions with its receptor.

4. Discussion

The ECM is an important structural scaffold for the organization of living tissues in the body. It provides an array of information for several key cellular functions, such as cell motility, polarity, migration, proliferation (Damsky and Werb, 1992; Schwartz et al., 1995; Damsky, 1999), and survival (Frisch and Francis, 1994; Damsky, 1999; Urbich et al., 2000), thus preventing apoptosis (Zhang et al., 1995; Globus et al., 1998). These functions require specialized ECM proteins for a number of cell types including osteoblasts. The resultant process of osteoblast-ECM adhesion also generates an abundance of signals designed to modulate vital osteoblastic responses. Transduction of signals from the ECM takes place through a variety of transmembrane proteins, including the integrin family of cell receptors (Clark and Brugge, 1995; Schwartz et al., 1995). Integrins are heterodimers comprised of two different subunits, α and β, and each subunit contains over 20 different types of integrins (Ingber, 1991). Consequently, the

specificity of integrin binding will be dependent on the unique combination of these subunits (i.e. integrin $\alpha_5\beta_1$ binds fibronectin, while $\alpha_2\beta_1$binds collagen) (Ingber, 1997).

In previous studies, we demonstrated that both stretch induced mechanical stimulation and cellular adhesion induce osteopontin expression. These previous studies further illustrated that integrin ligation induced common signal transduction processes that were facilitated by mechanical stimulation (Carvalho et al., 1998). The present studies investigate whether different ECM matrix proteins would equally mediate the adhesion of osteoblasts. If they did mediate selective cellular adhesion, we planned to next examine whether this would facilitate a common signal transduction process that induced osteopontin expression. The proteins we chose for our studies, native collagen (Col1), osteopontin (OPN), fibronectin (FN), denatured collagen/gelatin (G), vitronectin (VN), and laminin (LN), were selected based on previous studies which indicated that they interact with integrins on the cell surfaces of different populations of osteogenic cells. These proteins were also expressed by osteogenic cells or found in the ECM of bone (Grzesik and Robey, 1994). While FN, LN, collagen (Col1), and denatured collagen (G) interact with integrin receptors primarily containing β_1, VN and OPN were chosen as ligands that interact with integrins that contain β_3. Various cellular functions are associated with the different ligands, and integrins containing both β_1 and β_3 have been shown to promote cell survival and prevent apoptosis of osteogenic cells (Aplin et al., 1999; Urbih et al., 2000; Globus et al., 1997; Tanaka et al., 2002).

The results presented here demonstrate that FN, Col1, LN and G promoted selective osteoblast adhesion, while VN, and OPN did not, with FN being the most effective protein in promoting selective adhesion and LN being the weakest (Figure 1). This is consistent with a number of previous studies that also showed preferential adhesion or growth and differentiation

on β_1 interacting ligands (Gronthos et al., 1997; Tanaka et al., 2002). In contrast to the studies reported here, those of Aarden et al. (1996) demonstrated that osteoblasts bind equally well to β_3 interacting ligands. Some of the variations in the different studies, however, may be in part due to the variation in the complement of integrin isotypes that are found at different stages of osteogenic linage progression (Gronthos et al., 2001).

While these results indicate that adhesion of the osteoblast cell populations used in our studies was specifically promoted by β_1 and not β_3 containing integrins, these results also showed that there is a further discrimination between the individual integrin ligand's abilities to induce specific second signals and osteopontin gene expression. ECM protein-receptor specificity is an integral part of cellular signal transduction. It provides the means for initiation of second messenger signaling cascades (Schaller and Parsons, 1994; Damsky, 1999), which in turn regulate cellular function. We therefore looked at broad classes of key signaling mechanisms following osteoblast-ECM protein adhesion. Based on the relationship of the ligand-mediated adhesion with the second signal kinase activity, these data showed that kinase activities are dependent on the specific ligand interactions and not on the processes of cell attachment alone. This was evidenced by the inhibitory effect of gelatin coating on both PKA and PKC pathways, which at the same time promoted cell adhesion. Thus, the processes of cellular adhesion are most likely mediated solely through the RGD or other small integrin binding motifs, yet the down-stream activation of intracellular signaling responses are specifically related to the structural conformations of the intact ligand. Such a conclusion can further be appreciated as the activity of PKA fluctuated much more than that of PKC (i.e. 2-3 fold increase in response to Coll coated dishes as opposed to no changes on LN-coated dishes). While OPN did not promote cell adhesion, it did stimulate PKA activity. Conversely, G and LN

both strongly inhibited PKA activity. In contrast, the activity of PKC did not appear to change very much with exception of cells plated on FN-coated dishes, which showed a 2 fold increase versus that seen in cells plated on the control protein (BSA).

From our own studies and those of a number of other groups, it has been shown that *opn* mRNA expression is regulated by both mechanical stimulation and adhesion (Toma et al., 1997; Carvalho et al., 1998; Harter et al., 1995). In order to further investigate the molecular activation of intracellular signaling through ECM adhesion, we used the induction of *opn* expression as a functional assay. It is interesting to note that the strongest induction was seen with FN, Col1, and LN, with a weaker induction seen with denatured collagen (G). In contrast, OPN and VN were incapable of inducing *opn* mRNA expression (Figure 2). These results imply that the same integrin receptors that facilitate specific cell attachment also facilitate the induction of *opn* expression. As neither OPN nor VN mediate either of these cellular responses, these data suggest that the signal transduction processes that induce *opn* expression are not facilitated through a $\alpha_v\beta_3$ receptor, which further corroborates the adhesion assay results shown in Figure 1. The one difference that was observed, however, was in the comparison of cell attachment on gelatin vs. the induction of *opn* expression. This result may suggest that signal transduction through the collagen receptor is only mediated when it interacts with native collagen (Col1). The response of osteoblast adhesion, in its dependency to the ECM substrate onto which the cell adheres, has similar aspects to cell responses such as those elicited by mechanical stimulation (Wilson et al., 1995; Carvalho et al., 1998).

It is also known that ECM-derived signals are transduced to the cells through transmembrane molecules (i.e. integrins) primarily in zones of focal adhesions, which are known areas in which signal transduction takes place (Clark and Brugge, 1995; Burridge and

Chrzanowska-Wodnicka, 1996). We therefore further investigated the signal cascades by immunolabeling the well-known focal adhesion molecules, focal adhesion kinase (FAK). The immunolabeling also examined proteins containing phosphotyrosine (PT), which is the prevalent form of phosphorylation response mediated by FAK. Our data suggest that while FAK was seen in zones of focal adhesions (Burridge and Chrzanowska-Wodnicka, 1996; Kano et al., 2000) in osteoblasts plated on FN and VN, its distribution was localized more discreetly along the periphery of cells plated on fibronectin. Similarly, the distribution of p-tyrosine became more cytoplasmic in its localization and appeared in higher levels in the cells plated on FN. This result provides a potentially significant distinction between the signal transduction derived from cellular adhesion and that of mechanical stimulation. In the latter, FAK molecules localize to plaque-like areas of a $\alpha_v\beta_3$ integrins (Wozniak et al., 2000). It has also been shown that FAK autophosphorylation may be directly related to cell binding to OPN (Liu et al., 1997). This is consistent with the role of OPN in anchoring functional osteoclasts during bone remodeling (Reinholt et al., 1990). The role of FAK appears, however, to be highly relevant in ECM-mediated signal transduction. FAK transduces survival signals from the ECM, and these are monitored by p53 (Ilic et al., 1998). Lack of FAK redistribution following adhesion may reflect the early stage of the embryonic osteoblast phenotype studied here. In addition, PKC may also be activated by the interruption of survival signals from the ECM in conjunction with p53 (Damsky, 1999). This infers a close relationship between FN attachment and osteoblast survival, which is consistent with our results that showed the highest PKC activity response for dishes coated with FN as opposed to all the other ligands (Figure 4). As protein tyrosine phosphorylation occurs very often during intracellular signaling, the levels of phosphotyrosine were examined. Anti-phosphotyrosine staining was detected throughout the cells. It appeared to

be more intense immediately following cell adhesion to FN when there was a strong induction of PT levels and a generalization of its distribution throughout the cells. It is speculated that this response may be directly related to β_1 integrin-mediated binding, such as the one seen when osteoblasts were subjected to mechanical stress in vitro (Bierbaum and Notbohm, 1998).

Throughout this paper, we have speculated that as integrins are the mediators of specific ECM-osteoblast attachment, they also play a role in the selective signal transduction that induces *opn* expression. We did not directly examine the integrin receptors or their expression, yet the conclusion that integrins are transducing signals from the ECM is consistent with many other observations published in the literature (Clark and Brugge, 1995; Gronthos et al., 1997; Liu et al., 1997; Carvalho et al., 1998; Damsky, 1999; Yamada and Geiger, 1997; Zimmerman et al., 2000). The conclusion that implicates β_1 containing integrins as playing an important role in osteoblast development is supported by multiple recent experiments of transgenic cells expressing a dominant-negative truncated integrin β_1 subunit driven by an osteocalcin promoter that targets its expression to mature osteoblasts and osteocytes (Zimmerman et al., 2000). These studies illustrated that while wild type cells promoted osteoblast differentiation as characterized by the high levels of osteocalcin and alkaline phosphatase activity, the majority of transgenic cells expressing the dominant-negative β_1 integrin subunit lost attachment and died, which further suggests that β_1 integrin is very important in the regulation of cellular adhesiveness. Other studies have shown osteoblast interactions with the collagen type I binding integrin $\alpha_2\beta_1$ specifically activate MAPK mediated signal transduction, which in turn leads to Cbfa1 transcription factor activation (Xiao et al., 1998). In view of the number of results describing ECM-induced integrin-dependent signaling that have been previously reported, it is important to point out that our study deals with only a small number of signaling pathways. Some of the

other pathways include mitogen-activated protein kinase activation, Ca^{++} influx, pH alterations, and inositol phosphate turnover (Yamada and Geiger, 1997). The investigation of these may lead to additional clues as to the regulatory influences of ECM attachment proteins.

In conclusion, adhesion of osteoblasts to ECM proteins appears to be primarily mediated by the class of integrins containing β_1, as adhesion of these cells was primarily mediated by FN, Coll, or LN. This same class of integrins appears to be responsible for the signal transduction process that stimulates *opn* induction. The β_3 integrin containing receptors appear to play a lesser role in adhesion, since neither vitronectin nor osteopontin mediated specific adhesion nor induced *opn* gene expression. Therefore, even though cellular attachment may occur through non-specific binding, down stream activation of intracellular signaling responses that are mediated by ECM ligands are explicitly related to the ligand's structural conformation and its interactions with specific receptors.

Acknowledgements:

This work was supported by Supported by a grant from the Department of Defense Bone Health and Military Readiness Program DAMD17-98-1-8510

References

Aarden, E.M., Nijweide, P.J., van der Plas, A., Alblas, M.J., Mackie, E.J., Horton, M.A., Helfrich, M.H., 1996. Adhesive properties of isolated chick osteocytes in vitro. Bone 18, 305-313.

Aplin, A.E., Short, S.M., Juliano, R.L., 1999. Anchorage-dependent regulation of the mitogen-activated protein kinase cascade by growth factors is supported by a variety of integrin alpha chains. J. Biol. Chem. 274, 31223-31228.

Bierbaum, S., Notbohm, H., 1998. Tyrosine phosphorylation of 40 kDa proteins in osteoblastic cells after mechanical stimulation of beta1-integrins. Eur. J. Cell Biol. 77, 60-67.

Burridge, K., Chrzanowska-Wodnicka, M., 1996. Focal adhesions, contractility and signaling. Annu. Rev. Cell Dev. Biol. 12, 463-518.

Carvalho, R.S., Schaffer, J.L., Gerstenfeld, L.C., 1998. Osteoblasts induce osteopontin expression in response to attachment on fibronectin: demonstration of a common role for integrin receptors in the signal transduction processes of cell attachment and mechanical stimulation. J. Cell Biochem. 70, 376-390.

Clark, E.A., Brugge, J.S., 1995. Integrins and signal transductions pathways: the road taken. Science 268, 233-239.

Damsky, C.H., Werb, Z., 1992. Signal transduction by integrin receptors for extracellular matrix: cooperative processing of extracellular information. Curr. Opin. Cell Biol. 4, 772-781.

Damsky, C.H., 1999. Extracellular matrix-integrin interactions in osteoblast function and tissue remodeling. Bone 25, 95-96.

Dodds, R.A., Connor, J.R., James, I.E., Rykaczewski, E.L., Appelbaum, E., Dul, E., Gowen, M., 1995. Human osteoclasts, not osteoblasts, deposit osteopontin onto resorption surfaces: an in vitro and ex vivo study of remodeling bone. J. Bone Min. Res. 10, 1666-1680.

Frisch, S.M., Francis, H., 1994. Disruption of epithelial cell-matrix interactions induce apoptosis. J. Cell Biol. 124, 619-626.

Gerstenfeld, L.C., Chipman, S.D., Kelly, C.M., Lee, D.D., Landis, W.J., 1988. Collagen expression, ultrastructural assembly and mineralization in cultures of chicken embryo osteoblasts. J. Cell Biol. 106, 979-989.

Gerstenfeld, L.C., 1999. Osteopontin in skeletal tissue homeostasis: an emerging picture of the autocrine/paracrine functions of the extracellular matrix. J. Bone Min. Res. 14, 850-855.

Globus, R.K., Holmuhamedov, E., Morey-Holton, E., Moursi, A.M., 1997. Laminin as an autocrine factor for the differentiation and survival of osteoblasts. Bone 23(Suppl), 434.

Globus, R.K., Doty, S.B., Lull, J.C., Holmuhamedov, E., Humphries, M.J., Damsky, C.H., 1998. Fibronectin is a survival factor for differentiated osteoblasts. J. Cell Sci. 111, 1385-1393.

Gotoh, Y., Salih, E., Glimcher, M.J., Gerstenfeld, L.C., 1995. Characterization of the major non-collagenous proteins of chicken bone: identification of a novel 60 kDa non-collagenous phosphoprotein. Biochem. Biophys. Res. Commun. 208, 863-870.

Gronthos, S., Stewart, K., Graves, S.E., Hay, S., Simmons, P.J., 1997. Integrin expression and function on human osteoblast-like cells. J. Bone Miner. Res. 12, 1189-1197.

Gronthos, S., Simmons, P.J., Graves, S.E., Robey, P.G., 2001. Integrin-mediated interactions between human bone marrow stromal precursor cells and the extracellular matrix. Bone 28, 174-181.

Grzesik, W.J., Robey, P.G., 1994. Bone matrix RGD glycoproteins: Immunolocalization and interaction with human primary osteoblastic bone cells in vitro. J. Bone Min. Res. 9, 487-496.

Harter, L.V., Hruska, K.A., Duncan, R.L., 1995. Human osteoblast-like cells respond to mechanical strain with increased bone matrix protein production independent of hormonal regulation. Endocrin. 136, 528-535.

Ilic, D., Almeida, E.A., Schlaepfer, D.D., Dazin, P., Aizawa, S., Damsky, C.H., 1998. Extracellular matrix survival signals transduced by focal adhesion kinase suppress p53-mediated apoptosis. J. Cell Biol. 143, 547-560.

Ingber, D.E., 1991. Integrins as mechanochemical transducers. Curr. Opin. Cell Biol. 3, 841-848.

Ingber, D.E., 1997. Tensegrity: the architectural basis of cellular mechanotransduction. Ann. Rev. Physiol. 59, 575-599.

Jilka, R.L., Manologas, S.C., 1994. The cellular and biochemical basis of bone remodeling. In Marcus, R., (Ed.) Osteoporosis, Blackwell Scientific Publications, Cambridge, MA, USA. pp. 17-47.

Kano, Y., Katoh, K., Fujiwara, K., 2000. Lateral zone of cell-cell adhesion as the major fluid shear stress-related signal transduction site. Circ. Res. 86, 425-433.

Lanyon, L.E., 1987. Functional strain in bone tissue as an objective and controlling stimulus for adaptive bone remodeling. J. Biomech. 20, 1083-1093.

Lanyon, L.E., Goodship, A.E., Pye, C.J., MacFie, J.H., 1982. Mechanically adaptive bone remodeling. Biomech. 15, 141-154.

Liu, Y.K., Uemura, T., Nemoto, A., Yabe, T., Fujii, N., Ushida, T., Tateishi, T., 1997. Osteopontin involvement in integrin-mediated cell signaling and regulation of expression of alkaline phosphatase during early differentiation of UMR cells. FEBS Lett. 420, 112-116.

Meazzini, M.C., Toma, C.D., Schaffer, J.S., Gray, M.L., Gerstenfeld, L.C., 1998. Osteoblast cytoskeletal modulation in response to mechanical strain in vitro. J. Orthop. Res. 16, 170-180.

Moore, M.A., Gotoh, Y., Rafidi, K., Gerstenfeld, L.C., 1991. Characterization of a cDNA for chicken osteopontin: expression during bone development, osteoblast differentiation and tissue distribution. Biochem. 30, 2501-2508.

Mori, S., Burr, D.B., 1993. Increased intracortical remodeling following fatigue damage. Bone 14, 103-109.

Reinholt, F.P., Hultenby, K., Oldberg, A., Heinegard, D., 1990. Osteopontin: a possible anchor of osteoclasts to bone. Proc. Natl. Acad. Sci. USA 87, 4473-4475.

Schaffer, J.L., Rizen, M., L'ltalien, G.J., Benbrahim, A., Megerman, J., Gerstenfeld, L.C., Gray, M.L., 1994. Device for the application of a dynamic biaxially uniform and isotropic strain to a flexible cell culture membrane. J. Orthop. Res. 12, 709-719.

Schaller, M.D., Parsons, J.T., 1994. Focal adhesion kinase and associated proteins. Curr. Opin. Cell Biol. 6, 705-710.

Schwartz, M.A., Schaller, M.D., Ginsberg, M.H., 1995. Integrins: emerging paradigms of signal transduction. Annu. Rev. Cell Dev. Biol. 11, 549-599.

Shyy, J.Y., Chien, S., 1997. Role of integrins in cellular responses to mechanical stress and adhesion. Cur. Opin. Cell Biol. 9, 707-713.

Tanaka, Y., Nakayamada, S., Fujimoto, H., Okada, Y., Umehara, H., Kataoka, T., Minami, Y., 2002. H-Ras/mitogen-activated protein kinase pathway inhibits integrin-mediated adhesion and induces apoptosis in osteoblasts. J. Biol. Chem. 277, 21446-21452.

Terai, K., Takano-Yamamoto, T., Ohba, Y., Hiura, K., Sugimoto, M., Sato, M., Kawahata, H., Inaguma, N., Kitamura, Y, Nomura, S., 1999. Role of osteopontin in bone remodeling caused by mechanical stress. J. Bone Miner. Res. 14, 839-849.

Toma, C.D., Ashkar, S., Gray, M.L., Schaffer, J.L., Gerstenfeld, L.C., 1997. Signal transduction of mechanical stimuli is dependent on microfilament integrity: identification of osteopontin as a mechanically induced gene in osteoblasts. J. Bone Min. Res. 12, 1626-1636.

Urbich, C., Walter, D.H., Zeiher, A.M., Dimmeler, S., 2000. Laminar shear stress upregulates integrin expression: role in endothelial cell adhesion and apoptosis. Circ. Res. 87, 683-689.

Wang, N., Butler, J.P., Ingber, D.E., 1993. Mechanotransduction across the cell surface and through the cytoskeleton. Science 260, 1124-1127.

Wilson, E., Sudhir, K., Ives, H.E., 1995. Mechanical strain of rat vascular smooth muscle cells is sensed by specific extracellular matrix/integrin interactions. J. Clin. Invest. 96, 2364-2372.

Wozniak, M., Fausto, A., Carron, C.P., Meyer, D.M., Hruska, K.A., 2000. Mechanically strained cells of the osteoblast lineage organize their extracellular matrix through unique sites of alphavbeta3-integrin expression. J. Bone Min. Res. 15, 1731-1745.

Xiao, G., Wang, D., Benson, M.D., Karsenty, G., Franceschi, R.T., 1998. Role of the alpha2-integrin in osteoblast-specific gene expression and activation of the Osf2 transcription factor. J. Biol. Chem. 273, 32988-32994.

Yamada, K.M., Geiger, B., 1997. Molecular interactions in cell adhesion complexes. Curr. Opin. Cell Biol. 9, 76-85.

Zhang, Z., Vuori, K., Reed, J.C., Ruoslahti, E., 1995. The $\alpha_5\beta_1$ integrin supports survival of cells on fibronectin and up-regulates Bcl-2 expression. Proc. Nat. Acad. Sci. USA 92, 6161-6165.

Zimmerman, D.L., Jin, F., Leboy, P., Hardy, S., Damsky, C.H., 2000. Impaired bone formation in transgenic mice resulting from altered integrin function in osteoblasts. Dev. Biol. 220, 2-15.

Figure Legends

Figure 1. Comparison of osteoblast adhesion on different extracellular matrix proteins. Petri dishes were coated with 0, 0.1, 3.0, and 10 $\mu g/cm^2$ of the various ECM proteins as described in the materials and methods. Second passage chick osteoblasts ($1x10^4$ cells) were plated per 33 mm well. Fn=fibronectin, Ln=laminin, Opn=osteopontin, C=native collagen type 1, G=gelatin, Vn=vitronectin, and BSA=bovine serum albumin. Std errors of each measurement are denoted in the figure.

Figure 2. Relationship of adhesion mediated induction of osteopontin to specific ECM proteins. Panel A: Northern blot analysis of osteopontin mRNA expression at twenty-four hours after cell adhesion on various ECM coated cell surfaces. Panel B: Relative levels of osteopontin mRNA expression at either 4 or 24 hours after adhesion on various ECM coated surfaces. ECM surface coatings are as denoted in Figure 1. Pl=polylysine coated surfaces.

Figure 3. Relationship of adhesion induced kinase activity to specific ECM protein ligands. Panel A: Relative percent of adherent cells after one hour of adhesion compared to plating on polyL-lysine coated dishes. Panel B: The induction of two classes of kinases, PKA and PKC, that are involved in second signaling were determined in parallel cultures to those assayed in panel A. Total PKC and PKA kinase activities were determined as described in the materials and methods. ECM surface coatings are as denoted in Figure 1. Error bars denote the standard deviations from triplicate measurements.

Figure 4. Comparison of FAK and p-Tyrosine distribution in osteoblasts after plating on BSA, fibronectin, and vitronectin. The nature of the immunolocalized molecules and the protein used to coat surfaces are denoted in the figure. Magnifications are at 400x.

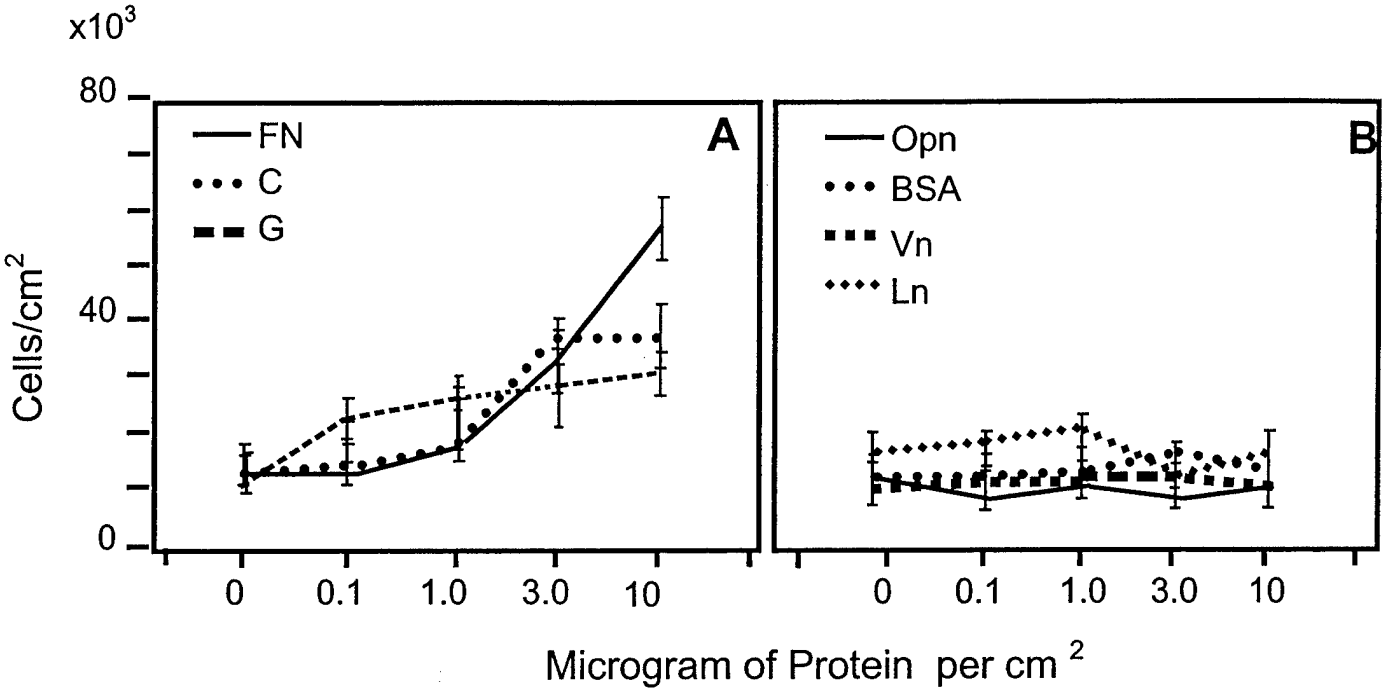
x10^3
80
40
0
Cells/cm^2
FN
C
G
A
Opn
BSA
Vn
Ln
B
0
0.1
1.0
3.0
10
Microgram of Protein per cm 2

Figure 1

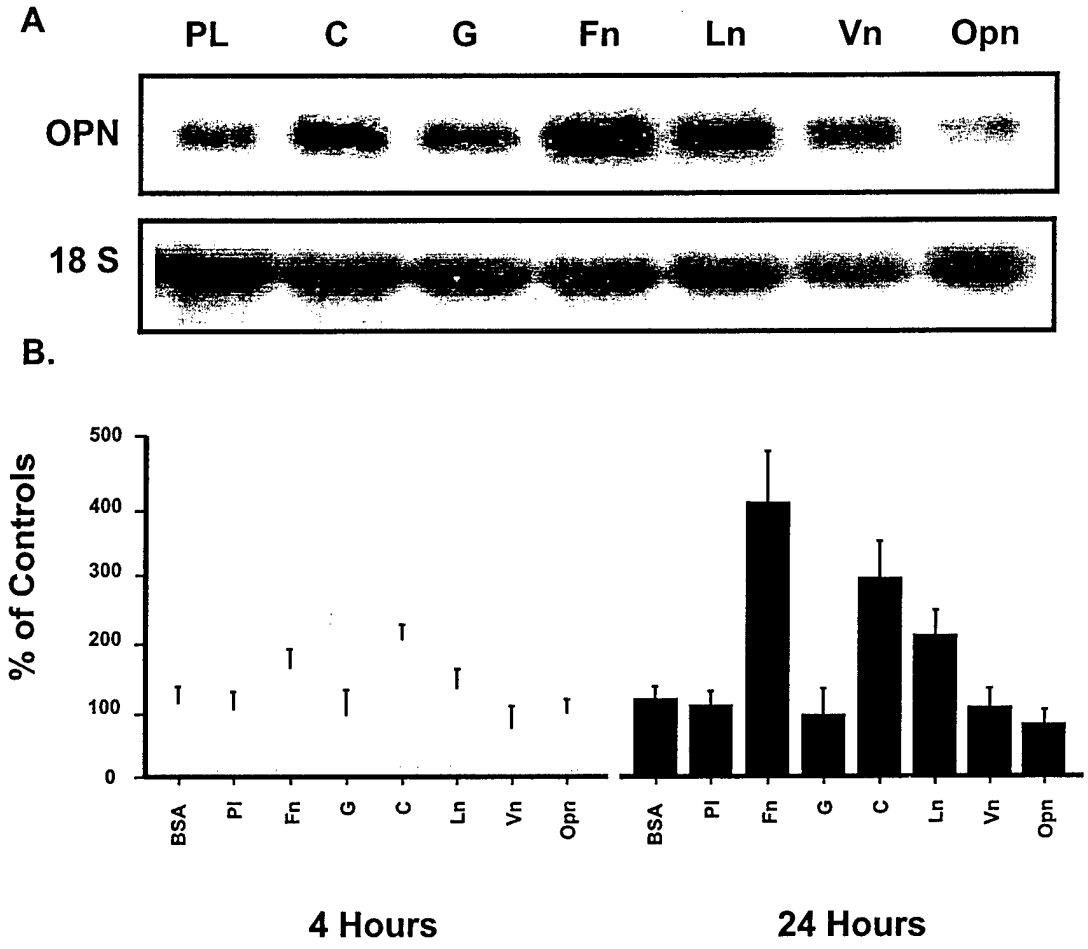
A
PL
C
G
Fn
Ln
Vn
Opn
OPN
18 S
B.
% of Controls
500
400
300
200
100
0
BSA
Pl
Fn
G
C
Ln
Vn
Opn
4 Hours
24 Hours

Figure 2

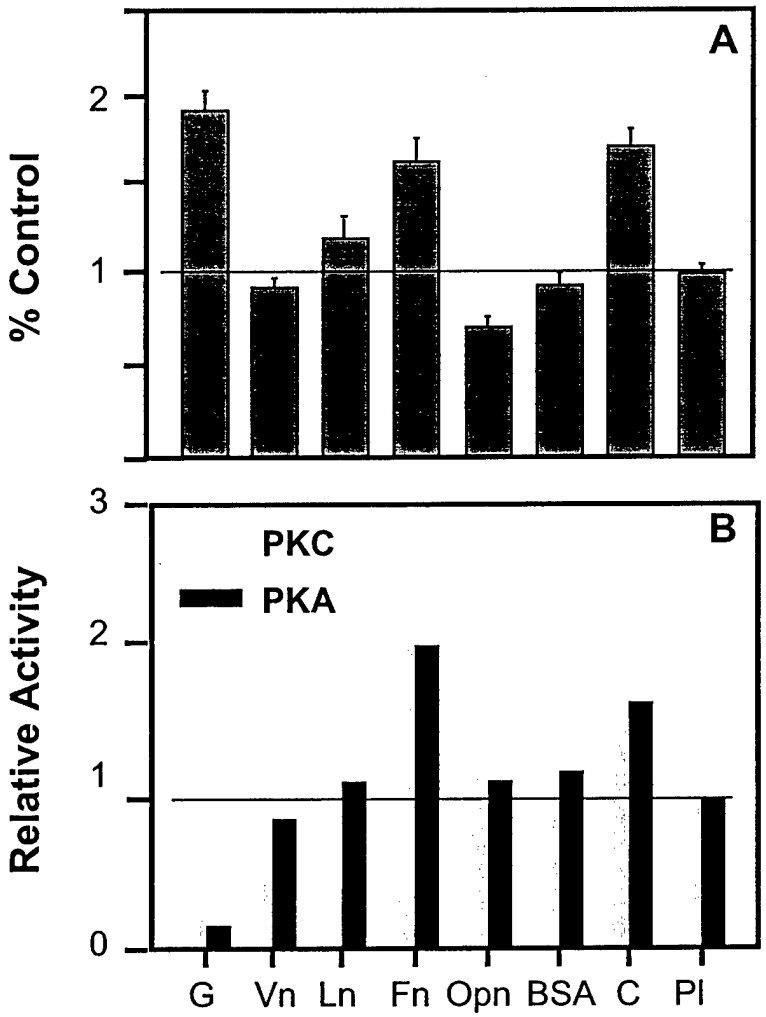
A
% Control
2
1
B
PKC
PKA
Relative Activity
3
2
1
0
G
Vn
Ln
Fn
Opn
BSA
C
Pl

Figure 3

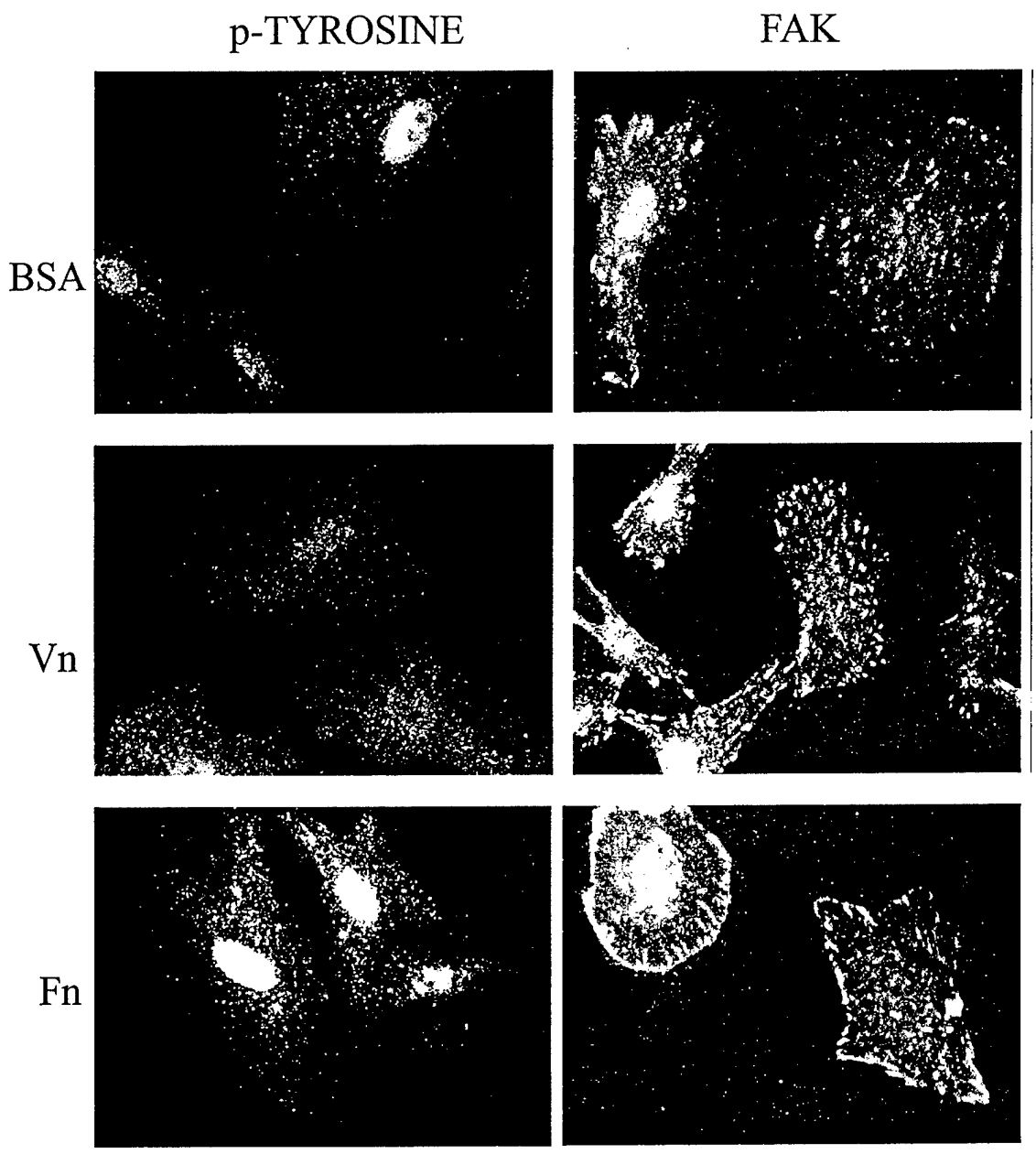

Figure 4

The Role of the Local Mechanical Environment on Tissue Differentiation During Skeletal Defect Repair: Can Repair Recapitulate Development?

Dennis M. Cullinane[α, δ]*, Kristy T. Salisbury[α, δ], Yaser Alkhiary[β],

Solomon Eisenberg[δ], Louis Gerstenfeld[α], and Thomas A. Einhorn[α]

Orthopaedic Research Laboratory, Department of Orthopaedic Surgery, Boston University Medical Center, 715 Albany Street, Housman-205, Boston, MA 02118-2526, USA

Department of Biomedical Engineering, Boston University, Boston, MA

Department of Restorative Sciences and Biomaterials, Boston University School of Dental Medicine, Boston, MA

*Corresponding Author
Dennis M. Cullinane, Ph.D.
Orthopaedic Surgery Laboratory
Housman 205
Boston University Medical Center
715 Albany Street
Boston, MA 02118

ABSTRACT

The local mechanical environment is a crucial factor in determining the differentiation of cells and tissues during skeletal development and repair. This includes cell molecular expression, tissue molecular organization and gross morphology, and resulting tissue mechanical properties. Theoretical, *in vitro,* and *in vivo* models have demonstrated that the regulation of cell molecular expression and the directed development of specific tissue types can be achieved by manipulation of the local mechanical environment. This study tests the hypothesis that precisely controlled mechanical stimulation can regulate cell molecular expression, tissue differentiation, and resulting tissue architecture in an adult rat bone defect model. Custom-designed external fixators capable of introducing daily bending, shear, or a combination of bending and shear load regimens were used to induce precisely controlled mechanical environments within healing femoral defects. These devices allowed the association of specific mechanical loads to cell molecular expression, tissue types, tissue histomorphometrics, and finite element model generated predictions of tissue differentiation. Our results demonstrated that the three experimentally induced mechanical environments 1) created a contiguous cartilage band that persisted within all experimental defects where bone would normally form during the healing process, 2) influenced the ratios of cartilage to bone in all experimental groups approximating that for the knee joint, 3) produced collagen fibril angle specializations between superficial, intermediate, and deep layers in all treatment groups ($p<0.0001$), and 4) resulted in the expression of the cartilage marker molecule collagen type II and the joint determining gene GDF-5 within the experimentally generated tissues. Finally, the finite element models predicted the

differentiation of cartilage within the defects, and that fibrous tissues would develop along the periphery in the bending group. Our results show that local mechanics are an important regulatory factor in cell molecular expression, tissue differentiation, and tissue architecture during healing; and that this relationship is quantitative and can be used to develop a predictive model of tissue differentiation based upon the local mechanical environment. We further demonstrate that mechanical intervention during adult skeletal defect repair can trigger events of early joint development, resulting in a joint-like structure with articular cartilage-like tissues.

INTRODUCTION

Mechanobiology, a science that relates local mechanical loading to cell molecular expression and tissue differentiation, has shown great promise in furthering our understanding of tissue development, ontological adaptation, and repair. For example, the local mechanical environment within the skeleton will directly influence the cells responsible for creating, maintaining, and repairing tissues, creating either cartilage or bone based on its specific characteristics (Carter, 1987; Carter et al., 1991; Cullinane et al., 1999; van der Meulen and Huiskes, 2001). Mechanical loads generated by daily physical activity have been shown to influence skeletal mass, density, and architecture (Carter, 1987; van der Meulen et al., 1995; van der Meulen et al., 1993; Whalen et al., 1993). This mechanosensitivity of the skeleton is also apparent during bone defect repair, with the mechanical environment directly influencing the type and morphology of repair tissues (Carter et al., 1998A; Claes and Heigele, 1999; Cullinane et al., 2000; Cullinane et al., 2002; Gardner et al., 2000; Loboa et al., 2001; Smith-Adaline et al, 2002; Waanders et al., 1998). Similarly, direct parallels have been made between joint development and fracture repair based on these same mechanobiological principles (Cullinane et al., 2002; Ferguson et al., 1999).

Appropriate mechanical stimulation is essential in directing complex tissue architecture such as during joint development (Carter et al., 1998B; Eckstein et al., 2002; Heegaard et al., 1999; Sarin and Carter, 2000; Smith et al., 1991). The mechanical properties of the resulting tissues can also be correlated to the applied load (Grodzinsky et al., 2000). Thus, cartilage, and specifically articular cartilage demonstrates direct dependency on the mechanical environment for normal development and maintenance

(Beaupre et al., 2000; Grodzinsky et al., 2000; Loboa-Polefka et al., 2002). Evidence of this relationship can similarly be found in studies of joint immobilization which significantly alters tissue developmental pathways (de Rooji et al., 2001; Hall, 1972; Smith et al., 1991).

This study was designed to empirically test the mechanobiological paradigm as it applies to cell molecular expression, tissue differentiation, and tissue architecture. The goal of our experimental design was to mimic, within an adult healing bone defect, the local mechanical environment during early joint development (post segmentation). Joint-like mechanical loads (bending and shear) were imposed on the cells and tissues differentiating within healing bone defects in adult animals using custom designed external fixation devices. We compared molecularly, histomorphometrically, and architecturally, the tissues resulting from three different mechanical loading environments imposed within a healing bone defect using histologic, morphometric, and molecular analyses. We also compared those results to native cartilage tissues as well as to predictions based on computer-generated finite element models. Finally, we assayed for the expression of type II collagen to confirm the presence of cartilage, as well as the expression of growth and differentiation factor-5 (GDF-5) which is a joint development-related gene. The goal of this study was to characterize the empirical relationship between the mechanical environment and cell molecular expressions, tissue type expression, and collagen architecture.

MATERIALS AND METHODS

Finite Element Models

Finite element models (FEMs) were used to create predictive models of tissue types and their spatial distribution within the defect of each mechanical treatment type. Their composition required a representative 3D reconstruction of the defect coupled with real input loads and material properties (Figure 1). The FEMs then generated experimentally imposed stress and strain distributions within the modeled defect. Our models were based on a bone defect FEM by Carter et al. (1988), using ideal geometric tubes to represent the femur and a mid-tube segment representing the defect. Tubes represent the cortical bone shaft and serve as rigid boundaries because the bone is orders of magnitude stiffer than the materials within the early healing defect. The defect is represented by a middle segment of the tube with different mechanical properties from the cortical bone portion of the tube and the medullary canal. The mechanical properties of the defect were taken from the literature for callus at an equivalent early stage of maturation (Gardner et al., 2000). We expected the early callus to be representative of a fluid to semi-solid phase material and so hydrostatic forces should dominate. The finite element models were used to 1) estimate local mechanical loading conditions, and using that information, to 2) predict the patterns of tissue differentiation within the defect. We modeled both the bending and shear actions.

A number of nodes comprise the brick elements of the model. We estimated the brick elements to be 0.05 mm in magnitude. The FE analysis was performed using I-DEAS software (Schroff Development Corp., Mission, KS). Solids including bone and condensed cell masses were meshed into elements using mesh generation software.

Stress and strain distributions are estimated by the model, and tissue types are assigned to these levels based on Carter et al., (1988, 1998). Hydrostatic stress and maximum principal tensile strain are calculated for the different mechanical actions, and spatial tissue predictions are assigned based upon quantitative and relative stress and strain levels according to Giori et al., (1993). The tissues we expected from our stimulations included cartilage (under relatively high hydrostatic compressive stress), fibrocartilage (under relatively high hydrostatic stress and high tensile strain), bone (under relatively lower hydrostatic stress and lower hydrostatic strain), and fibrous tissue (under relatively low hydrostatic stress but high tensile strain).

External Fixation

A total of twelve Sprague-Dawley rats weighing 421 $\pm$ 34 grams were used in this study. Animal care and experimental protocols were followed in accordance with NIH guidelines and approved by Boston University's Laboratory Animal Science Center IACUC. Four animals were used in each group, bending, shear, and the alternating combination group. The external fixator is modified from a model used in a previous study while the surgical procedure is identical to the one used in that study (Cullinane et al., 2002). The external fixator is surgically applied to the right femur and an osteotomy is created leaving a 2 mm defect within the femoral diaphysis. The external fixator, in conjunction with the linkage system, is capable of imposing both 12° symmetrical bending and 10% symmetrical cortical shear, depending on the locking screw insertion configuration (Figure 2A). The fixator body is made of two articulating solid aluminum rectangular prisms with cortical pin holes, and clamping and locking screws. The

clamping screws fasten the cortical pins into the fixator and the locking screws arrest the fixator pivot or shear actions (Figure 2B).

Mechanical Stimulation

To perform the mechanical stimulations an oscillating linkage system was built that supplied a rotational moment which could be applied to the fixators as an oscillating vertical displacement (Figure 3). Our stimulation protocol followed that established by a previous study (Cullinane et al., 2002). The vertical displacement is then translated by the fixator into either 10% shear or 12° bending. The motion was applied using a servomotor (model #2602-010, QCI-23-5-E-01 Quicksilver Controls Inc., Covina, CA). The speed of the motor was controlled using a PC computer-based software). The shaft of the servomotor was coupled to one of two eccentric shafts of a torque transducer (model #1102-50, Lebow Products, Troy, MI). One eccentric shaft of the transducer was connected to the linkage. A torque sensor connected to an external data acquisition board (model #100, InstruNet Inc., Cambridge, MA) acted as a bridge voltage sensor and controlled the torque transduced to the fixator. Based on the manufacturer's specifications the torque sensor was mapped to 1.967 millivolts/ounce-inches, with the input torque sampled at 60 Hertz for the duration of each experimental session. The peak torque required to induce the respective motions was recorded as the baseline value. The loading apparatus was then calibrated prior to every application using InstruNet, PC-based software.

There were three mechanical stimulation protocols executed during this study: bending at 12°, 10% shear, and alternating 12° bending and 10% shear on even and odd

days (% of cortex diameter), with both the bending and shear actions symmetrical to the longitudinal axis. All mechanical stimulations were symmetrical to the alignment of the cortices, and cyclical. Starting at post-operative day three and continuing for six weeks, the mechanical stimulations were induced for six consecutive days, with one day of rest each week. The fixator on each animal was attached to the linkage system which instituted the respective bending and shear actions initiated by the motor. The results from these three treatment groups were compared to previous control specimens.

Prior to each mechanical session the treatment animals were anesthetized, the fixators were attached to the linkage, the locking screws were removed, and cyclic stimulations were applied for 15 min at a frequency of 1 Hz. A dedicated computer coordinated the application of the mechanical treatment and data acquisition during calibration and treatment. The locking screws were replaced upon completion of each session. Once recovered from the anesthesia the animals are returned to the housing room and allowed to ambulate freely in their cages.

Histology

Animals were euthanized at the termination of the study and the femora excised. Standard histological methods were employed to generate serial 5 μm thin sections from the specimens which were used for standard histology (Cullinane et al., 2002). The sections were mounted on glass slides, and every tenth slide stained using a Safranin-O stain, while every other eleventh slide was stained with alcian blue and counter stained with eosin for detection of proteoglycans. The five micron decalcified histological specimens were examined under a light microscope using 1.25X through 40X objectives

and a polarizing filter. Dark field images were obtained through the use of a polarizing filter which highlighted collagen fibrils for quantification of their orientation and conformity within the new extracellular matrices.

Histomorphometrics: Tissue type composition

Tissue type area composition was quantified for bone and cartilage percentage for each of the treatment groups and the control group, as well as rat knee and lumbar intervertebral joints. The entire defect and joint were quantified for tissue percentage within a standardized area of interest including 2.5 mm in both directions, proximal and distal, from the defect or joint center. Tissue type ratios were generated for each treatment group and the controls, as well as actual native rat joints. Comparisons were made to identify similarities in tissue composition ratios between the treatment groups and the native rat joints.

Histomorphometrics: Collagen architecture quantification

In order to characterize the molecular organization of the newly formed cartilage tissues, collagen fibril orientation and angular agreement were quantified using polarizing light microscopy and histomorphometric analyses using MatLab© and ImagePro©. Fast Fourier transforms were performed on digitized images of polarized light micrographs, and the preferred collagen fibril orientation was determined by the most intense region in their power spectra (Figure 4). This procedure was performed as previously described by Cullinane et al. (2002). Polarized light micrographs were taken from predetermined superficial, intermediate, and deep regions of the experimentally derived cartilage tissues

in order to highlight collagen fibrils. These images were then incorporated into a MatLab Fourier Transform analysis to determine mean collagen fibril orientation and fibrillar agreement.

Molecular Analyses

Molecular analyses of the expression of specific genes or proteins was carried out by either *in situ* hybridization or immunostaining in order to confirm tissue types and to identify the expression of the joint-development-related gene. *In situ* hybridization was carried out for collagen type II using a commercially available probe for RNA run of labeling. Linearized plasmids containing this gene were purchased from PharMingen Corp. (San Diego, CA, USA). Single stranded ^{35}S-labeled cRNA probes were generated by *in vitro* transcription (PharMingen Corp, San Diego, CA, USA). Linearized plasmids containing each of the selected genes for analysis were transcribed with use of ^{35}S-uridine triphosphate (UTP) (NEN Life Science Products, Inc., Boston, MA, USA) and T7 RNA polymerase, then digested with DNase, phenol extracted and ethanol precipitated. The labeling efficiency for the cRNA products was determined by scintillation counting, and adjusted to a concentration of 3×10^5 cpm/μl of probe for each *in situ* assay.

Tissue Procurement: Tissue samples were fixed overnight in freshly prepared 0°C 4% paraformaldehyde, followed by decalcification in 14% EDTA for up to eight weeks. Decalcified samples were paraffin embedded.

Tissue preparation and sectioning: Fixed and decalcified tissues were dehydrated in graded ethanol up to 100%, transferred to xylenes, then embedded in paraffin. Five-micron thin paraffin sections were placed on poly L-lysine coated slides, dried overnight and used immediately or stored at 4 C.

Probe preparation. Sense and antisense ^{35}S-labeled cRNA probes were used for hybridization. Vectors were appropriately linearized and incubated with either T7 or SP6 RNA polymerase in the presence of ^{35}S-UTP (New England Nuclear, Boston, MA), unlabeled nucleotides, 10mM DTT, and RNasin RNase inhibitor (Promega, Madison, WI). Labeled cRNA probes were separated from free nucleotides using Mini Quick Spin RNA column (Roche Molecular Biochemicals, Indianapolis, IN).

Prehybridization. Slides were deparaffinized in xylenes followed by rehydration in graded ethanol solutions, rinsed in 0.85% NaCl (5 minutes) and 1X PBS (5 min). Sections were treated with proteinase K (20μg/ml) for 8 minutes at 37°C. Slides were dipped successively in 1X PBS (5 min), 4% paraformaldehyde (5 minutes), acetylated in 0.25%. GDF-5 expression was examined by immunohistochemical. For these studies an antibody to GDF-5 was obtained from Santa Cruz Biotechnology, Inc. (Santa Cruz, CA). Briefly, histochemical staining was carried out using antigen retrieved at 199° F for 10 min in 10mM sodium citrate. The GDF-5 antibody (0.5 μg/ml) was applied to the sections followed by a biotinylated secondary antibody and HRP conjugated Strepavidine complex, and visualized with DAB chromogen.

RESULTS

Finite Element Models

The results from the finite element models indicate that unique distributions of stress and strain exist within the defects between the bending and shear groups (Figure 5). The distribution of tensile strain within the bending defect peaks at the defect periphery and subsides linearly in the direction of the defect center. Compressive stress acts in opposite response to the tensile strain, peaking almost simultaneously but in the vicinity of the opposite cortex. These strain levels correspond with the magnitude of displacement of the cortices on the tensile side during bending excursion. This distribution of tensile strain (and compressive stress) spans the entire defect with diminishing values approaching the defect center. Finite element model estimated peak strain levels in the bending group reach 7.87×10^{-6} E, while peak strain in the shear groups reaches only 1.95×10^{-11} E, with a more narrow range of strain distribution in the proximal-distal direction. According to the relative scale used by this study, fibrous tissues would form in the bending group within the estimated range of 7.87×10^{-6} to 6.07×10^{-6}E, with cartilage forming in the range from 5.84×10^{-6} to 3.37×10^{-6}E, and bone within the range from 2.70×10^{-6} to 2.20×10^{-6} E. The shear group tissue differentiation ranges for strain include 1.95 X 10-11 to 1.56×10^{-11} E for fibrous tissue, 1.47×10^{-11} to 8.79×10^{-12} E for cartilage, and 7.82×10^{-12} to 2.93×10^{-12} E for bone.

The architecture of the bone and cartilage structures formed within the defect of the bending group specimens reflect not only the distribution of stress and strain, but the motion of the bending action, where the bone has formed an arch closely following the action of the fixator, and whose anatomical peak is located at the neutral axis of bending.

The shear group distribution is linearly aligned with the arches being much more flat in profile. The stress and strain distributions were then incorporated into graphic models of expected tissue differentiation for each of the mechanical stimulations (Figure 6). The areas of higher compressive stress were predicted to foster cartilage differentiation whereas the areas of extreme tensile strain are predicted to foster the differentiation of fibrous tissue. The areas within the high compressive stress region, but that are shielded by previous cartilage formation, are predicted to foster bone.

Radiology

Radiographs were taken weekly to determine the progress of mineralized tissue formation within and around the defects. The weekly radiographs illustrated the onset of bony bridging across the defects in the control specimens while the treatment defects each demonstrated defect lucency and complete nonunion in all specimens (Figure 7). Areas of reduced density represent cartilage or fibrous tissue while high density areas represent mineralized tissues such as bone. A distinctive arch-shaped structure spanning the defect cortices can be seen in the bending group.

General Histology

The shear treatment was preceded by an experimental test to determine an appropriate shear magnitude. This test, using two shear magnitudes demonstrated two completely different tissue outcomes. One group experienced 10% shear magnitude while the other experienced 25% shear. The 10% magnitude shear group developed a cartilage band

across the entire defect while the 25% shear defect developed only fibrous tissue across the defect (Figure 8).

The mechanical treatment groups all demonstrated the presence of a cartilage band spanning the entire defect while the control specimens demonstrated bony bridging of the defect (Figure 9). The cartilage tissues stained red while the bone and fibrous tissues stained blue-green. The bending specimens acquired an arched appearance to their cartilage and the underlying subchondral bone arch on at least one side of the defect, while the shear and combination groups showed parallel and evenly distributed cartilage bands.

Histomorphometrics: Tissue type composition

The ratio of cartilage to bone is one of the basic defining characters of a synovial joint. We examined this ratio in our experimental tissues and compared them to the rat knee joint. We found that the ratio of cartilage to bone in our experimental tissues were each very similar to articular cartilage, and especially in comparison to control endochondral healing callus (Table 1). The control specimens ratio of bone to cartilage averaged 94:6. In the experimental results the bending group ratio of bone to cartilage average 78:22 and the shear group averaged 80:20. The combination group ratio averaged 82:18. None of the treatment groups were significantly different from the knee joint but all were significantly different from the control ($p<0.05$). Thus, we found consistent ratios of cartilage to bone in our experimental tissues and ones which mirrored the knee joint average of roughly 80:20. The intervertebral joint was unique in that its cartilage to bone ratio was significantly different from all others ($p<0.00062$), approximating 50:50.

Histomorphometrics: Collagen architecture quantification

The experimentally generated cartilage tissues demonstrated visually distinct zones of collagen fibril organization with specialized fiber orientations in each zone (Figure 10). Obvious were the superficial and deep zones, with a less obvious transitional intermediate zone. Mean collagen fibril angles were not significantly different between the different treatment groups for each of the layers: superficial, intermediate, and deep, except the shear intermediate group (Table 2). The intermediate shear layer was significantly different from both the bending and combination groups' ($p<0.001$). The intervertebral joint tissue was not used in this analysis due to its specialized and very different structural configuration.

Molecular analysis

In situ hybridization confirmed the presence of type II collagen within the tissues differentiating in the experimental defects (Figures 11A&B). Type II collagen is a marker molecule for all forms of cartilage and its presence confirms that the tissue differentiating within the defect is cartilage. We observed collagen type II expression at constant but relatively low levels throughout the tissue. However, higher levels of expression were seen in a band of cells adjacent to the area of fibrous tissue where cartilage cavitation was initiating. We also saw a weaker band of labeled cells adjacent to the subchondral bone formed under the cartilage band. Immunohistology also identified the presence of GDF-5 within the cells of the bending experimental cartilage (Figure 12). The positive presence of this molecule is indicated by a brown stain located

around the cells differentiating within the defect. Its presence in the experimental tissues is contrasted by its absence in the controls.

Discussion

Mechanobiological theory dictates that the local mechanical environment influences the differentiation of cells and tissues during the processes of development and healing. Our experimental results have confirmed that an empirical relationship exists between the mechanical environment and the resulting tissues within a mechanically stimulated healing bone defect. Quantifications of resulting tissue types and their molecular architecture verify that a direct and quantifiable relationship can be established between different mechanical treatments and their respective tissue outcomes. We also found that specific mechanical stimuli can trigger the expression of molecules such as collagen type II (cartilage formation) and GDF-5 (bone and joint formation). These results further suggest that mechanical stimulation, during the process of bone defect repair, can recapitulate developmental events from joint development.

Our results, based upon precise mechanical stimulations, demonstrate uniform cartilage bands across the defects whose collagen organization shows a complex, multilayered architecture reminiscent of articular cartilage. These cartilages are maintained well past the time of healing in the controls and we predict they will remain so long as the respective mechanical environments continue. This is an intuitive outcome in our estimation, as our mechanical interventions were designed to mimic the actions of a developing joint. The histomorphometric results verify that the ratio of tissues differentiating within the experimentally treated defects is in large part controlled by the mechanical interventions, varying by intervention type. The organizations of collagen fibrils within the experimentally derived tissues demonstrate highly organized, multilayered patterns that resemble articular cartilage. The experimental tissues

demonstrate a three layer structure with different collagen fibril orientations in each layer, as well as between the different treatment types. The results of the shear pilot study are particularly interesting because they underline the extremely divergent results one can expect based solely on differences in the mechanical environment. We believe those results serve as a tremendous example of the predictive power of the mechanobiological paradigm.

Our molecular results are encouraging because they demonstrate two principal findings: First, that the presence of collagen type II confirms our experimentally derived tissues are indeed cartilage, and second, that a gene associated with the *in utero* development of joints (GDF-5) is upregulated as a result of the bending stimulation. The comparison between the *in situ* reactions in normal post-natal long bones to those obtained from the mechanically induced cartilage was very informative. It is interesting to note that high levels of cartilage mRNA expression were not observed in fully differentiated joint tissues, but were observed with very intensely labeled areas of cartilage formation within the epiphyseal growth plate. Similarly, in the areas of mechanically induced cartilage formation we observed collagen type II expression at low levels throughout the tissue. However, higher levels of expression were seen in a band of cells adjacent to the area of fibrous tissue where cartilage cavitation was initiating. We also saw a weaker band of labeled cells adjacent to the subchondral bone that formed under the cartilage band.

These results suggest that the mechanical environment has a direct and quantifiable effect on cell expression and tissue differentiation within healing bone defects. Specifically, we have documented that molecular expression, tissue type, and

tissue molecular architecture are influenced by the local mechanical environment. In this particular case our mechanical stimulation regimens were designed to simulate the action of a developing joint. As a result, the experimental tissues and their molecular architecture took on joint-like characteristics in several aspects of our analyses. We believe these results emphasize, on numerous levels, the importance of the mechanical environment in tissue differentiation. This relationship is an important one and will help us to better understand the factors controlling tissue development and repair.

Cases of mechanically unstable fractures will likewise demonstrate the presence of cartilage within a healing bone defect, but the location, amount, and architecture of that cartilage differs markedly from our precise mechanical intervention cartilage. Classic pseudoarthroses or "false joints" are typically a random conglomeration of fibrotic tissue, cartilage, and bone. This configuration is directly related to the randomness of the local mechanical environments and their variant magnitudes.

The outcomes of this study confirm that mechanobiological principles can accurately predict cell molecular expression, tissue differentiation, and tissue architecture. They further emphasize the important role the local mechanical environment plays in the everyday development and repair of the vertebrate body. Further studies need to be conducted in order to determine the precise relationship between the physical environment and cell molecular expression, tissue differentiation, development, and repair.

LITERATURE CITED

Armstrong CG, Lai WM, Mow VC (1984) An analysis of the unconfined compression of articular cartilage. J Biomech Eng 106:165-173.

Arokoski JP, Hyttinen MM, Helminen HJ, Jurvelin JS (1999) Biomechanical and structural characteristics of canine femoral and tibial cartilage. J Biomed Mater Res 48(2):99-107.

Athanasiou KA, Rossenwasser MP, Buckwalter JA, Malini TI, Mow VC (1991) Interspecies comparison of in situ intrinsic mechanical properties of distal femoral cartilage. J Orthop Res 9(3):330-40.

Beaupre GS, Stevens SS, Carter DR (2000) Mechanobiology in the development, maintenance, and degeneration of articular cartilage. J Rehabil Res Dev 37(2):145-51.

Carter DR (1987) Mechanical loading history and skeletal biology. J Biomech. 20(11-12):1095-109.

Carter DR, Blenman PR, Beaupre GS (1988) Correlations between mechanical stress history and tissue

differentiation in initial fracture healing. J Orthop Res 6:736-748.

Carter DR, Wong M, Orr TE (1991) Musculoskeletal ontogeny, phyolgeny, and functional adaptation. J

Biomech 24(S1):3-16.

Carter DR, Beaupre GS, Giori NJ, Helms JA (1998A) Mechanobiology of skeletal regeneration. Clin Orthop

355S:S41-S55.

Carter DR, van der Meulen MCH, Beaupre GS (1998B) Mechanobiologic regulation of osteogenesis and athrogenesis. In: Skeletal Growth and Development: Clinical Issues and Basic Science Advances. Ed by JA Buckwalter, MG Ehrlich, LJ Sandell, SB Trippel. pp 99-130. Am Acad Orthop Surg, Rosemont, IL.

Carter DR, Beaupre GS (2001) Skeletal tissue histomorphometry and mechanics. In Skeletal function and form. DR Carter and GS Beaupre Eds. Cambridge University Press:31-52.

Claes LE, Heigele CA (1999) Magnitudes of local stress and strain along bony surfaces predict the course and type of fracture healing. J Biomech 32:255-66.

Cullinane DM, Inoue N, Meffert R, Tis J, Rafiee B, Chao EYS (1999) Regulating bone at the cellular level: A little evidence for Wolff's Law. Am Zool 39(5):96.

Cullinane DM, Fredrick A, Eisenberg SR, Pacicca D, Elman MV, Lee C, Salisbury K, Gerstenfeld LC, Einhorn

TA (2002) Induction of Articular-like Cartilage and a Joint-like Structure by Controlled Motion in an Experimental Mid-Femoral Defect. J Orthop Res 20(3):579-586.

de Rooji PP, Siebrecht MA, Tagil M, Aspenberg P (2001) The fate of mechanically induced cartilage in an unloaded environment. J Biomech 34(7):961-6.

Dowthwaite GP, Edwards JC, Pitsillides AA (1998) An essential role for the interaction between hyaluronan and hyaluronan binding proteins during joint development. J Histochem Cytochem 46(5):641-51.

Eckstein F, Faber S, Muhlbauer R, Hohe J, Englmeier KH, Reiser M, Putz R. (2002) Functional adaptation of human joints to mechanical stimuli. Osteoarthritis Cartilage 10(1):44-50.

Elder SH, Goldstein SA, Kimura JH, Soslowsky LJ, Spengler DM (2001) Chondrocyte differentiation is modulated by frequency and duration of cyclic loading. Ann Biomed Eng 29(6):476-82.

Ferguson C, Alpern E, Miclau T, Helms JA (1999) Does adult fracture recapitulate embryonic skeletal formation? Mech Dev 87(1-2):57-66.

Gardner TN, Stoll T, Marks L, Mishra S, Tate MK (2000) The influence of mechanical stimulus on the pattern of tissue differentiation in a long bone frature-a FEM study. J Biomechanics 33(4):415-25.

Grodzinsky AJ, Leveston ME, Jin M, Frank EH (2000) Cartilage tissue remodeling in response to mechanical forces. Ann Rev Biomed Eng 2:691-713.

Hall BK (1972) Immobilization and cartilage transformation into bone in the embryonic chick. Anat Rev 173:391-403.

Hartmann C, Tabin CJ (2001) Wnt-14 plays a pivotal role in inducing synovial joint formation in the developing appendicular skeleton. Cell 104(3):341-51.

Heegaard JH, Beaupre GS, Carter DR (1999) Mechanically modulated cartilage growth may regulate joint surface morphogenesis. J Orthop Res 17(4):509-17.

Loboa EG, Beaupre GS, Carter DR (2001) Mechanobiology of initial pseudoarthrosis formation with oblique fractures. J Orthop Res 19:1067-1072.

Loboa-Polefka EG, Wren TAL, Carter DR (2002) Mechanobiology of soft tissue regeneration. 48th Annual Meeting Orthop Res Soc, Dallas.

Mow VC, Kuei SC, Lai WM, Armstrong CG (1980) Biphasic creep and stress relaxation of articular cartilage in compression: Theory and experiments. J Biomech Eng 102:73-84.

Mow VC, Zhu W, Ratcliffe A (1991) Structure and function of articular cartilage and meniscus. In Basic Orthopaedic Biomechanics, VC Mow and WC Hayes eds. Raven Press, New York :143-98.

Narmoneva DA, Cheung HS, Wang JY, Howell DS, Setton LA (2002) Altered swelling behavior of femoral cartilage following joint immobilization in a canine model. J Orthop Res 20(1):83-91.

Sarin VK, Carter DR (2000) Mechanobiology and joint conformity regulate endochondral ossification of sesamoids. J Orthop Res 18(5):706-12.

Smith RL, Thomas KD, Schurman DJ, Carter DR, Wong M, van der Meulen (1991) Rabbit knee immobilization: Bone remodeling precedes cartilage degredation. J Orthop Res 10:88-95.

Smith-Adaline EA, Ignelzi MA, Volkman SK, Slade JM, Goldstein SA (2002) Chondrogenesis is influenced by mechanical environment during fracture healing concommitant with altered expression of BMP-4, VEGF, and IHH. 48th Annual Meeting Orthop Res Soc, Dallas.

Stegmann H, Stalder K (1967) Determination of hydroxyproline. Clin Chim Acta 18:267-73.

Storm EE, Kingsley DM (1999) GDF-5 coordinates bone and joint formation during digit development. Dev Biol 209(1):11-27.

Suh JK, Youn I, Fu FH (2001) An in situ calibration of an ultrasound transducer: a potential application for an ultrasonic indentation test of articular cartilage. J Biomech 34(10):1347-53.

van der Meulen MC, Beaupre GS, Carter DR (1993) Mechanobiologic influences in long bone cross-sectional growth. Bone 14(4):635-42.

van der Meulen MC, Morey-Holton CR, Carter DR (1995) Hindlimb suspension diminishes femoral cross-sectional growth in the rat. J Orthop Res 13(5):700-7.

van der Meulen MCH, Huiskes R (2001) Why mechanobiology? J Biomechanics 35(4):401-414.

Waanders NA, Richards M, Steen H, Kuhn JL, Goldstein SA, Goulet JA (1998) Evaluation of the mechanical environment during distraction osteogenesis. Clin Orthop 349:225-34.

Whalen S (1993) Musculoskeletal adaptation to mechanical forces on Earth and in space. Physiologist 36(1 Suppl):S127-30.

Wong M, Siegrist M, Wang X, Hunziker E (2001) Development of mechanically stable alginate/chondrocyte
constructs: effects of guluronic acid content and matrix synthesis. *J Orthop Res* 19:493-9.

Figure 1 A finite element model of the defect. The cortical bone is represented as an ideal tube with relative thickness while the defect is represented as a mid-segment of the tube. The mechanical properties of the defect are taken from the literature for callus mechanics while the cortical bone is modeled as an incompressible solid. The model is given geometry, mechanical properties, and load characteristics. The model generates stress and strain distribution fields that are used to create tissue differentiation predictions.

Figure 2 An external fixator mounted on a rat femur with an AutoCad representation of the device below. Top: The pin clamping screws can be seen facing out from the animal. The device is in the straight and locked position, maintaining rigid fixation within the defect. The healed surgical incision site can be seen below the fixator. Bottom: The bicortex pins are situated in the pin channels (green arrows) and are fixed by clamp screws (yellow arrows). When the locking screws are in place (white arrows) the device is capable of rigid fixation

Figure 3 The linkage system which connects the motor and torque sensor to the fixator, inserted by pins into the rat femur. As the wheel (bottom right) rotates, the horizontal actuator arm (bottom) drives the vertical piston (bottom left) which is attached to one side of the fixator (occulted by the plate). As the fixator bends on its axis or displaces in shear the defect is stimulated. The rat is lying in a sling hammock with its tail protruding to the left.

Figure 4 An example Fourier transform of collagen fibril architecure. The panels represent the stages of Fourier analysis including a thresholded image, ellipse, and frequency distribution. The transform identifies the predominant pattern within an image (in this case fibrillar orientation). The predominant angle, identified by highest frequency, is relative to the original captured image's orientation but in our final analysis we make the angle relative to a presumed defect midline, perpendicular to the bone long axis.

Figure 5 A FEM illustrating strain distribution within the defect for shear (A&B) and bending (C&D). The 3D models are to the left while their respective cross section representations are to the right. The models presented are from an intermediate stage of loading to illustrate the strain progression. The distribution of strain is illustrated using the color bars to the right of each active model. Note the strain distribution in the 12° bending model has not yet spanned the defect from one cortex to the other, which would predict that a threshold may exist in that area for the differentiation of tissues such as cartilage or bone. Altering the mechanical properties of the defect tissues alters the results of the models. The number of brick elements and the composition of the structure also play a role in determining the models effectiveness in estimating local mechanical loads.

Figure 6 Stress and strain based tissue prediction diagrams based on finite element results for 12° bending (left) and shear (right). The area in green represents putative cartilage, the areas in red represent putative fibrous tissues, and the blue areas represent

bone. The bending model predicts two opposing convex bone elements but does not predict that the cartilage element will completely segment between the proximal and distal halves. The shear model predicts cartilage segmentation between the halves.

Figure 7 Radiographs of control, bending, and shear specimens with the external fixators attached. In every case the mechanically stimulated defects resulted in nonunion. The cartilage tissues in the experimental treatment defects are represented by lucencies in the gaps between the segments. All experimental treatments were for a 35 day (6 week) duration. The control specimen example is from a four week control specimen, demonstrating the rapid bony bridging occuring in the controls.

Figure 8 An illustrative example of the mechanobiological paradigm at work. Here the magnitude of strain graphically dictates the differentiation of cartilage versus fibrous tissue within the mechanically stimulated defects. The defect to the left underwent 10% cortex diameter shear whereas the defect to the right underwent 25% shear. Thus, a threshold exists between these shear magnitudes which determines cartilage versus fibrous tissue outcomes.

Figure 9 The histological results from our A) control, B) bending, C) bending & shear, and D) shear pilot stimulations. Note the control exhibits almost no cartilage while the treatment groups all present cartilage bands spanning the defect. Note also the arched nature of the cartilage band in the bending specimen, a further mechanobiological response to the bending action.

Figure 10 Fourier transformation of control cartilage collagen fibril orientation. Very little cartilage is produced within the control specimens due to the reduced magnitude of the local mechanical environment. This example also demonstrates the randomness of the collagen fibril architecture within the control specimens.

Figure 11A In situ hybridization analysis of type II collagen mRNA expression in control murine femoral joint tissues and in mechanically induced tissues. Left upper panel: 10X magnification analysis comparing light and dark field images of in situ hybridization profiles of a normal murine joint and the underlying epiphyseal plate. Note the intense primary expression of type II collagen in the epiphyseal plate but not in the area of mature joint cartilage collagen. Lower panels: 20X magnification analysis of the cartilage tissue produced by controlled mechanical loading, forming an artificial joint like structure. Collagen type II expression is seen at low levels throughout the tissue but shows higher levels of expression in a band of cells adjacent to the area of fibrous tissue where cartilage cavitation is beginning to occur.

Figure 11B In situ hybridization analysis of type II collagen mRNA expression in control murine femoral joint tissues and in mechanically induced tissues. The 40X magnification shows silver grain localization over cartilage cells of native cartilage within the epiphysis and over chondrocytes within mechanically generated tissues.

Figure 12 Immunohistologically stained sections of bending stimulated (left) and control (right) cartilages. The brown stain in the mechanically stimulated cartilage indicates the expression of growth and differentiating factor-5 (GDF-5) whereas the control section (right) demonstrates no reaction. The positive reaction to GDF-5 indicates that the mechanical stimulation therapy is causing the expression of this joint determining gene.

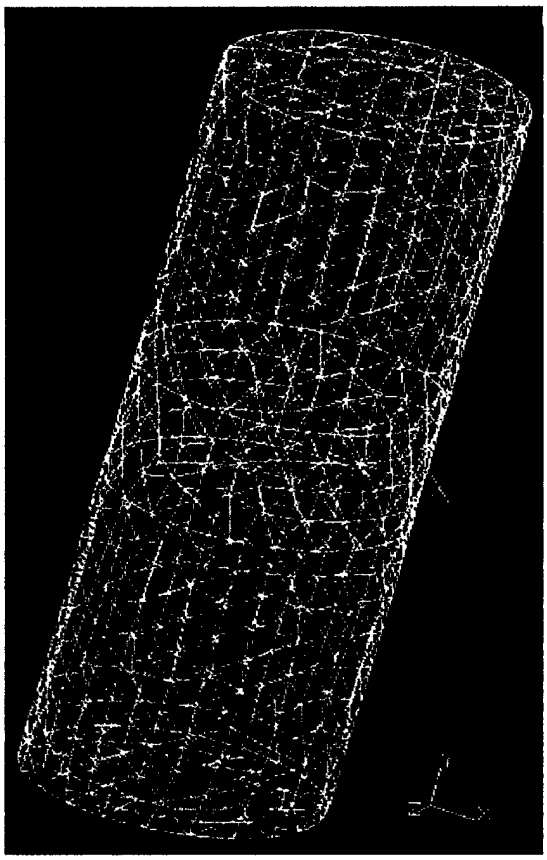

Figure 1

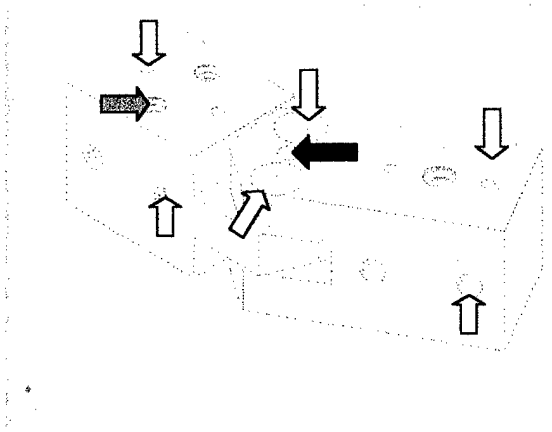

Figure 2

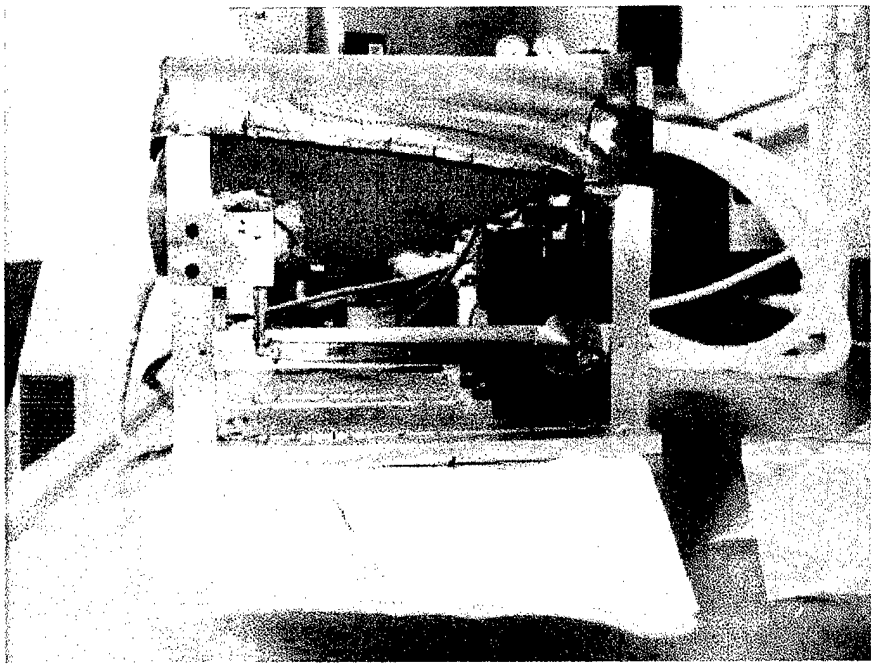

Figure 3

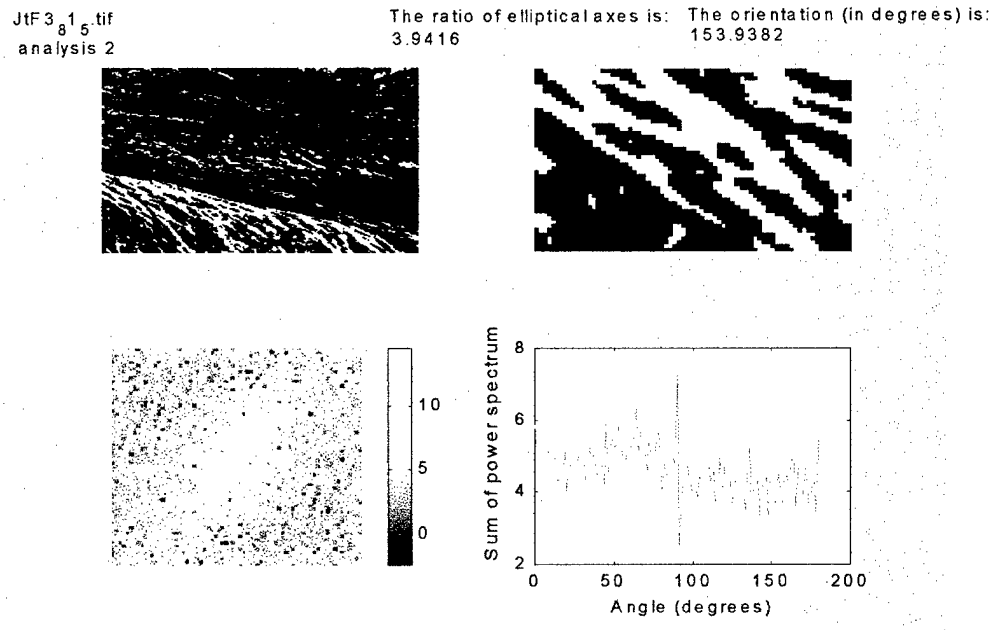
JtF3_8 1_5.tif
analysis 2
The ratio of elliptical axes is:
3.9416
The orientation (in degrees) is:
153.9382
10
5
0
Sum of power spectrum
8
6
4
2
0
50
100
150
200
Angle (degrees)

Figure 4

A

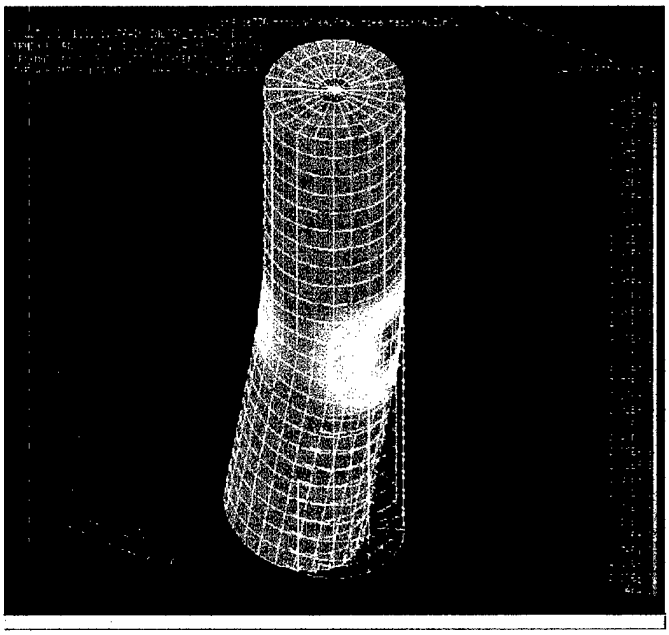

B

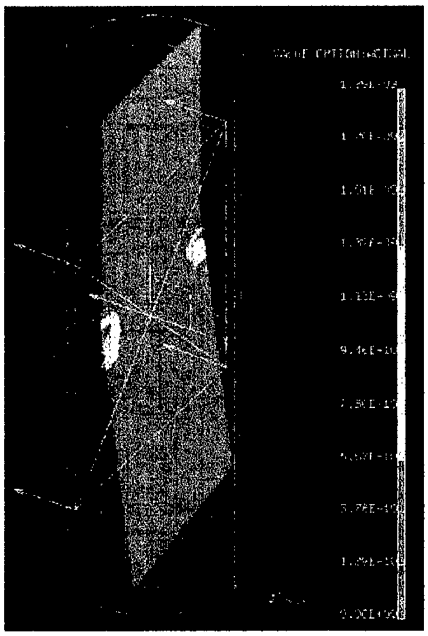

C

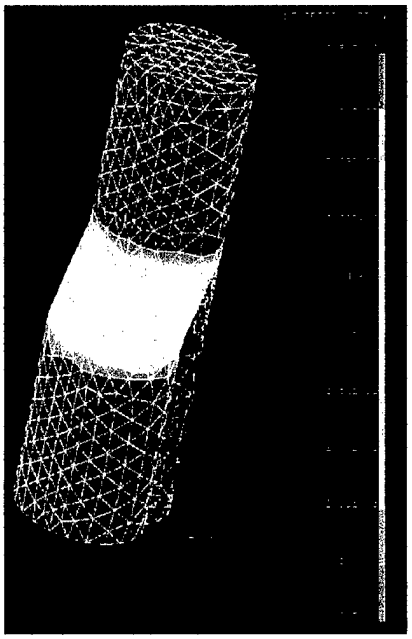

D

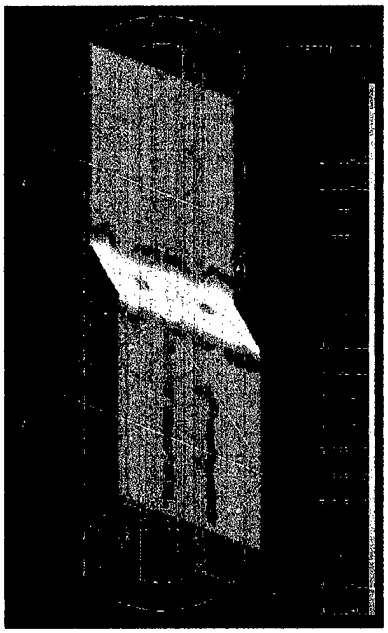

Figure 5

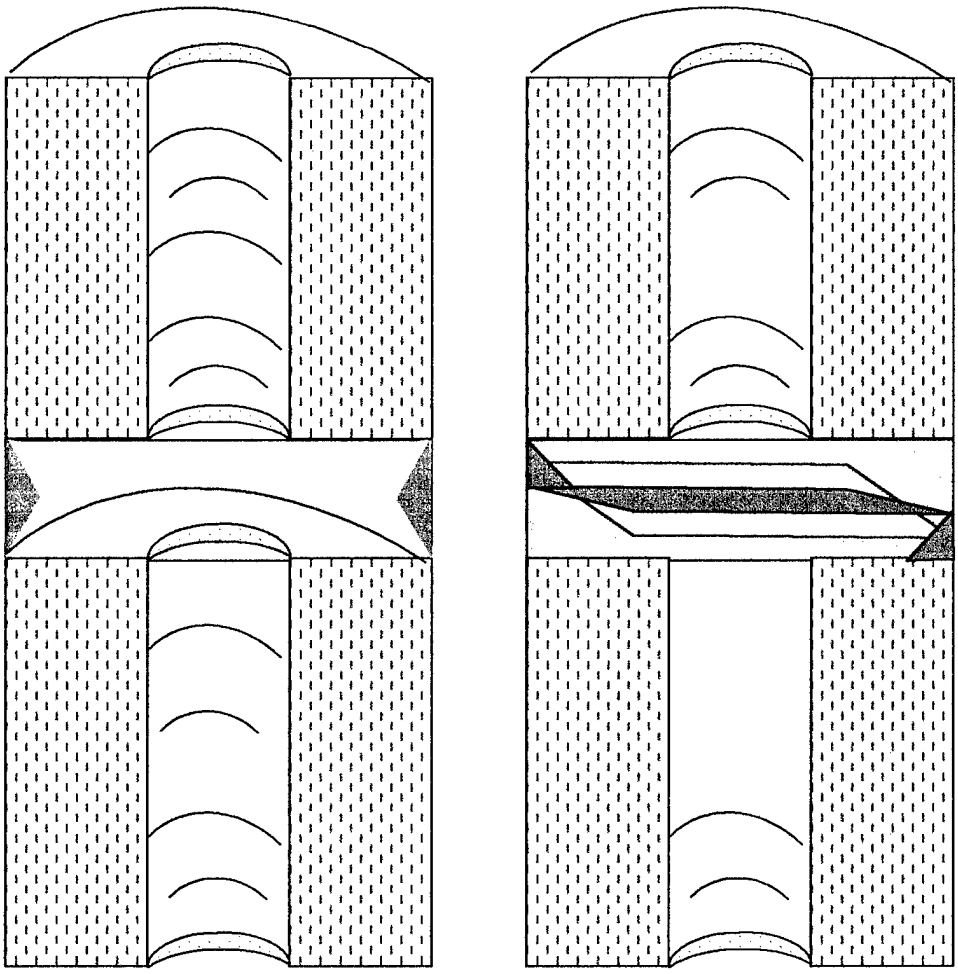

Bone

Cartilage

Fibrous

Figure 6

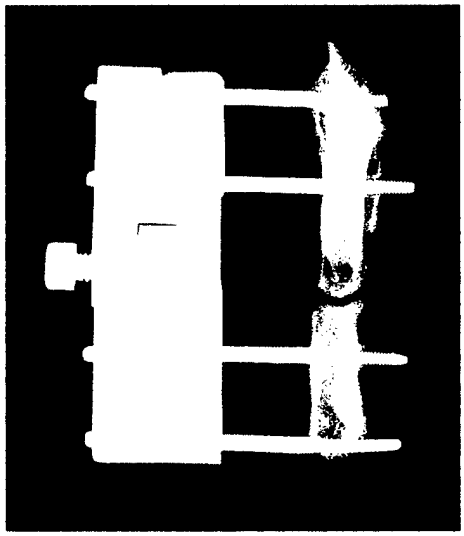

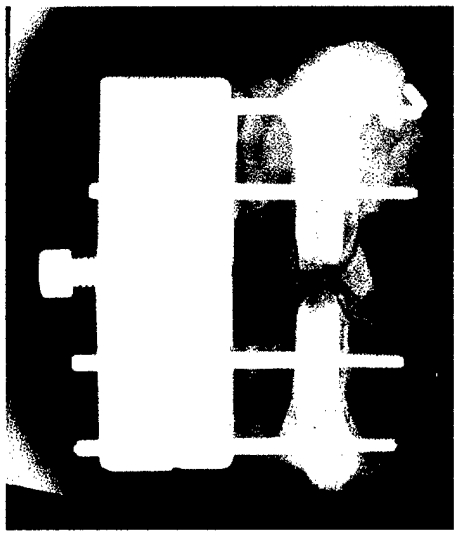

Figure 7

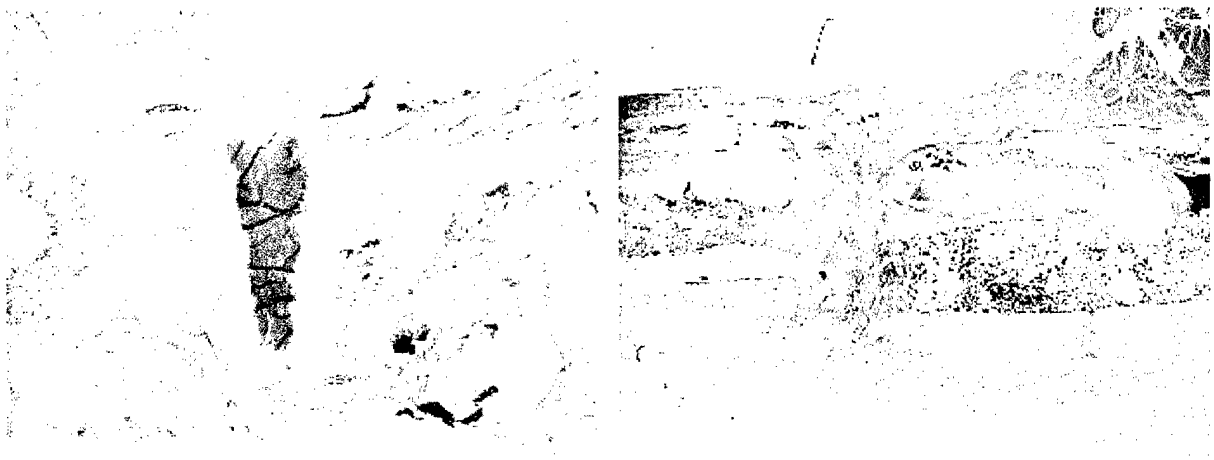

Figure 8

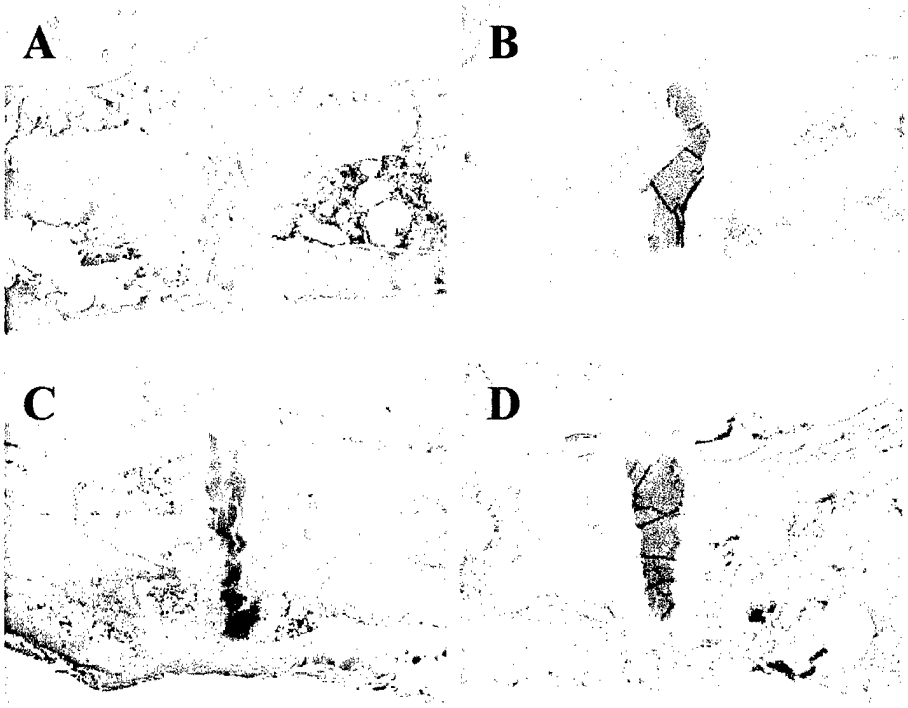

Figure 9

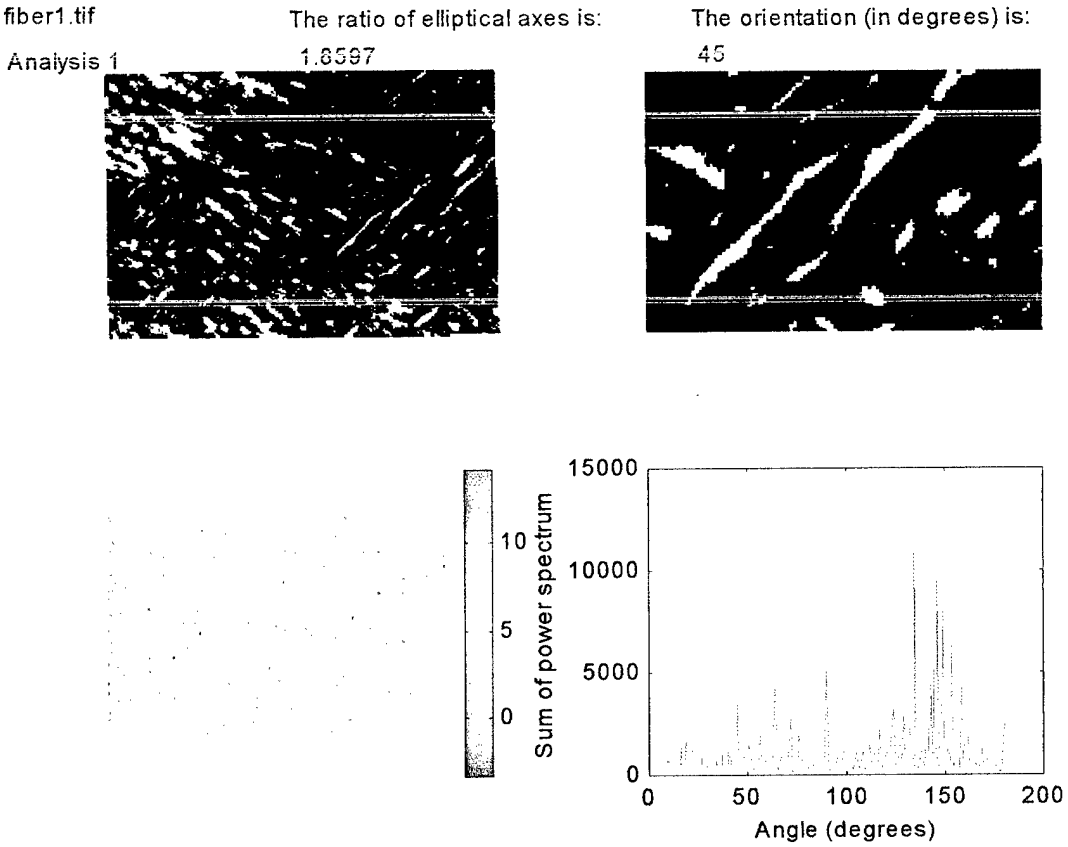
fiber1.tif
Analysis 1
The ratio of elliptical axes is:
1.8597
The orientation (in degrees) is:
45
10
5
0
Sum of power spectrum
15000
10000
5000
0
0
50
100
150
200
Angle (degrees)

Figure 10

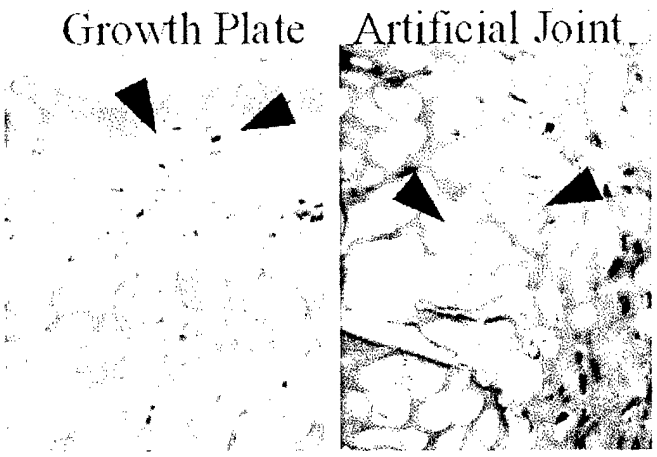

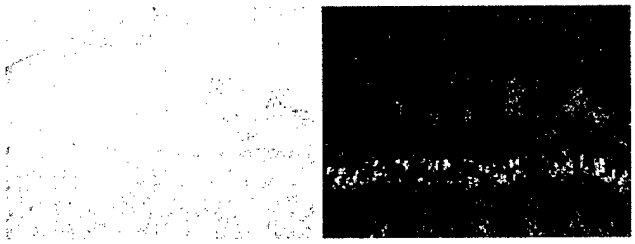

Type II collagen *in situ* on mouse growth plate

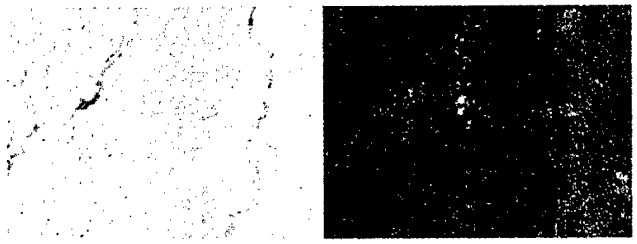

Type II collagen *in situ* on rat artificial joint

Figure 11

Figure 12